INSIGHTS INTO THE FUNCTIONS OF MUNC18-1 IN NEUROTRANSMITTER RELEASE

APPROVED BY SUPERVISORY COMMITTEE

_____

Jose Rizo-Rey, Ph.D.

_____

Yi Liu, Ph.D.

_____

Ege T. Kavalali, Ph.D.

_____

Xuelian Luo, Ph.D.

Dedication

This work is dedicated to my family for their support and love.

INSIGHTS INTO THE FUNCTIONS OF MUNC18-1 IN NEUROTRANSMITTER RELEASE

by

LIJING SU

DISSERTATION

Presented to the Faculty of the Graduate School of Biomedical Sciences

The University of Texas Southwestern Medical Center at Dallas

In Partial Fulfillment of the Requirements

For the Degree of

DOCTOR OF PHILOSOPHY

The University of Texas Southwestern Medical Center at Dallas

Dallas, TX

May, 2013

Acknowledgements

I would like to acknowledge my mentor Dr. Jose Rizo-Rey in the first place. He is the person who helped me to transfer from Oklahoma state university to UT Southwestern Medical Center at Dallas. My life changed completely from the moment I joined his laboratory. His lab is full of fantastic and talented people where I am happy and learn a lot of scientific knowledge. Dr. Jose Rizo-Rey is not only a great scientist, but also a great teacher and a warmhearted friend. As a scientist, he guided me with patience and enthusiasm in all my projects to think, to experiment and to pursue new ideas. As a teacher, he provided me tremendous help in learning NMR spectroscopy and other biophysical techniques. As a friend, he offers as much help as possible whenever I have difficulties in life. Overall, I can say that I couldn't have been able to achieve what I did at UT Southwestern Medical Center without him.

I also would like to acknowledge two previous lab members who are important for my dissertation work, Dr. Cong Ma and Dr. Yi Xu. Dr. Cong Ma was a very talented postdoc in the lab, who provided me an opportunity to join his project. It was our collaborative work that made it possible for me to complete my dissertation. He is also a good friend to me. He encourages and guides me to think deeper and more critically in scientific questions. Dr. Yi Xu was a former graduate student working on Munc18-1. She helped me to learn skills in protein purification, and gave me advices in many of my experiments.

I want to thank my dissertation committee members, Dr. Yi Liu, Dr. Ege Kavalali and Dr. Xuelian Luo, for their constructive suggestions and support during my graduate study. I also thank Dr. Diana Tomchick for her help and guidance in crystallography. I want to thank many current and previous lab members in the Rizo-Rey lab. Alpay B. Seven, who likes to read and

think, gave many suggestions to my experiments whenever I asked him for help. Yilun Sun, a wonderful technician in the lab, provided excellent technical assistance. I thank Amy Zhou, Kyle Brewer, Dr. Tim Craig, Dr. Junjie Xu, Dr. Yinbin Xu, Dr. Wei Li, Dr. Mengru Ho, Yi Zhang, and Wenhao Li for their support, discussions and friendship. I also thank my friend Tingting Weng for her help and encouragement.

Finally, I would like to thank my family with all my heart, my parents Yongchao Su and Jinzhi Ye, my sister Bisang Su and her family, my brother Ningke Su and his family, for their love, support and encouragement during my Ph.D. journey.

INSIGHTS INTO THE FUNCTIONS OF MUNC18-1 IN NEUROTRANSMITTER RELEASE

LIJING SU, Ph.D.

The University of Texas Southwestern Medical Center at Dallas, 2013

JOSE RIZO-REY, Ph.D

Neurotransmitter release is an exquisitely regulated process that transmits signals between neurons. The release process includes: docking of synaptic vesicles at the active zone of the pre-synaptic plasma membrane, priming to a release ready state, and then membrane fusion and release of neurotransmitters triggered by Ca^{2+}. Several conserved proteins are involved in regulating the entire process.

The central membrane fusion machinery in neurons includes Munc18-1 and the SNARE proteins syntaxin-1, SNAP-25 and synaptobrevin. The SNAREs form tight SNARE complexes that bring the vesicle membrane and plasma membrane into close proximity and provide forces

to induce membrane fusion. Munc18-1 is essential because deletion of Munc18-1 in mice leads to a complete loss of neurotransmitter secretion. However, its molecular mechanism of action is still unclear. This work is aimed to unravel the critical roles of Munc18-1 in regulating neurotransmitter release.

The functions of Munc18-1 discovered so far are related to the SNAREs. Recently we found that Munc18-1 interacts with synaptobrevin and the SNARE four-helix bundle with week affinity, which have been shown to stimulate in vitro SNARE-dependent liposome fusion. Biophysical characterization of these two interactions could provide important information to uncover the roles of Munc18-1 in membrane fusion. Cross-linking and NMR spectroscopy experiments showed that Munc18-1 interacts with the C-terminus of the synaptobrevin SNARE motif through some positively charged residues located in its domain 3a. NMR spectroscopy and ITC experiments revealed that the Munc18-1 N-terminal domain interacts with the C-terminal part of synaptobrevin and syntaxin-1 on the SNARE four-helix bundle, and that the affinity is higher than full length Munc18-1.

In our in vitro reconstitution experiments that try to establish the vital functions of Munc18-1 and Munc13 in neurotransmitter release, I found that Munc18-1 displaces SNAP-25 from syntaxin-1/SNAP-25 complex to form Munc18-1/syntaxin-1 complex on liposomes in the presence of NSF/α-SNAP/ATP. When NSF/α-SNAP were incorporated in the lipid mixing assays between synaptobrevin-liposmes and syntaxin-1/SNAP-25-liposomes, Munc18-1 together with Munc13 activate lipid mixing that is inhibited by NSF/α-SNAP. These results suggest that Munc18-1 functions with Munc13 to promote SNARE complex formation in an NSF/α-SNAP resistant manner and to guide the synaptic vesicle exocytosis through a tightly regulated pathway.

TABLE OF CONTENTS

PRIOR PUBLICATIONS

- Cong Ma*, **Lijing Su***, Alpay B. Seven, Yibin Xu and Josep Rizo. Reconstitution of the Vital Functions of Munc18 and Munc13 in Neurotransmitter Release. ***Science***. 2013, 339(6118):421-5 **(* co-first authors)**

- Weng T, Mishra A, Guo Y, Wang Y, **Su L**, Huang C, Zhao C, Xiao X, Liu L. Regulation of lung surfactant secretion by microRNA-150. ***Biochem Biophys Res Commun.*** 2012, 422(4):586-9.

- Xu Y, Seven AB, **Su L**, Jiang QX, Rizo J. Membrane bridging and hemifusion by denaturated Munc18. ***PLoS One.*** 2011, 6(7): e22012.

- Mishra A, Chintagari NR, Guo Y, Weng T, **Su L**, Liu L. Purinergic P2X7 receptor regulates lung surfactant secretion in a paracrine manner. ***J Cell Sci.*** 2011, 124(Pt4): 657-68.

- Xu Y, **Su L**, Rizo J. Binding of Munc18-1 to synaptobrevin and to the SNARE four-helix bundle. ***Biochemistry.*** 2010, 49(8): 1568-76.

- Chintagari NR, Mishra A, **Su L**, Wang Y, Ayalew S, Hartson SD, Liu L. Vacuolar ATPase regulates surfactant secretion in rat alveolar type II cells by modulating lamellar body calcium. ***PLoS One.*** 2010, 5(2):e9228.

- Yang C, **Su L**, Wang Y, Liu L. UTP regulation of ion transport in alveolar epithelial cells involves distinct mechanisms. ***Am J Physiol Lung Cell Mol Physiol.*** 2009, 297(3):L439-54.

- Gou D, Mishra A, Weng T, **Su L**, Chintagari NR, Wang Z, Zhang H, Gao L, Wang P, Stricker HM, Liu L. Annexin A2 interactions with Rab14 in alveolar type II cells. ***J Biol Chem***. 2008, 283(19):13156-64.

- Wang P, Chintagari NR, Gou D, **Su L**, Liu L. Physical and functional interactions of SNAP-23 with annexin A2. ***Am J Respir Cell Mol Biol.*** 2007, 37(4):467-76.

LIST OF FIGURES

LIST OF TABLES

LIST OF ABBREVIATIONS

1D, 2D, 3D	one dimensional, two dimensional, three dimensional
C.elegans	caenorhabditis elegans
CMC	critical micellar concentration
DLS	dynamic light scattering
DOPS	1,2-dioleoyl-sn-glycero-3-phospho-L-serine
DTT	dithiothreitol
E.coli	Eschericheria coli
EDTA	ethylene diamine tetraacedic acid
EGTA	ethylene glycol-bis (β-aminoethyl ether)-tetraacetic acid
FPLC	fast performance liquid chromatography
FRET	fluorescence resonance energy transfer
GST	glutathione S-transferase
HEPES	N-(2-hydroxyethyl) piperizine-N'2-ethanesulphonic acid
HOPS	homotypic fusion and vacuole protein sorting
hr	hour
HSQC	heteronuclear single quantum coherence spectroscopy
IPTG	isopropyl β-D-thiogalactopyranoside
Kd	dissociation constant
KDa	kilodalton
LB	luria broth
NBD PE	1,2-dipalmitoyl-sn-glycero-3-phosphoethanolamine-N-(7-nitro-2-1,3-benzoxadiazol-4-yl)
Ni-NTA	nickel-nitrilotriacetic acid
NMR	nuclear magnetic resonance
NSF	N-ethylmaleimide-sensitive factor

OD	optical density
PBS	phosphate buffered saline
PCS	pseudocontact chemical shift
PCR	polymerase chain reaction
POPC	1-palmitoyl, 2-oleoyl-sn-glycero-3-phosphocholine
POPE	1-palmitoyl-2-oleoyl-sn-glycero-3-phosphoethanolamine
ppm	part per million
PRE	Paramagnetic resonance enhancement
Rho PE	1,2-dioleoyl-sn-glycero-3-phosphoethanolamine-N-(lissamine rhodamine B sulfonyl)
RT	room temperature
SDS-PAGE	sodium dodecyl sulfate- polyacrylamid gel electrophoresis
SM	Sec1/Munc18
sMunc18-1	squid Munc18-1
SNAP-25	rat synaptosome associated protein- 25KDa
SNAPs	soluble NSF attachment proteins
α-SNAP	soluble NSF attachment protein isoform α
SNARE	SNAP receptor
SNC	the C-terminal SNARE motif of rat SNAP25
SNN	the N-terminal SNARE motif of rat SNAP25
Syb	synaptobrevin
TRIS	tris (hydroxymethyl) aminomethane
t-SNARE	target membrane SNARE
UV	ultraviolet
VAMP	vesicle associated membrane protein
v-SNARE	vesicle SNARE

WT	wild type
β-OG	octyl-β-D-glucopyranoside

Chapter 1 General Introduction

1.1 Neurons and Signal Transduction

The brain is one of the most important organs of a body. It is the center of the nervous system and it controls all actions of an animal through a complex neural network. The human neural network is composed of approximately 100 billion neurons (Figure 1.1) (Williams *et al.* 1988) which receive, process and transmit information through electrical and chemical signaling.

Neurons are the functional units of the brain. They are specialized cells that have special structures in order to conduct signals from one to another. A typical neuron includes three different parts: a cell body or the soma, dendrites, and an axon. The cell body is the heart of a neuron. It contains the nucleus and machineries to synthesize almost all the proteins for the cell activities, and gives rise to multiple dendrites and an axon. Dendrites are thin and branching extensions from the cell body. They are hundreds of micrometers long and normally branch several times to provide an enlarged surface area to receive signals from axons of other neurons. The cell body and dendrites can both receive signals. The axon is a long structure that arises from the cell body and extends from less than 1 mm to more than 1 m. It transmits signals away from the cell body to distant targets through its multiple terminals. The axon terminals form synapses where signal transduction occurs.

Neurons communicate with each other through synapses. Synapses transmit electrical or chemical signals from one neuron cell to another. Normally, a synapse is a structure formed by one axon terminal (presynaptic neuron) and one part of a dendrite or cell body (postsynaptic neuron), which are in close apposition, with a synaptic cleft in between. There are extensive arrays of molecular machinery in the presynaptic and postsynaptic sites of the synapse, which exquisitely regulates signal transduction.

Signals pass through two different types of synapses, electrical synapse and chemical synapse. In an electrical synapse, the cell membranes of presynapse and postsynapse are connected by gap junctions that transfer the voltage changes from the presynaptic cell to the postsynaptic cell and induce a series of molecular events in the postsynaptic cell. In a chemical synapse (Figure 1.2), signals are transmitted through neurotransmitters released from the presynaptic cell to the postsynaptic cell. Neurotransmitters bind to receptors in the postsynaptic cell membrane and initiate some molecular pathways or electrical responses that regulate the activities of the postsynaptic neuron. Signal transductions through chemical synapses are indirect and tightly regulated by a protein machinery. This work focused on neurotransmitter release in chemical synapses that provide the majority of nerve cell connections.

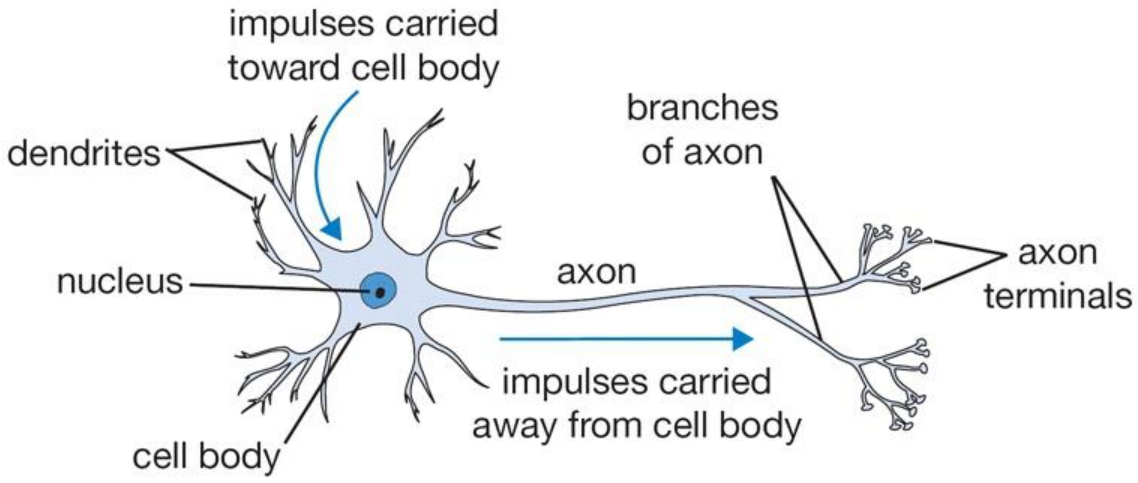

Figure 1.1 Structure of a typical neuron

A typical neuron includes a cell body, an axon and axon terminals, and dendrites. Impulses are accepted from the cell body, and then carried away through the axon to the axon terminals.
(http://www.wpclipart.com/medical/anatomy/cells/neuron/neuron.png.html)

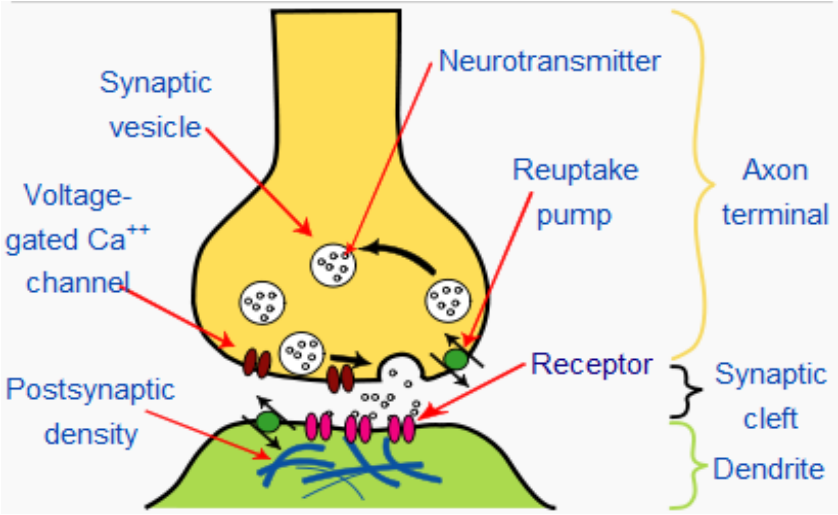

Figure 1.2 Structure of a typical chemical synapse

The structure of a typical chemical synapse is composed of an axon terminal, one part of a dentrite and the synaptic cleft between them. Neurotransmitters are released from the axon terminal, and then act on the receptors in the dendrite to transmit signals (From Wikipedia).

1.2 The Synaptic Vesicle Cycle

The release of neurotransmitters from the presynaptic cell is mediated by synaptic vesicle exocytosis at the active zone of the axon terminal. Synaptic vesicles undergo a trafficking cycle (Sudhof 2004) (Figure 1.3) to support frequent rounds of exocytosis and neurotransmitter release. Synaptic vesicles first actively uptake neurotransmitters in the cytoplasm (step 1), and then cluster in a place close to the active zone (step 2). After that, synaptic vesicles translocate and dock at the active zone (step 3), and are primed to a release-ready state (step 4). Upon stimulation by an action potential, the Ca^{2+} channels in the active zone open and induce a sudden influx of Ca^{2+}, which triggers fast membrane fusion and neurotransmitter release (step 5). After fusion, synaptic vesicles are proposed to be recycled through three different pathways: (1) Vesicles close the fusion pore and remain docked at the active zone, and then reacidify and reload neurotransmitters to start a new cycle (step 6); (2) Empty vesicles leave the active zone but reacidify and reload neurotransmitters locally (step 7); (3) Vesicles undergo clathrin mediated endocytosis (step 8) and go through endosome (step 9) to reacidify and reload neurotransmitters (Sudhof 2004). Of the three pathways, (1) and (2) are fast, and (3) is slower. The synaptic vesicle cycle is regulated by a number of molecular machineries to rapidly respond to stimulation and release neurotransmitters to communicate with other neuron cells. Of all the steps, Ca^{2+} triggered membrane fusion is the most important one.

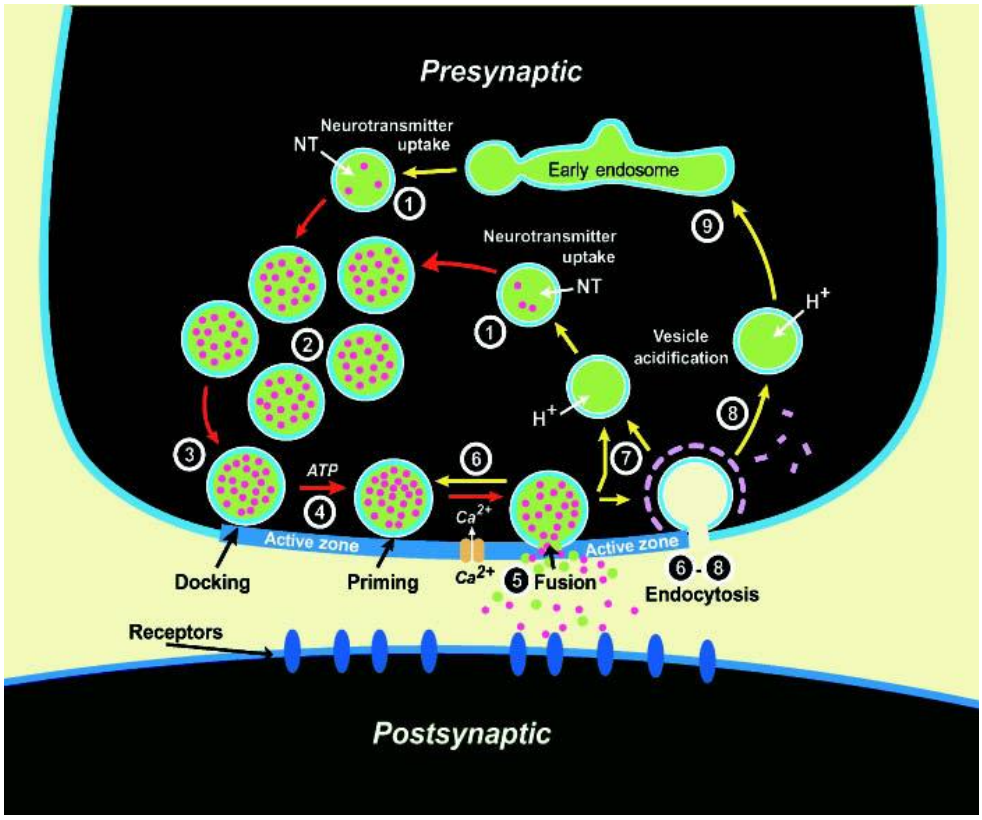

Figure 1.3 The synaptic vesicle cycle.

Neurotransmitters are first actively transported into synaptic vesicles (step 1). The filled synaptic vesicles form clusters that may represent the reserve pools (step 2) and then dock at the active zone (step 3). After docking, synaptic vesicles undergo a priming step (step 4) to make them ready for Ca^{2+} triggered vesicle exocytosis (step 5). After release, synaptic vesicles are recycled through several different routes: local reuse (step 6), recycling without going through endosome (step 7), or clathrin mediated endocytosis (step 8) and recycling through endosomes (step 9). Red arrows represent steps in exocytosis and yellow arrows represent steps in endocytosis and recycling. (Sudhof 2004).

1.3 Membrane Fusion

Membrane fusion is fundamental for many biological processes, such as exocytosis, protein sorting, fertilization and enveloped virus infection. Neurotransmitter release is a specialized type of exocytosis. Despite the differences in the biological processes, all kinds of fusion reactions proceed through the same elementary processes: membrane contact, membrane merger, and the opening of a fusion pore (Jahn *et al.* 2003). Membrane fusion doesn't occur spontaneously. It is highly regulated by conserved protein families.

Biological membranes are covered by a layer of water molecules that adhere to the hydrophilic surface of the membranes and hinder approximation of two opposing membranes through hydration repulsion. Besides, phospholipid bilayers create other forces, such as electrostatic repulsion of the negatively charged phospholipid headgroups and van der Walls forces, to keep the opposing membranes away from each other. In order to fuse, membranes first need to be brought into proximity, which is called docking and it is regulated by some tethering factors.

However, actual fusion requires a much closer apposition. A small area of the two opposing phospholipid bilayer needs to approach closer than 3 nm in order for membrane merger to occur (Helm *et al.* 1993). When two phospholipid bilayers are within 3 nm, the repulsion between each other becomes huge, which makes a very high energy barrier for membrane fusion to occur. Specialized proteins can lower the energy barrier and make the fusion favorable. Membrane merger also requires lipid reorganization, which needs some local packing defects of the phospholipid bilayers. The packing defects can be created by changes of membrane curvature or lipid composition, insertion of membrane proteins or some regulating amphipathic proteins.

Once the energy barrier is overcome and the packing defects are achieved, membranes start to fuse, and eventually a fusion pore forms to connect the contents of the two compartments. There are transition states during the process of fusion pore formation to minimize the exposure of hydrophobic surfaces of phospholipids to the aqueous environment. Right now, the most favored model of describing the transition states of membrane fusion is the stalk hypothesis (Kozlov *et al.* 1983; Chernomordik *et al.* 1987). The stalk hypothesis proposes some distinct steps in the formation of a fusion pore: merging of the two opposing proximal leaflets, stalk formation, generation of hemifusion intermediates, and opening of a fusion pore (Figure 1.4) (Jahn *et al.* 2003). Membrane proximity is facilitated by a combination of thermal fluctuations of phospholipid, application of mechanical energy, and shielding of charges, which temporarily reduce the repulsive forces of the two membranes. The proximal leaflets can merge and form metastable intermediates because of the membrane temporary relaxation. The first step of merging is stalk formation, in which the two proximal leaflets are merged while the two distal leaflets are still separated. After stalk formation, the radial expansion of the two proximal leaflets pulls the two distal leaflets toward each other, and eventually causes the merging of the distal leaflets, which is the hemifusion intermediate. Then the relaxation of energetically unfavorable void interstices will cause the opening of a fusion pore. The stalk hypothesis is supported by both theoretical calculations and experimental evidence in several model systems (Chernomordik 1996; Lee *et al.* 1997; Basanez *et al.* 1998).

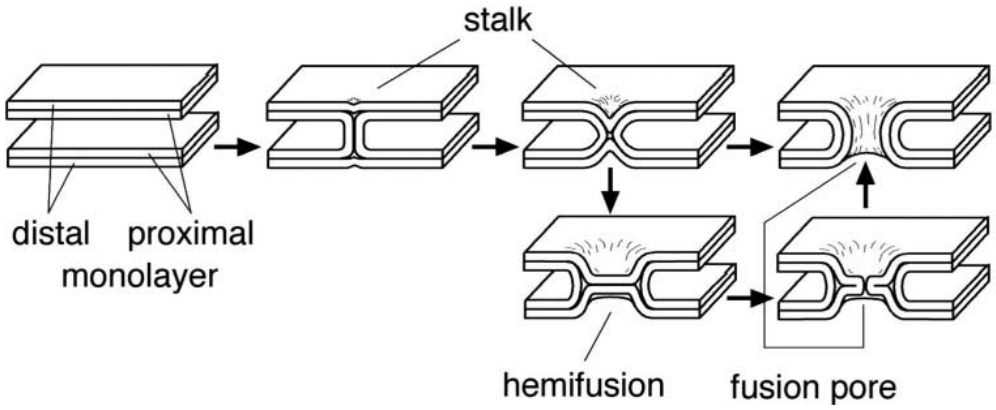

Figure 1.4 Transition states in membrane fusion.

The smooth and bendable sheets on the left represent the phospholipid bilayers or leaflets. The two membrane bilayers are first separated. When membrane fusion initiates, the two proximal layers merge but not the two distal layers, which is called stalk intermediate. The radial expansion of the proximal leaflets causes the two distal leaflets to contact with each other and leads to a hemifusion intermediate. The subsequent merging of the two distal leaflets causes formation of a fusion pore (Jahn *et al.* 2003).

1.4 Proteins involved in Neurotransmitter Release

The release of neurotransmitters from presynaptic terminals is a process that is mediated by synaptic vesicle exocytosis and incudes several steps. Ca^{2+} triggered neurotransmitter release is a very fast process. It is strictly regulated by intracellular Ca^{2+} concentration, and can happen within a few hundred microseconds. To achieve this highly precise spatial and temporal regulation, a series of conserved proteins are involved in each step of neurotransmitter release. The central protein machinery consists of N-ethylmaleimide sensitive factor (NSF), soluble NSF adaptor proteins (SNAPs), the neuronal SNAP receptors (SNAREs) syntaxin-1, SNAP-25 and synaptobrevin, and the Sec1/Munc18 (SM) protein Munc18-1 (Brunger 2005; Jahn *et al.* 2006; Rizo *et al.* 2008; Sudhof *et al.* 2009). These proteins have homologs in most types of intracellular membrane traffic, suggesting that this central protein machinery comprises a conversed mechanism of membrane fusion in synaptic vesicle exocytosis and other membrane traffic events. Besides these universally required proteins, there are other neuronal specific proteins involved in regulating Ca^{2+} triggered fast release, such as the Ca^{2+} sensor synaptotagmin-1 (Fernandez-Chacon *et al.* 2001), Rab3, the priming factors RIMs (Rab3-interating molecules) and the large active zone proteins Munc13s, and the small SNARE complex associating protein complexins.

1.4.1 SNARE proteins

SNARE proteins are a conserved protein superfamily required for most intrancellular membrane trafficking processes from yeast to neurons (Clary *et al.* 1990; Bennett *et al.* 1993). SNAREs include a v-SNARE from the vesicle membrane and t-SNAREs from the target membrane. The most known and best characterized SNAREs are the neuronal SNAREs, which include the synaptic vesicle membrane protein synaptobrevin, known as v-SNARE, and the

plasma membrane proteins syntaxin-1 and SNAP-25, known as t-SNAREs. All SNAREs contain one or two SNARE motifs, which are 60-70 residues long and have a tendency to form coil-coils.

Synaptobrevin 2 is a member of the vesicle associated membrane protein (VAMP) family. It is the v-SNARE protein responsible for synaptic vesicle exocytosis in forebrain synapses. It consists of a short NH_2-terminal sequence, a SNARE motif, and a COOH-terminal transmembrane region (Figure 1.5). The first indication of synaptobrevin being involved in neurotransmitter release is that tetanus toxin and botulinum-B toxin block neurotransmitter release by specific proteolytic cleavage of synaptobrevin (Link *et al.* 1992; Schiavo *et al.* 1992). Synaptobrevin 2 knockout mice died immediately after birth probably due to impaired exocytosis in the brown fat cells which accumulate in the upper back and cause an abnormal body shape (Schoch *et al.* 2001). Analysis of the knockout hippocampal neurons from embryos revealed that spontaneous synaptic vesicle fusion and fusion induced by hypertonic sucrose were decreased around 10 fold, while Ca^{2+}-triggered fast fusion was decreased more than 100 fold (Schoch *et al.* 2001). The strong impairment but not complete abrogation of neurotransmitter release by knocking out synaptobrevin 2 suggests that synaptobrevin 2 is not strictly required for synaptic vesicle fusion, but it is essential for keeping a normal rate of fusion without or with stimulation (Schoch *et al.* 2001).

Syntaxin-1 is a plasma membrane protein with a short NH_2-terminal sequence (N-peptide), an NH_2-terminal 3 helix bundle Habc domain, a short flexible linker, a SNARE motif and a COOH-terminal transmembrane region (Figure 1.5) (Fernandez *et al.* 1998). In human neurons, syntaxin-1 has two isoforms, syntaxin-1A and syntaxin-1B, which are highly homologous and might perform similar functions (Fujiwara *et al.* 2006). Syntaxin-1 can adopt two different conformations: a closed conformation and an open conformation (Figure 1.6). In

closed conformation, syntaxin-1 Habc domain can fold back and bind to the syntaxin-1 SNARE motif to form a four helix bundle, which is stabilized through binding to Munc18-1 and is incompatible for SNARE complex formation (Dulubova *et al.* 1999; Misura *et al.* 2000). The SNARE motif of syntaxin-1 together with the SNARE motifs of synaptobrevin and SNAP-25 form the SNARE complex, in which syntaxin-1 is in the open conformation. The closed conformation of syntaxin-1 is important for its trafficking to the plasma membrane, but it has to undergo a conformational change in order to allow SNARE complex formation, which is central for neurotransmitter release. This conformation switch has been shown to be regulated by Munc13-1 (Ma *et al.* 2011) and syntaxin-1 N-peptide (Burkhardt *et al.* 2008). The syntaxin-1 N-peptide binds to a hydrophobic pocket on the surface of Munc18-1 according to the refined crystal structure of Munc18-1/syntaxin-1 (Figure 1.9) (Burkhardt *et al.* 2008). N-peptide also plays a role in Munc18-1 stimulation of SNARE-dependent liposome fusion (Shen *et al.* 2007).

SNAP-25 is a plasma membrane associated protein which consists of an NH_2-terminal SNARE motif (SNN), a flexible linker region that has four cysteines, and a COOH-terminal SNARE motif (SNC) (Figure 1.5) (Chapman *et al.* 1994). SNAP-25 contributes two SNARE motifs to the SNARE complex. It is associated to the plasma membrane through palmitoylation of the four cysteines in the flexible linker. In vitro, SNAP-25 can cause oligomerization of the SNARE complexes probably because the two SNARE motifs can be assembled into different SNARE complexes. To simplify experiments, the two SNAP-25 SNARE motifs SNN and SNC are often used. Experiments from SNAP-25 knockout mice revealed that SNAP-25 is not required for normal nervous system development, normal axonal outgrowth and stimulus-independent spontaneous neurotransmitter release. However, it is essential for Ca2+-triggered

release at the neuromuscular junctions and central synapses (Washbourne *et al.* 2002), suggesting that regulated exocytosis requires the specialized SNAREs and SNARE complexes.

The SNARE motifs of synaptobrevin, syntaxin-1 and SNAP-25 form a highly stable four-helix bundle complex called the SNARE core complex (Figure 1.5c), which is SDS and proteolysis resistant and stable at temperatures below 90 ℃ (Hayashi *et al.* 1994; Fasshauer *et al.* 1998). Early electron microscopy (EM), electron paramagnetic resonance (EPR) spectroscopy and fluorescence resonance energy transfer (FRET) revealed that the SNARE complex is a parallel four-stranded coiled-coil structure with the membrane anchors of syntaxin-1 and synaptobrevin located at the same end (Hanson *et al.* 1997; Lin *et al.* 1997; Poirier *et al.* 1998). Later, the crystal structure of the neuronal SNARE complex showed that it is a parallel four-helix bundle structure with a length of 120 Å (Figure 1.7) (Sutton *et al.* 1998). This complex is mainly stabilized by hydrophobic interactions at the core. The surface of this four-helix bundle consists of distinct hydrophilic, hydrophobic and charged regions, with negative charges at the middle regions and positive charges at the ends. These characteristics of the complex might be important for inducing membrane fusion and for the regulatory factors that are involved in neurotransmission (Sutton *et al.* 1998).

The SNARE complex is proposed to zipper from the membrane distal N-termini to the membrane proximal C-termini to form trans-SNARE complex (two transmembrane regions located in two different membranes) (Fig 1.7) and release energy from assembly (Hanson *et al.* 1997; Lin *et al.* 1997). Thus the SNARE complex formation might be able to overcome the repulsion between two opposing membranes and bring them into close proximity, facilitating or driving membrane fusion (Figure 1.7) (Hanson *et al.* 1997). However, if there is any flexibility in the linker region between the SNARE core complex and the transmembrane region, energy

released from assembly may not be able to transfer to the membrane and SNARE complex may not be able to directly execute fusion (Rizo *et al.* 2006). Recently, a group reported the X-ray structure of the SNARE complex with the C-terminal linkers and transmembrane regions of syntaxin-1 and synaptobrevin (Stein *et al.* 2009). The structure shows that the assembly proceeds from the known SNARE core complex all the way to the linker and transmembrane region (Figure 1.8), suggesting that the final phase of the SNARE complex assembly is directly coupled to membrane merger (Stein *et al.* 2009). However, this structure is about the cis-SNARE complex (two transmembrane regions located in the same membrane), thus it is unclear that whether the trans-SNARE complex assemble in the same way.

Previous studies showed that SNAP-25 binds to syntaxin-1 with high affinity (EC_{50} of about 0.4uM) (Pevsner *et al.* 1994). Later work revealed that the two target-SNAREs, SNAP-25 and syntaxin-1, can form stable coiled coil complex (Fasshauer *et al.* 1997). This finding led to the hypothesis that SNAP-25 and syntaxin-1 form the acceptor t-SNARE heterodimers at the plasma membrane, when synaptic vesicles dock at the active zones, synaptobrevin sequentially associates with the t-SNARE heterodimer and form the SNARE complex (Chen *et al.* 2001; Fasshauer *et al.* 2004; Rickman *et al.* 2004). In vitro reconstitution experiments with synaptobrevin and syntaxin-1/SNAP-25 incorporated into different liposomes showed efficient lipid mixing upon the SNARE complex formation, suggesting that the SNAREs constitute the minimal membrane fusion machinery (Weber *et al.* 1998). However, the efficiency of these experiments depends strongly on the protein to lipid ratios and homogeneity of the liposomes (Kweon *et al.* 2003; Chen *et al.* 2006). Moreover, these experiments provide no explanation of the physiologically strict requirements of Munc18-1 and Munc13. Knock out Munc18-1 or Munc13-1/2 mice resulted in the total abrogation of neurotransmitter release (Verhage *et al.*

2000; Varoqueaux *et al.* 2002). Hence, the model that SNAREs alone cause membrane fusion is still under debate.

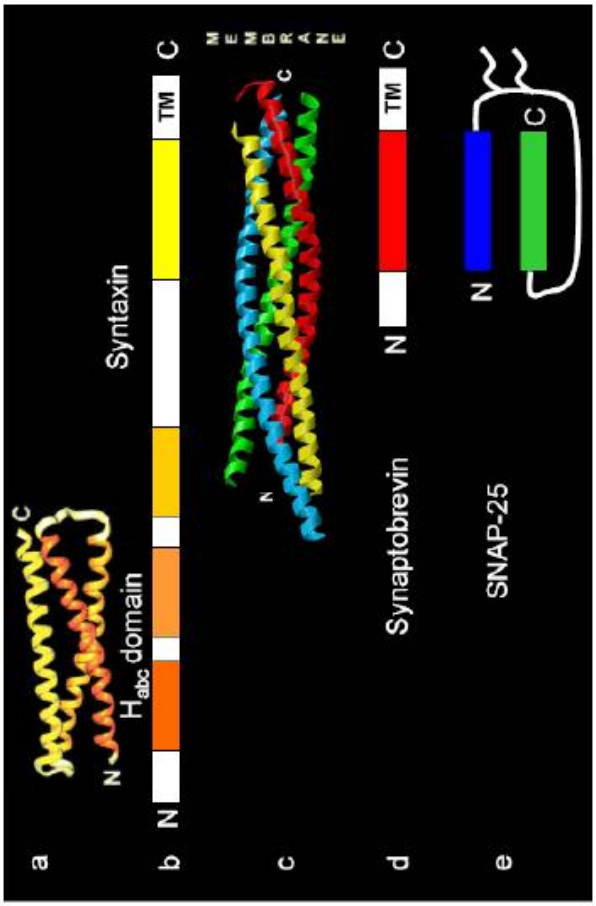

Figure 1.5 Structure of the SNARE complex and its components.

(A)Ribbon diagram of the structure of the Syntaxin Habc domain (Fernandez *et al.* 1998); (B) Domain diagram of syntaxin-1. Syntaxin-1 is composed of a SNARE motif (yellow), a transmembrane region (TM), and a self folded (A) three α-helix bundle Habc domain (orange). (C) Ribbon diagram of the crystal structure of the SNARE complex (Sutton *et al.* 1998) with each of the 4 SNARE motifs: Syntaxin-1 (Yellow), Synaptobrevin (Red), and the N (Blue) and C (Green)-terminal SNARE motifs of SNAP25 (SNN and SNC). (D) Domain diagram of synaptobrevin with one SNARE motif (Red) and one transmembrane region (TM). (E) Domain diagram of SNAP 25 with SNN in blue and SNC in green.

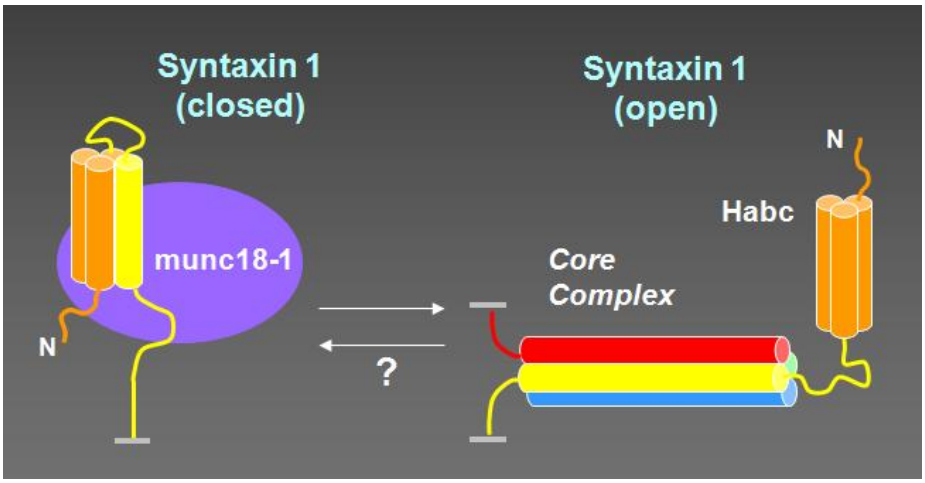

Figure 1.6 Models of the closed and open conformations of syntaxin-1.

Left panel represents the closed conformation of syntaxin-1 with the SNARE motif (yellow) bound to the Habc domain (orange), forming a four-helix bundle. The closed conformation is stabilized through binding to Munc18-1 (purple). Right panel represents the open conformation of syntaxin-1 in the SNARE complex with synaptobrevin in red, SNN in green, and SNC in blue.

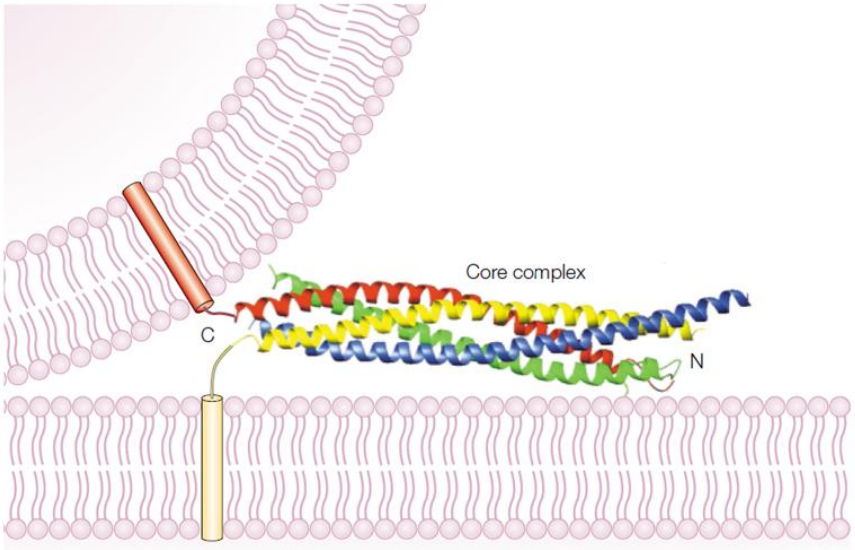

Figure 1.7 Model of the assembled SNARE core complex in two opposing membranes.

The ribbon diagram represents the crystal structure of the core complex with the SNARE motifs of SNC in greem, SNN in navy blue, synaptobrevin in red, and syntaxin-1 in yellow. The cylinders represent the transmembrane regions of syntaxin-1 and synaptobrevin, which are inserted into the plasma and synaptic vesicle membranes, respectively. The curved lines represent short sequences that connect the SNARE motifs and the transmembrane regions.(Sutton *et al.* 1998; Rizo *et al.* 2002)

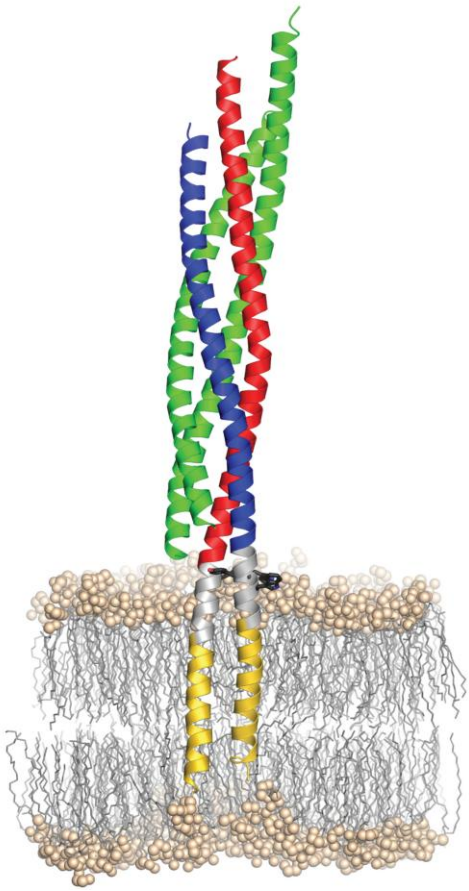

Figure 1.8 Model of the synaptic SNARE complex inserted into a membrane.

The SNARE complex here includes two SNARE motifs of SNAP-25 (green), syntaxin-1 with SNARE motif in red, transmembrane region in yellow, and the linker in grey, and synaptobrevin with SNARE motif in navy blue, transmembrane region in yellow, and linker in grey. The aromatic residues (black sticks) within the linker regions of synaptobrevin (grey) are shown. The hydrophilic head groups of the phospholipids are shown as balls, their aliphatic chains as sticks. They stand for the membrane.
(Stein *et al.* 2009)

1.4.2 Sec1/Munc18 (SM) protein Munc18-1

Sec1/Munc18 (SM) proteins are highly conserved 60-70 KDa proteins that are universally required for intracellular membrane fusion (Rizo *et al.* 2002; Toonen *et al.* 2007; Sudhof *et al.* 2009). Structure studies of SM proteins revealed that these proteins are highly conserved in the overall fold in different organisms and trafficking steps (Misura *et al.* 2000; Bracher *et al.* 2001; Bracher *et al.* 2002). UNC-18 is the first identified SM protein through genetic screens for uncoordinated phenotypes in *C. elegans* (Brenner 1974). Deletion of UNC-18 results in deficient locomotions in *C. elegans (Brenner* 1974*).* Mutation studies revealed that UNC-18 plays important roles in axon transport system, the acetylcholine flow in motor neurons, and synaptic vesicle docking (Gengyo-Ando *et al.* 1993; Weimer *et al.* 2003). Later, Sec1 was identified to be involved in the yeast secretory pathway in genetic screens (Novick *et al.* 1980). The mammalian homolog of UNC-18, Munc18-1, was first connected to synaptic vesicle fusion by the identification that Munc18-1 interacts tightly to the t-SNARE syntaxin-1 (Hata *et al.* 1993).

The SM protein structure is globular arch shape, and consists of three domains (domains 1-3) as shown in Figure 1.9. Domains 1 and 3 form a cavity where syntaxin-1 binds (Misura *et al.* 2000). Domains 1 and 2 form a groove that is involved in yeast SM protein Sec1p binding to the yeast SNARE complex (Hashizume *et al.* 2009). The structure of diverse SM proteins is highly conserved with some conformational flexibility in domain 1 and part of domain 3 (Bracher *et al.* 2001), which affects the shape of the cavity and might influence the binding to SNAREs.

Munc18 has 3 isoforms: Munc18-1, Munc18-2, and Munc18-3. Munc18-1 is neuron specific and expressed throughout the brain. Deletion of Munc18-1 in mice resulted in complete loss of neurotransmitter release throughout development without affecting normal brain

assembly, which suggests that Munc18-1 is essential for synaptic vesicle exocytosis (Verhage *et al.* 2000). Munc18-2 is 62% sequence identical to Munc18-1 (Tellam *et al.* 1995). It is predominantly expressed in epithelial cells and forms a complex with syntaxin 3, which is involved in the regulation of apical membrane transport (Riento *et al.* 1998). Munc18-3 is 51% sequence identical to Munc18-1 and it is ubiquitously expressed (Tellam *et al.* 1995). It interacts with syntaxin 4, which is required for the integration of GLUT4 storage vesicles into the plasma membrane in adipocytes (Thurmond *et al.* 2000).

Analysis of neurons from Munc18-1 knockout mice revealed that Ca^{2+}-triggered release, minis or exocytosis evoked by hypertonic sucrose or by α-latrotoxin were completely abrogated (Verhage *et al.* 2000), suggesting that Munc18-1 is absolutely required for neurotransmitter secretion. However, the functions of Munc18-1 are still not well understood. Munc18-1 has been shown to play an important role in secretory vesicle docking to the plasma membrane in chromaffin cells from Munc18-1 knockout mice (Voets *et al.* 2001), but docking was not affected in brain synapses, which suggests that the most important function is downstream of docking. The functions of Munc18-1 have been tightly linked to the SNAREs since Munc18-1 interacts with the SNAREs in different modes. So far, two different binding modes have been discovered, and they play different roles in synaptic vesicle exocytosis: (1) Munc18-1-syntaxin-1 interaction; (2) Munc18-1-SNARE complex interaction.

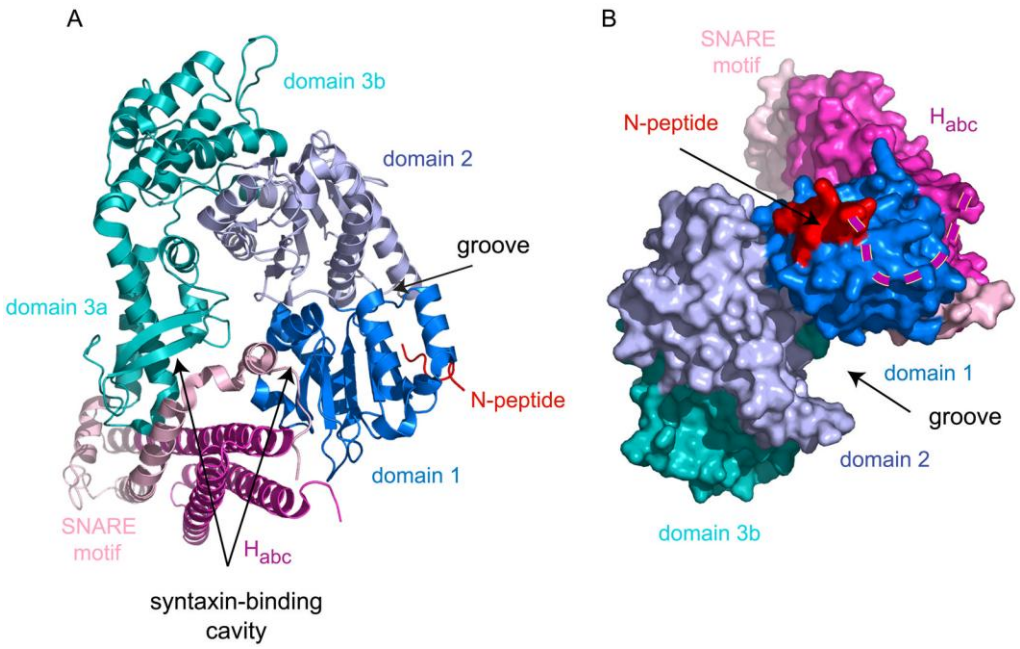

Figure 1.9 Structure of Munc18-1 bound to syntaxin-1.

(A) A ribbon diagram of Munc18-1 bound to the helical bundle of synaxin-1 in the closed conformation. Munc18-1 domain 1 (blue) binds the syntaxin N-peptide (red) and forms an arch with domains 2 (light blue) and 3 (teal). The cavity of the arch binds the syntaxin-1 helical bundle formed by the SNARE motif helix (light pink) bound to the Habc domain (hot pink) in the closed conformation. The location of the groove between domains 1 and 2 and the syntaxin-binding cavity are indicated with arrows. (B) Surface presentation of a rotated view of Munc18-1 bound to syntaxin-1 [domains colored as in (A)]. The view reveals two syntaxin-binding sites and a groove implicated in SNARE complex binding. The syntaxin N-peptide is bound to domain 1 of Munc18-1, and is connected to the syntaxin-1 Habc helical bundle by an unresolved linker (aa 10–26; hatched line). (Carr *et al.* 2010)

Munc18-1-syntaxin-1 interaction. The observation that Munc18-1 interacts tightly with syntaxin-1, and that other SM protein homologs also bind to their cognate syntaxins (Grabowski *et al.* 1997; Nichols *et al.* 1998), led to the assumption that Munc18-1 functions by interacting with syntaxin-1. The crystal structure of Munc18-1-syntaxin-1 showed that Munc18-1 cradles syntaxin-1 in its central cavity and that syntaxin-1is in a closed conformation (Figure 1.9) (Misura *et al.* 2000). In the structure, Munc18-1 domain 1 and domain 3a are involved in the binding. Domain 1 contributes a large contact surface to the interaction. The syntaxin Habc domain and SNARE motif form a four-helix bundle, which is called 'closed' conformation. The very N-terminus of syntaxin-1, called syntaxin-1 N-peptide, binds to a hydrophobic pocket of domain 1. The biological relevance of Munc18-1/syntaxin-1 interaction was supported by several findings. First, the expression level of syntaxin-1 was 70% decreased in Munc18-1 knockout neurons (Verhage *et al.* 2000). In Munc18-1 knock down PC12 cells, the expression level of syntaxin-1 was reduced and the plasma membrane localization of syntaxin-1 was also severely perturbed. The localization of syntaxin-1 and the impaired secretion capability were restored by reintroduction of Munc18-1 (Arunachalam *et al.* 2008). These results suggest that Munc18-1 plays a role in stabilizing syntaxin-1 and syntaxin-1 trafficking to the plasma membrane. Second, the Munc18-1-syntaxin-1 interaction is important in stimulating vesicle docking in chromaffin cells. Munc18-1 null chromaffin cells showed a vesicle docking defect, and this defect is associated with binding to syntaxin-1 and can be rescued by Munc18 (Gulyas-Kovacs *et al.* 2007). Third, when binds to Munc18-1, syntaxin-1 is in the closed conformation, which competes with the SNARE core-complex (syntaxin-1 is in an open conformation) formation (Yang *et al.* 2000). The syntaxin-1 N-peptide has been shown to connect the two binding modes of syntaxin-1 to each other and is essential for synaptic vesicle exocytosis (Khvotchev *et al.*

2007). Moreover, syntaxin-1 N-peptide binding to Munc18-1 domain 1 was reported to play a role in controlling SNARE core-complex assembly (Burkhardt *et al.* 2008; Rathore *et al.* 2010). Overall, the Munc18-1-syntaxin-1 interaction is important in synaptic vesicle exocytosis, but has never been shown to be critical for membrane fusion so far.

Munc18-1-SNARE complex interaction. After many years of characterizing Munc18-1-syntaxin-1 interaction, Munc18-1 was shown to bind directly to the SNARE complex by our group and Rothman's group (Dulubova *et al.* 2007; Shen *et al.* 2007). Yeast SM protein Sec1p binds specifically to the ternary SNARE complex rather than the closed conformation of the cognate syntaxin Sso1p (Togneri *et al.* 2006). Thus, Munc18-/SNARE complex interaction might represent the most general role of Munc18-1, and might underlie its crucial function in fusion. Mutations on Munc18-1 domain 1 that disrupt Munc18-1-SNARE complex interaction result in impaired synaptic vesicle priming (Deak *et al.* 2009). In vitro reconstitution studies revealed that Munc18-1 enhances SNARE-dependent lipid mixing in a manner that associates with SNARE complex binding (Shen *et al.* 2007; Rodkey *et al.* 2008). Later, further characterization of Munc18-1-SNARE complex interaction showed that Munc18-1 directly binds to the SNARE four-helix bundle with a much weaker affinity (6-13 μM) than the SNARE core complex that includes syntaxin Habc domain, and that syntaxin Habc domain competes with the SNARE four-helix bundle for binding to Munc18-1 (Xu *et al.* 2010). The Munc18-1/SNARE four-helix bundle binding mode might be crucial for membrane fusion and the idea is supported by in vitro reconstitution data showing that Munc18-1 binding to SNARE four-helix bundle is sufficient for its stimulation of lipid mixing (Diao *et al.* 2010; Shen *et al.* 2010). However, the physiological relevance of this weak interaction is not known yet. In vitro characterization of the

binding sites involved in Munc18-1/SNARE four-helix bundle interaction would certainly provide key information for in vivo study.

Overall, why is Munc18-1 essential for neurotransmitter release and what is the function of Munc18-1? The functional data summarized above revealed that Munc18-1 participates in several steps in synaptic vesicle exocytosis and interacts with the SNAREs in different modes. These different binding modes might be compatible with each other. Integrating these binding modes might provide a better idea to understand the roles of Munc18-1 in neutrotransmitter release. Figure 2.7 shows our current working model of Munc18-1. Munc18-1 initially binds to the closed syntaxin-1, working as a molecular chaperon for syntaxin-1 trafficking to the plasma membrane, stabilizaing syntaxin-1, inhibiting SNARE core complex assembly, and also mediating vesicle docking. At some point, Munc13 opens syntaxin-1 to allow SNARE core complex assembly (Ma *et al.* 2011), while Munc18-1 remains bound to the tsyntaxin-1 N-peptide and Habc domain, which is important for synaptic vesicle priming and also Munc18-1 localization on plasma membrane. After that, Munc18-1 translocates to the SNARE motif to promote SNARE four-helix bundle assembly or directly translocates to the assembled SNARE four-helix bundle, probably with the help of membranes or allosteric regulation of Munc18-1 by other factors. Munc18-1 together with the SNARE four-helix bundle might cooperate to initiate membrane fusion. Clearly, these ideas need to be further proved and need to be integrated with the functions of complexins and synaptotagmins.

1.4.3 NSF/SNAPs

NSF (N-ethylmaleimide-sensitive factor) and SNAPs (Soluble NSF attachment proteins) are both required for intracellular vesicle fusion. NSF, SNAP, and SNARE complex assemble into a 20S particle (Wilson *et al.* 1992). NSF is an ATPase, which functions as a homohexamer

(Fleming *et al.* 1998). Each subunit of NSF hexamer consists of three domains: the N-terminal domain and two nucleotide binding domains (D1 and D2) (Tagaya *et al.* 1993; Zhao *et al.* 2012). The N domain is essential for interaction with the SNAP-SNARE complex, while the D1 domain provides the main ATPase activity required for NSF function, and the D2 domain mediates nucleotide –dependent hexamerization (Nagiec *et al.* 1995). SNAPs contain three isoforms: α-, β-, and γ-SNAP. β-SNAP is specifically expressed in the brain. α- and γ-SNAPs are ubiquitously expressed in all cell types. α- and β-SNAPs share 83% identity to each other. γ-SNAP is less related to α- and β-SNAP, but has similar overall structure (Whiteheart *et al.* 1993). NSF and α-SNAP are homologs to yeast Sec18p and Sec17p, which are required for all types of intracellular fusion in yeast (Mayer *et al.* 1996). α-SNAP binds to the SNARE complex and serves as an adaptor protein for NSF binding to form the 20S particle. The ATPase activity of NSF couples the energy released from ATP hydrolysis to disrupt the cis-SNARE complexes and recycle the SNAREs for another round of fusion, while the trans-SNARE complexes are resistant according to Rothman's group (Sollner *et al.* 1993; Weber *et al.* 2000). Meanwhile, NSF and α-SNAP were reported to be capable of disrupting the t-SNARE complex in in vitro reconstitution assays (Weber *et al.* 2000).

1.4.4 Munc13s

Munc13s are mammalian homologs of *C. elegans* Unc13, which plays a role in regulating neurotransmitter release and is essential for normal worm movements (Brose *et al.* 1995). Munc13s are critical for synaptic vesicle exocytosis because their absence leads to strong impairment of neurotransmitter release, which is largely caused by a defect in synaptic vesicle priming (Aravamudan *et al.* 1999; Augustin *et al.* 1999; Varoqueaux *et al.* 2002). Munc13s are

also reported to play a role in synaptic vesicle docking (Augustin *et al.* 1999; Weimer *et al.* 2006; Hammarlund *et al.* 2007; Siksou *et al.* 2009).

There are three isoforms of Munc13 expressed in the brain, Munc13-1, Munc13-2, and Munc13-3. Munc13-1 is enriched in synaptosomes and localized to plasma membranes, and is not expressed in synaptic vesicles (Brose *et al.* 1995). Munc13s are large and brain specific proteins with multiple domains, including three C_2 domains (C_2A, C_2B, and C_2C), one C_1 domain, one calmodulin binding site and a large central executive domain called MUN domain (Fig 1.10 A). The C_2B domain functions as a Ca^{2+}-phospholipid binding module, while the other two C2 domains do not bind Ca^{2+} (Lu *et al.* 2006; Shin *et al.* 2010). The MUN domain is the major domain responsible for the priming activity of Munc13s, although the C_2C domain may also be involved in the activity (Basu *et al.* 2005; Madison *et al.* 2005; Stevens *et al.* 2005). Munc13-1 and Munc13-2 double knockout mice revealed no primed vesicles, and also total abrogation of spontaneous and evoked release (Varoqueaux *et al.* 2002), while the MUN domain was sufficient to rescue release in hipocampal neurons lacking Munc13-1/2 (Basu *et al.* 2005). Previous studies suggested that the C-terminal part of Munc13-1, which includes the MUN domain and C_2C, directly interacts with N-terminal part of syntaxin-1 (Betz *et al.* 1997). Another study showed that a constitutively open form of syntaxin-1 (LE mutant) partially rescued synaptic vesicle priming and neurotransmitter release in unc13 null C. elegans (Richmond *et al.* 2001). These data together suggest that Munc13 functions in priming by directly interacting to the syntaxin-1 N-terminus and thus opening the ‘closed’ conformation syntaxin-1, therefore modulating or regulation the SNARE core complex formation. However, no binding of Munc13-1 MUN domain to syntaxin-1 was observed at low micromolar concentrations (Basu *et al.* 2005). Instead, the MUN domain binds weakly to the membrane anchored SNARE four-helix bundle, the

syntaxin-1 SNARE motif, and the SNARE complex in solution through cooperation with Munc18-1 (Guan *et al.* 2008; Ma *et al.* 2011). In vitro biochemistry experiments demonstrated that the MUN domain catalyzes the opening of syntaxin-1 from the closed syntaxin-1/Munc18-1 complex to form the SNARE core complex (Ma *et al.* 2011). This transition might be mediated by MUN domain through extracting the syntaxin-1 SNARE motif from the closed conformation and providing a template for SNARE complex formation (Figure 1.10 B). However, the syntaxin-1 LE mutant can only partially rescue the release in Unc13 null C. elegans, and the LE mutant does not rescue the release in Munc13-1/2 double knockout mice (Gerber *et al.* 2008). These data suggest that MUN domain probably also plays important roles in other processes of neurotransmitter release.

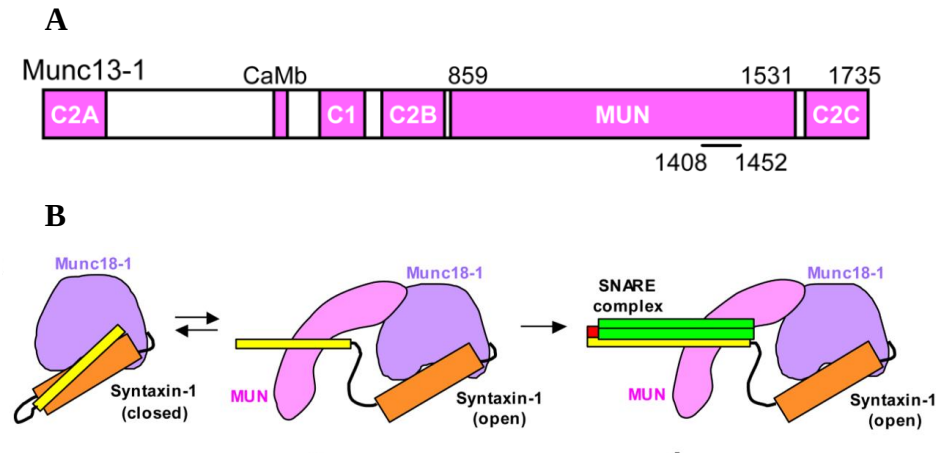

Figure 1.10 Domain diagram and functional model of Munc13-1.

(A) Domain diagram of Munc13-1. Munc13-1 comprises 1735 residues, one C2A domain at the N-terminus, one calmodulin binding site (CaMb), one C1 domain, one C2B domain, one MUN domain (residues 859-1532 with a loop from residues 1408 to 1452), and one C2C domain; (B) Functional model of Munc13-1. The Munc13-1 MUN domain mediates the transition of syntaxin-1 from the closed conformation (left panel) to the open conformation (middle panel) to allow SNARE complex formation (right panel). (Ma *et al.* 2011)

1.4.5 Complexins

Complexins are neuron specific small cytoplasmic proteins that play important roles in late stage of synaptic transmission. There are four isoforms of complexins in mammals (McMahon *et al.* 1995; Reim *et al.* 2005), and they bind tightly to the SNARE complex (Chen *et al.* 2002; Pabst *et al.* 2002; Bowen *et al.* 2005; Liu *et al.* 2006; Li *et al.* 2007). Complexin is unstructured in isolation, but it forms a central α-helix when it binds to the SNARE complex (Pabst *et al.* 2000; Chen *et al.* 2002). The crystal structure of the complexin central helix region/SNARE four-helix bundle showed complexin-I binds in an antiparallel α-helical conformation to a groove on the SNARE four-helix bundle, which is formed by syntaxin-1 and synaptobrevin helices (Figure 1.11B) (Chen *et al.* 2002). This interaction is proposed to stabilize the fully assembled SNARE complex (Chen *et al.* 2002). Later studies revealed that the N terminus of complexin-I interacts with the C terminus of the SNARE complex, which increases synaptic vesicle fusogenicty at a step after Ca^{2+}-triggered release. Disrupting this interaction abrogate the facilitatory function of complexin-I (Xue *et al.* 2010).

The function of complexins in synaptic vesicle exocytosis is complicated. Complexin null mice died at birth and showed a dramatically decreased neurotransmitter release in neurons (Reim *et al.* 2001). However, overexpression of complexin in PC12 cells inhibits exocytosis probably by preventing SNARE complex recycling (Liu *et al.* 2007). These biological data suggest that complexins play both stimulatory and inhibitory roles in synaptic transmission. The central helix of complexin is not sufficient for its function, and the N-terminus is required for its facilitation of fusion, while the regions flanking the central helix likely have an inhibitory role. So far two alternative models have been proposed to accommodate the stimulatory and inhibitory functions of complexin (Brose 2008; Sorensen 2009; Stein *et al.* 2009; Sudhof *et al.* 2009; Neher

2010). First, the complexin central helix and N-terminus binding to the SNARE four-helix bundle might stablilize the partially assembled SNARE complex, then promotes the progression of SNARE complex formation, therefore sensitizes them to activation of synaptotagmin (Jahn *et al.* 2012). Second, complexin directly competes with synaptobrevin binding to the C-terminal part of the SNARE complex (Xue *et al.* 2007; Yang *et al.* 2010; Kummel *et al.* 2011), then blocks the progression of SNARE complex formatiom and acts as a clamp that inhibits neurotransmitter release. The clamp is released by synaptotagmin upon Ca^{2+} triggering (Jahn *et al.* 2012).

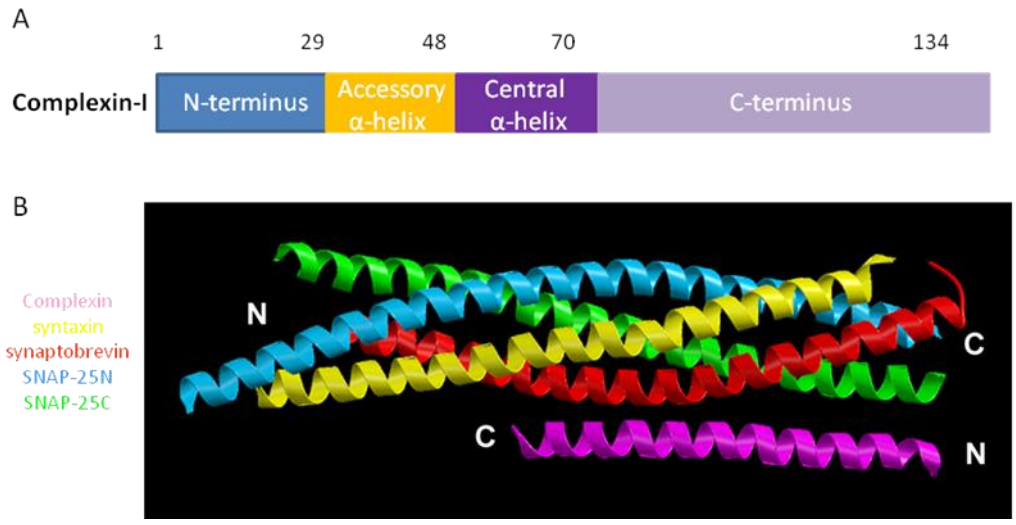

Figure 1.11 Structure of the complexin-I-SNARE complex.

(A) Domain diagram of Complexin-I. Complexin-I contains an N-terminal sequence (residues 1-29), an accessory α-helix (residues 30-48), a central α-helix (residues 49-70), and a C-terminal sequence (residues 71-134). (B) Ribbon diagram of the complexin/SNARE complex with complexin in pink, syntaxin-1 in yellow, synaptobrevin in red, SNAP-25 N-terminal SNARE motif (SNN) in blue, SNAP-25 C-terminal SNARE motif (SNC) in green. Only residues 32-72 of complexin were observable in the crystal structure. (Chen *et al.* 2002)

1.4.6 Synaptotagmins

Synaptotagmins constitute a large family of membrane trafficking proteins that consist of a short N-terminal intravesicular sequence, a transmembrane region, a short linker sequence, and two C2-domains (C2A and C2B) in their cytoplasmic region (Figure 1.12) (Bai *et al.* 2004; Sudhof 2004). There are 15 isoforms of synaptotagmins discovered so far in vertebrates (Sudhof 2002), of which synaptotagmin 1 and 2 are abundantly expressed in synaptic vesicles but differentially distributed in brain (Geppert *et al.* 1991; Ullrich *et al.* 1994). The C2 domains of eight synaptotagmins bind to Ca^{2+}, which is crucial for their functions in neurotransmitter release. Synaptotagmin binds phospholipids in a Ca^{2+} dependent manner, which suggest that synaptotagmin might be a Ca^{2+} receptor in exocytosis (Brose *et al.* 1992). Synaptotagmin 1 knockout hippocampal neurons showed severely impaired synaptic transmission, abrogation of Ca^{2+}-triggered synchronous release, but unaffected asynchronous release (Geppert *et al.* 1994). The in vivo results indicate that synaptotagmin 1 acts as a Ca^{2+} sensor for fast synchronous release, but not for asynchronous release.

Structural and biophysical studies showed that both C2A and C2B domains adopt a β sandwich structure (Figure 1.12). The C2A domain binds three Ca^{2+} ions through five conserved aspartates from the top loops of the β sandwich, while the C2B domainm binds two Ca^{2+} ions through the same conserved aspartates residues (Figure 1.12) (Ubach *et al.* 1998; Fernandez *et al.* 2001). The two C2 domains bind to Ca^{2+} ions with low affinities in solution (0.5-5mM), but the affinities for Ca^{2+} increase dramatically (up to 1000 fold) when the C2 domains bind to phospholipid membranes because of the additional coordination sites provided by the negative charged headgroups of the phospholipids (Fernandez-Chacon *et al.* 2001). However, mutations that disrupt the C2A domain binding to Ca^{2+}-phospholipids have little effect on release

(Fernandez-Chacon *et al.* 2002; Robinson *et al.* 2002; Stevens *et al.* 2003). Similar mutations on the C2B domain that disrupt its Ca^{2+}-phospholipids binding decrease evoked transmitter release by >95%, which suggests that Ca^{2+} binding to the C2B domain is essential for synaptic transmission but Ca^{2+} binding to the C2A domain is not (Mackler *et al.* 2002; Nishiki *et al.* 2004). Why the C2B domain is essential but not the C2A domain? Later in vitro experiments showed that synaptotagmin is able to bring two membranes into close proximity (~ 4 nm) upon Ca^{2+} binding, and that the C2B domain is sufficient for this activity because of the abundance of basic residues around its surface (Arac *et al.* 2006). In addition of binding to the Ca^{2+}-phospholipids, synaptotagmin also binds to the SNARE complexes in a partially Ca^{2+} dependent manner (Bennett *et al.* 1992; Chapman *et al.* 1995; Li *et al.* 1995; Shin *et al.* 2003). Together, a model for synaptotagmin function in neurotransmitter release was proposed by our group: after Ca^{2+} influx into the presynapse, synaptotagmin binds to membranes, and cooperates with the SNAREs to bring the synaptic vesicle and plasma membrane together and stimulate membrane fusion mainly through the highly positive charged C2B domain (Arac *et al.* 2006). There are other models proposed by other groups. McMahon's group proposed that: the C2 domains of synaptotagmin insert into the target membranes in response to Ca^{2+} binding, induce high positive curvature in the membranes, which lowers the energy barrier for bilayer-bilayer membrane fusion, and then trigger fusion in a SNARE-dependent manner (Martens *et al.* 2007).

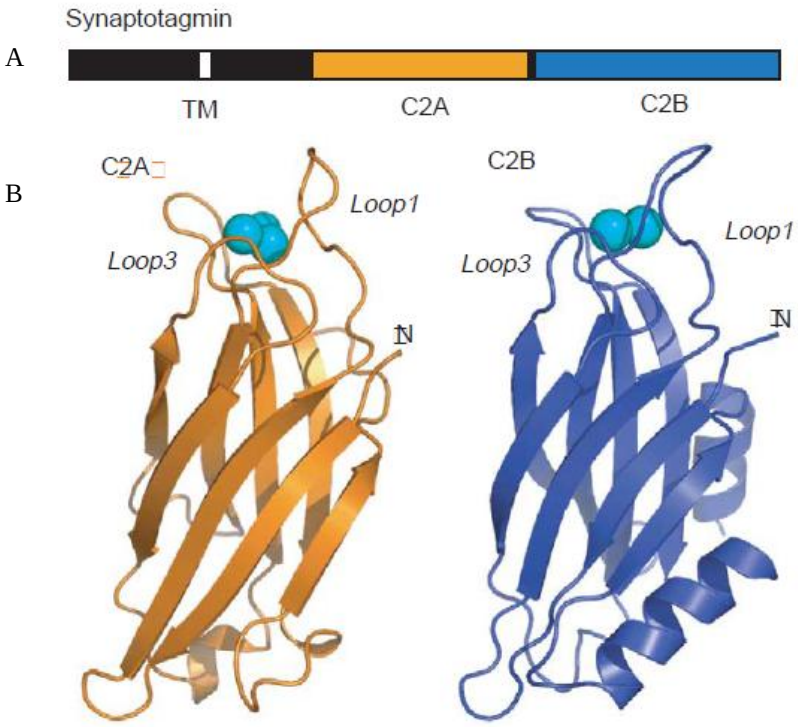

Figure 1.12 Structure of synaptotagmin-I.

(A) The domain diagram of Synaptotagmin-I. The C_2A domain is colored in orange, the C_2B domain is colored in blue, and the transmembrane domain (TM) is in black; (B) Ribbon diagrams of the individual synaptotagmine-I C_2A and C_2B domains. Ca^{2+} ions are represented by blue spheres (Rizo *et al.* 2006).

Chapter 2 Characterization of interaction between Munc18-1 and synaptobrevin

2.1 Introduction

Intracelluar membrane fusion is regulated by a conserved machinery composed of several protein families (Brunger 2005; Jahn *et al.* 2006). The most important components are soluble N-ethylmaleimide sensitive factor attachment protein receptors (SNAREs) and Sec1/Munc18 (SM) proteins, which form the core of the fusion machinery (Sudhof 2004; Verhage *et al.* 2007; Rizo *et al.* 2008). The neuronal SNAREs, synaptobrevin from synaptic vesicles, syntaxin-1 and SNAP-25 from the plasma membranes, form tight SNARE complexes that bring the two opposing membranes into close proximity and provide forces to induce membrane fusion. The neuronal SM protein Munc18-1 is essential for synaptic transmission (Verhage *et al.* 2000). A lot of research has been carried out to investigate the functions of Munc18-1, but its key role is still highly unclear.

Munc18-1 was first found to bind tightly to 'closed' syntaxin-1 (Hata *et al.* 1993), which plays a role in syntaxin-1 membrane trafficking and synaptic vesicle docking (Pabst *et al.* 2000; Arunachalam *et al.* 2008), and gates entry of syntaxin-1 into SNARE complexes (Gerber *et al.* 2008). Later, like other SM proteins, Munc18-1 was reported to bind directly to SNARE complexes and the syntaxin N-terminal sequences often contribute to this binding (Carr *et al.* 1999; Peng *et al.* 2002; Carpp *et al.* 2006; Latham *et al.* 2006; Stroupe *et al.* 2006; Dulubova *et al.* 2007; Shen *et al.* 2007). This interaction enhances SNARE-dependent lipid mixing in in vitro reconstitution assays (Shen *et al.* 2007; Rodkey *et al.* 2008) and suggests a role of Munc18-1 in assisting SNARE complex assembly after the opening of syntaxin-1, and the interaction is important for neurotransmitter release (Khvotchev *et al.* 2007). Moreover, the interactions of Munc18-1 with the syntaxin-1 Habc domain within the SNARE complex are crucial for the

synaptic vesicle priming step that makes the synaptic vesicles into a release ready state (Deak *et al.* 2009). However, none of these interactions are important for the downstream membrane fusion step. Munc18-1 and SM proteins are strictly required for general membrane fusion (Rizo *et al.* 2002), and some evidence supported a role of yeast SM protein Sec1p in a step after SNARE complex formation (Grote *et al.* 2000). These data together lead to a hypothesis that Munc18-1 might function directly in fusion besides regulates SNARE complex formation.

We proposed a model that Munc18-1 binding to the SNARE complex is more efficient in exerting mechanical force on the membranes to induce fusion than the SNARE complex alone, and this model assigns a direct role for Munc18-1 in the fusion step, which might explain the physiological requirement of Munc18-1 (Rizo *et al.* 2006). Binding of Munc18-1 to the SNARE four-helix bundle formed by the motifs of synaptobrevin, syntaxin-1 and SNAP-25 is the central aspect of this model. Some data showed that Munc18-1 indeed binds to the SNARE four-helix bundle (Dulubova *et al.* 2007; Shen *et al.* 2007), and Munc18-1 binding to synaptobrevin in the SNARE four-helix bundle is important for Munc18-1 stimulation of lipid mixing in reconstitution assays (Shen *et al.* 2007). However, no directly interaction of Munc18-1 to synaptobrevin was ever detected, and some isothermal titration calorimetry (ITC) data from another group showed that Munc18-1 interacts with the SNARE complex and syntaxin N-terminal region with similar affinities, which suggested that Munc18-1 binding to syntaxin N-terminal region is solely responsible for the SNARE complex binding (Burkhardt *et al.* 2008). Hence, it is still unclear whether Munc18-1 directly binds to synaptobrevin and the SNARE four-helix bundle. Dr. Yi Xu from the lab demonstrated that Munc18-1 binds directly to the synaptobrevin SNARE motif and the SNARE four-helix bundle at low micromolar affinities, and that the syntaxin-1 N-terminal region competes with the SNARE four-helix bundle for binding to

Munc18-1. I characterized the interaction of Munc18-1 with synaptobrevin, and made great efforts to crystallize the Munc18-1/synaptobrevin complex and solve the complex structure. However, the complex structure was not obtained at the end.

2.2 Materials and methods

2.2.1 Recombinant DNA constructs

Bacterial expression vectors to express rat Munc18-1, and fragments corresponding to the cytoplasmic regions of rat syntaxin-1A (residues 2-253) or the SNARE motifs of rat synaptobrevin-2 (29-93, 29-96, and 49-96) and human SNAP-25B (11-82 as SNN and 141-203 as SNC) as GST-fusion proteins were available in the lab (Dulubova *et al.* 2007; Xue *et al.* 2008). A vector to express squid Munc18-1 as a His-tagged protein was a kind gift from W. Weissenhorn (Bracher *et al.* 2000). Later, squid Munc18-1 was cloned into pGEX-KG vector as GST-fusion protein.

2.2.2 Expression and purification of recombinant proteins

The DNA constructs were transformed into *Escherichia coli* BL21 (DE3) cells for expression. The expression and purification of four SNARE proteins, Munc18-1 and squid Munc18-1 are similar except minor differences in the induction temperature and purification chromatography (table 2.1). First, one colony of bacteria in the transformation plate was picked into 100 ml LB with 100 μg/ml ampicillin, and was incubated in a 37 ℃ shaker at 250 rpm overnight. The next day, 15 ml of the overnight culture cells was transferred to 1 L LB media with 100 μg/ml ampicillin. The big flasks were incubated in a 37 ℃ shaker for 2.5-3 hr till OD_{600} reached 0.8-0.9. Then the temperature was lowered to 25 ℃ (for SNN, SNC, Syb, squid Munc18-1) or 20 ℃ (for Syx and Munc18-1), and 0.4 mM IPTG (isopropyl β-D-

thiogalactopyranoside, from Sigma) was added into each 1 L culture to induce protein expression. Cells were then incubated at 25 ℃ or 20 ℃ for 18-20 h to allow protein expression.

For isotopic labeled synaptobrevin-2 29-96, a similar growth and expression strategy was used except using ^{15}N M9 minimal media instead of LB. 1L ^{15}N M9 minimal media is composed of 6.8 g Na_2HPO_4, 3.0 g KH_2PO_4, 0.5 g NaCl, 2.0 mM $MgSO_4$, 100 μM $CaCl_2$, 1.0 g $^{15}NH_4Cl$ and 4.0 g D-(+)-glucose.

After expression, the cells were harvested by centrifugation at 4000 rpm for 30 minutes in swing buckets rotor (Beckman Instruments) and the cell pellets were re-suspended in 15 ml PBS buffer containing 2 mM EDTA, 2 mM EGTA, 1 mM AEBSF, and 10 μl/ml sigma inhibitor cocktail (Sigma). The cell suspension was then frozen in liquid nitrogen and then can be stored in -80 ℃ freezer for further purification.

For purification, the frozen cell suspension was thawed in a room-temperature water bath and then passed through a high pressure homogenizer (Emulsiflex C-5, Avestin Inc.) at 10,000 psi for 3 to 4 times. The lysate was then clarified by centrifugation at 20,000 rpm in a JA-20 rotor (Beckman Instruments) for 30 minutes. The supernatant was incubalted with 1.5 ml (each liter cell culture) prewashed glutathione sepharose beads (Amersham Pharmacia Biotech.) at 4 ℃ overnight or 3 hr at room temperature to allow the GST-fusion protein binding to the glutathione beads. Sepharose 4B beads were prewashed with at least 10 bed volumes of H_2O and then PBS. After incubation, the supernatant and beads mixture was then run through a gravity flow chromatography column (Bio-Rad) to remove most of non-binding proteins. The beads were then successively washed with 100 ml PBS containing 1% triton X-100, 1 M NaCl, and PBS to remove non-specific bound proteins. Then benzonase was used to remove protein-bound

DNA. Beads were washed with Benzonase buffer (50 mM Tris pH 8.0, 2 mM $MgCl_2$) and then incubated with 10 units per liter culture Benzonase at room temperature for 1 hr to digest bound DNA. After Benzonase treatment, the beads were washed with PBS, equilibrated with thrombin cleavage buffer (50 mM Tris pH 8.0, 150 mM NaCl, 2.5 mM $CaCl_2$), and then incubated with 3-5 units of thrombin at room temperature for two hours or at 4 ℃ overnight to cleave proteins from GST tag. After thrombin cleavage, the flow through was collected and purified through a Superdex 75 HiLoad 16/60 size exclusion chromatography column (Amersham Pharmacia Biotech.). For syntaxin-1 (2-253) and synaptobrevin-2 (29-96), proteins were first purified by ion exchange chromatography (Source Q and Source S). Briefly, a linear gradient of salt (0-1 M NaCl) was used to separate the protein from other proteins. Then size exclusion chromatography was performed. The purity of the fractions of proteins was assessed by SDS-PAGE and Coomassie blue staining. The right protein fractions were collected and concentrated to a desired concentration, and protein inhibitors containing 1 mM 1:100 Sigma Inhibitor cocktail, 1 mM AEBSF, 2 mM EDTA, 2 mM EGTA, and 2 mM TCEP were added. Small aliquots of proteins were made, and were frozen in liquid nitrogen and stored at -80 ℃. A typical yield was 3-5 mgs per liter of culture.

SNARE complexes were assembled and purified as described (Chen *et al.* 2002; Dulubova *et al.* 2007; Deak *et al.* 2009). A C-terminal fragment of synatobrevin-2 (77-96) was synthesized as a peptide in UTSouthwestern Medical Center protein chemistry facility.

	Induction Temperature	Purification Chromatography
SNN	25 ℃	Superdex75
SNC	25 ℃	Superdex75
Syb(29-93)	25 ℃	Superdex75
Syb(29-96)	25 ℃	Source S, Superdex75
Syb(49-96)	25 ℃	Superdex75
Syx(2-253)	20 ℃	Source Q, Superdex75
Munc18-1	25 ℃	Source Q, Superdex200
Squid Munc18-1	25 ℃	Source S, Superdex75

Table 2.1 The specific information for expression and purification of the SNARE proteins and Munc18-1.

2.2.3 Chemical cross-linking

17uM Rat Munc18-1 and 1X, 2X, 5X synaptobrevin (29-96) were incubated with 5 mM 1-Ethyl-3-[3-dimethylaminopropyl]carbodiimide (EDC) or 1 mM Bis (sulfosuccinimidyl) suberate (BS3) in 20mM HEPES pH7.2 200mM KCl for 1 hr at room temperature, and then quenched with 25 mM Tris, pH8.0. 8ul of samples, Munc18-1 alone, synaptobrevin (29-96) alone and Munc18-1 with synaptobrevin were loaded to SDS gels for PAGE. The cross-linked bands in the gel were cutted and sent for LC-MS-MS analysis.

2.2.4 1H-15N Heteronuclear Single Quantum Coherence (HSQC) Experiments

^{1}H-^{15}N HSQC spectra of ^{15}N Synaptobrevin (29-96) were recorded on Varian INOVA600 spectrometers at 25 ℃. 40 μM ^{15}N synaptobrevin(29-96) without and with 40 μM squid Munc18-1 in 20mM HEPES (pH 7.2) and 120 mM KCl were used in the HSQC experiments.

2.2.5 Isothermal Titration Calorimetry (ITC) Experiments

ITC experiments were performed using a VP-ITC (MicroCal, Northhampton, MA) calorimeter at 20 ℃. Squid Munc18-1 and synaptobrevin(49-96) or synaptobrevin(77-96) were prepared in a buffer containing 20 mM HEPES (PH7.4) and 100 mM KCl. 0.4 mM synaptobrevin(49-96) or 0.5 mM synaptobrevin(77-96) was successively injected 20 μM squid Munc18. The data were fitted with a nonlinear least squares routine using a single-site binding model with MicroCal Origin^{TM} software for ITC version 5.0.

2.2.6 Gel filtration binding assay

Purified 5 μM 400 μl Munc18-1, 6 μM 400 μl syntaxin-1 (2-253), 6 μM 400 μl SNARE complex composed of Syx(2-253), Syb(29-93), SNN, and SNC in a buffer containing 20 mM Tris, pH7.4, and 120mM NaCl were injected to a Superdex S200 (10/300GL) column to get gel filtration profiles of these proteins alone. 400 μl complex samples containing 5 μM Munc18-1 and 6 μM SNARE complexes or 6 μM syntaxin-1 (2-253) were incubated on ice for 30 minutes, and then injected into the column to detect complex formation. Data were analyzed by UNICORN 5.01 (Amersham Biosciences).

2.2.7 Carr Purcell Meiboom Gill (CPMG) experiments

Unlabeled 50 μM squid Munc18-1, 50 μM synaptobrevin (77-96), and 50 μM squid Munc18-1 with 50 μM synaptobrevin (77-96) were used to record methyl regions of 1D ^{1}H NMR spectra without (^{1}H-NMR) and with application of a Carr Purcell Meiboom Gill (CPMG)

sequence for 100 ms (CPMG 100 ms). Data were used to analyze the binding of synaptobrevin (77-96) to squid Munc18-1.

2.2.8 Crystallization of squid Munc18-1 and squid Munc18-1 with synaptobrevin (77-96)

Purified squid Munc18-1 was concentrated to 10 mg/ml in 20 mM HEPES, pH 7.4, 100 mM KCl, 10 mM DTT, and then was used to set up crystallography trays. Initial screening conditions were adapted and modified from squid Munc18-1 crystallization paper (Bracher *et al.* 2000) using hanging drop trays. Later, optimization of conditions was performed to get nice and single crystals (6%-8% PEG 1,000, 0.4 M ammonium sulfate, 0.1 M sodium citrate pH 6.6-7.6, 10 mM $CaCl_2$, and 10 mM DTT at 20 ℃ and 20 mM HEPES, pH 7.4, 100 mM KCl, 10 mM DTT at 4 ℃). 1mM synaptobrevin peptide (77-96) was added to nice and single crystals in cryo buffer overnight to soak synaptobrevin peptide into sMunc18-1 crystals. For sMunc18-1 and synaptobrevin (77-96) co-crystallization, 9.3 mg/ml sMunc18-1 was mixed with 1 mM peptide, and the mixture was incubated at room temperature for 1 hour. Crystallization screening was performed with the mixture using screens from Hampton Research. Some crystals were optimized using additive screen from Hampton Research.

2.3 Results

2.3.1 Munc18-1 domain 3a binds to the C-terminus of the SNARE motif of synaptobrevin (29-96)

Dr. Yi Xu found that Munc18-1 interacts with the SNARE motif of synaptobrevin (29-96) with an affinity of 6uM. However, we didn't know which part of Munc18-1 and synaptobrevin (29-96) bind to each other. To find out the residues involved in binding, I first performed chemical cross-linking experiments between WT Munc18-1 and synaptobrevin (29-96). Two kinds of cross-linkers were used: EDC, which links close carboxyl groups with primary amines, and BS3, which cross-links close primary amines with primary amines. No cross-linking was

observed in EDC reactions even when 5 times excess of synaptobrevin (29-96) was added (Fiure 2.1A). However, BS3 was able to cross-linking Munc18-1 and synaptobrevin (29-96) in all concentrations of synaptobrevin (Figure 2.1A). LC-MS-MS analysis of one of the cross-linked products from the gel revealed that one peptide of synaptobrevin (KYWWK, residues 87-91) was cross-linked to a sequence of Munc18-1 (KMPQYQK, residues 333-339). These sequences were mapped to a helix in domain 3a of Munc18-1 located in the cavity where syntaxin-1 binds and to the very C-terminus of synaptobrevin SNARE motif (Figure 2.1B), which is adjacent to the synaptic vesicle membrane.

To confirm the binding site on synaptobrevin with a more accurate method, Dr.Yi Xu performed ^{1}H-^{15}N heteronuclear single quantum coherence (HSQC) experiments of 5 μM ^{15}N-labeled synaptobrevin(29-96) in the presence and absence of 6 μM rat Munc18-1. The HSQC spectra suggested that Munc18-1 indeed binds to the C-terminus of synaptobrevin, however, the quality of the data was not very good because of insolubility of rat Munc18-1 in 120 mM salt. Hence, I turned to use squid Munc18-1 (sMunc18-1) which behaves much better than rat Munc18-1 *in vitro*. Moreover, squid Munc18-1 shares high identify both sequentially (66.4%) and structurally to rat Munc18-1 (Bracher *et al.* 2000).

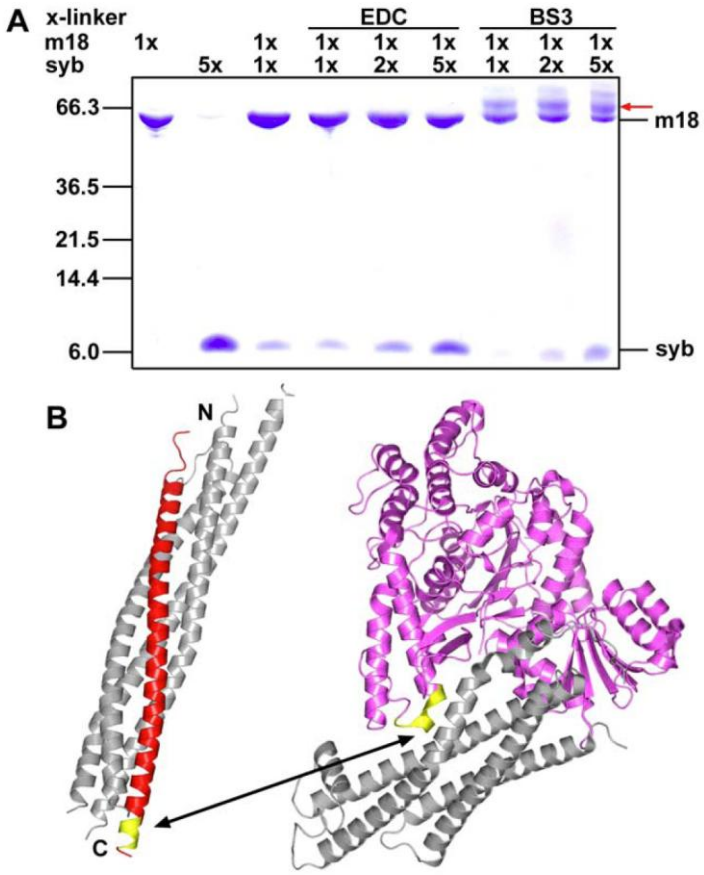

Figure 2.1 Cross-linking of synaptobrevin and Munc18-1

(A) SDS−PAGE of samples containing synaptobrevin(29−96), Munc18-1, or both after cross-linking with EDC or BS3. The relative concentrations of both proteins are indicated above the lanes. The positions of molecular mass markers are indicated at the left. The red arrow at the right indicates the position of the cross-linked product.

(B) Ribbon diagrams of the crystal structure of the SNARE complex (Sutton 1998) and the Munc18-1−syntaxin-1 complex (Misura et al., 2000) with synaptobrevin colored red and Munc18-1 colored purple (other proteins colored gray). The sequences of synaptobrevin and Munc18-1 that were cross-linked are colored yellow.

2.3.2 Squid Munc18-1 binds to the C-terminus of synaptobrevin (29-96) with similar affinity

Squid Munc18-1 co-elutes with the cytoplamic domain of rat syntaxin-1 (2-253) and with mammalian SNARE complex (Figure 2.2), which suggests that sMunc18-1 binds tightly to the mammalian SNAREs and functions like rat Munc18-1 *in vitro*. Hence, I used this protein in the following experiments. To find out exactly which residues in synaptobrevin (29-96) are involved in Munc18-1 binding, we acquired HSQC spectra of 40 μM ^{15}N synaptobrevin (29-96) in the absence and presence of 40 μM sMunc18-1. Synaptobrevin (29-96) is unstructured in solution (Hazzard *et al.* 1999), so the cross-peaks of the residues are very sharp by itself. The residues involved in interaction would be broadened due to binding to a large protein like sMunc18-1 (70 KDa), behaving like sMunc18-1, while other residues would remain flexible and would have no change in their cross-peaks. The results indeed showed selective broadening of some specific cross-peaks of synaptobrevin (29-96) upon sMunc18-1 addition (Figure 2.3A). Those cross-peaks correspond to the C-terminal residues (75-95) of synaptobrevin (29-96) (Figure 2.3B), which correlates well with the cross-linking results obtained with rat Munc18-1. The results also showed that synaptobrevin residues 60-70, which were previously suggested to mediate the SNARE complex dependent Munc18-1 enhancement of liposomes lipid mixing (Shen *et al.* 2007), are not involved in sMunc18-1 binding by itself.

We also wanted to find out which residues of Munc18-1 interact with synaptobervin (29-96), but NMR experiments were hindered by the large molecular weight of Munc18-1. We turned to use crystallography, intending to get the X-ray structure of the sMunc18-1/synaptobrevin complex. Since synaptobrevin C-terminus is responsible for Munc18-1 binding, we obtained a synthetic peptide including residues 77-96 of synaptobrevin for crystallography. To assure that the peptide synaptobrevin (77-96) still binds to sMunc18-1, I recorded 1D ^{1}H

NMR spectra of sMunc18-1 alone, peptide alone, and a mixture of the peptide and sMunc18-1 without and with application of a Carr−Purcell−Meiboom−Gill (CPMG) pulse sequence for 100 ms. Large proteins like sMunc18-1 relax much faster than small peptides like synaptobrevin (77-76) upon CPMG application. If the peptide binds to sMunc18-1, the mixture behaves like sMunc18-1; otherwise the mixture behaves like the peptide. Within 100 ms, the CPMG sequence leads to almost complete relaxation of the sMunc18-1 methyl signals, and also the mixture of sMunc18-1 and synaptobrevin peptide, but not the synaptobrevin peptide alone (Figure 2.4), which indicates that the synaptobrevin C-terminus alone indeed binds to sMunc18-1. In addition, I also measured the affinity of this peptide (77-96) and another fragment of synaptobrevin (49-96) to sMunc18-1 using ITC. The results showed Kd values of 13.5 and 13.3 μM for binding of the peptide and synaptobrevin (49-96) to sMunc18-1 (Figure 2.3C,D). These values are comparable to the Kd values (obtained by Dr. Yi Xu) obtained by FRET for binding of rat Munc18-1 to synaptobrevin(1-96), and their similarity confirms that the C-terminus of the SNARE motif is responsible for synaptobrevin binding to Munc18-1. Hence, the synaptobrevin peptide (77-96) was used for following crystallography experiments.

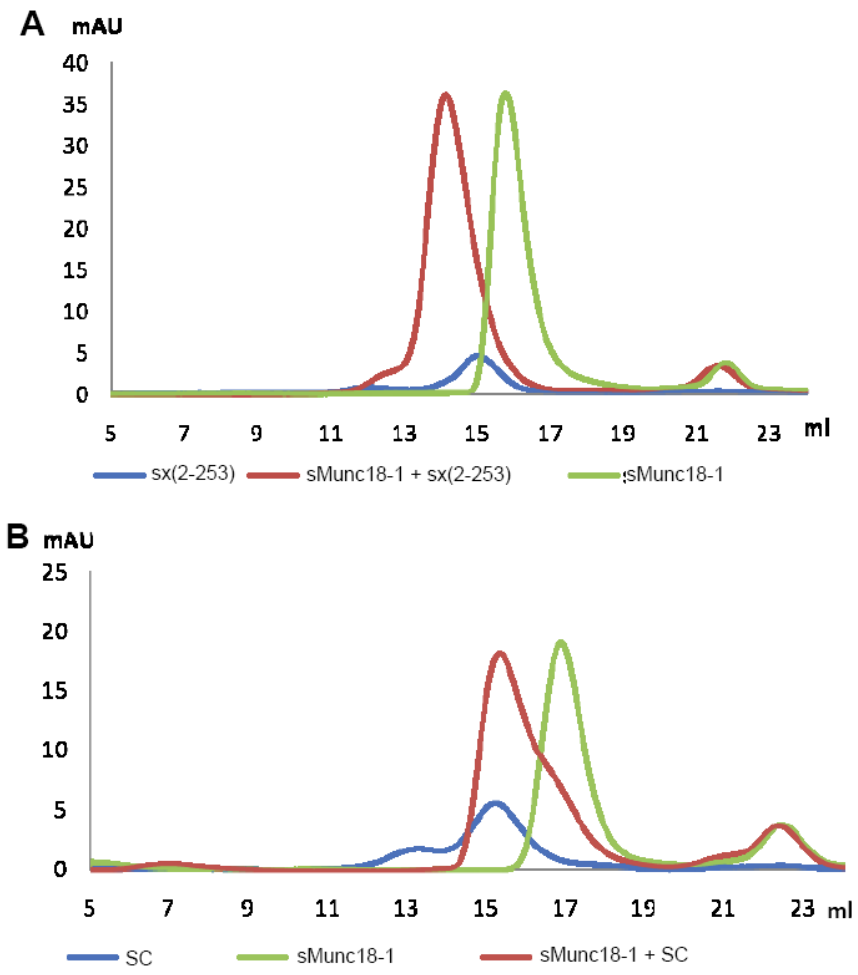

Figure 2.2 sMunc18-1 binds to mamalian syntaxin-1 and SNARE complex.

(A,B) Gel filtration profiles on Superdex 200 10/30HR (Amersham) of sMunc18-1 alone (green) or mixed with rat syntaxin-1(2-253) (red, panel A) or SNARE complex formed with rat syntaxin-1(2-253) and the SNARE motifs of rat synaptobrevin and human SNAP-25 (red, panel B). In blue are shown the controls with rat syntaxin-1(2-253) alone (A) or SNARE complex alone (B). The shifts in the elution profiles of sMunc18-1 observed in both cases demonstrate binding to the mammalian syntaxin-1 and SNARE complex.

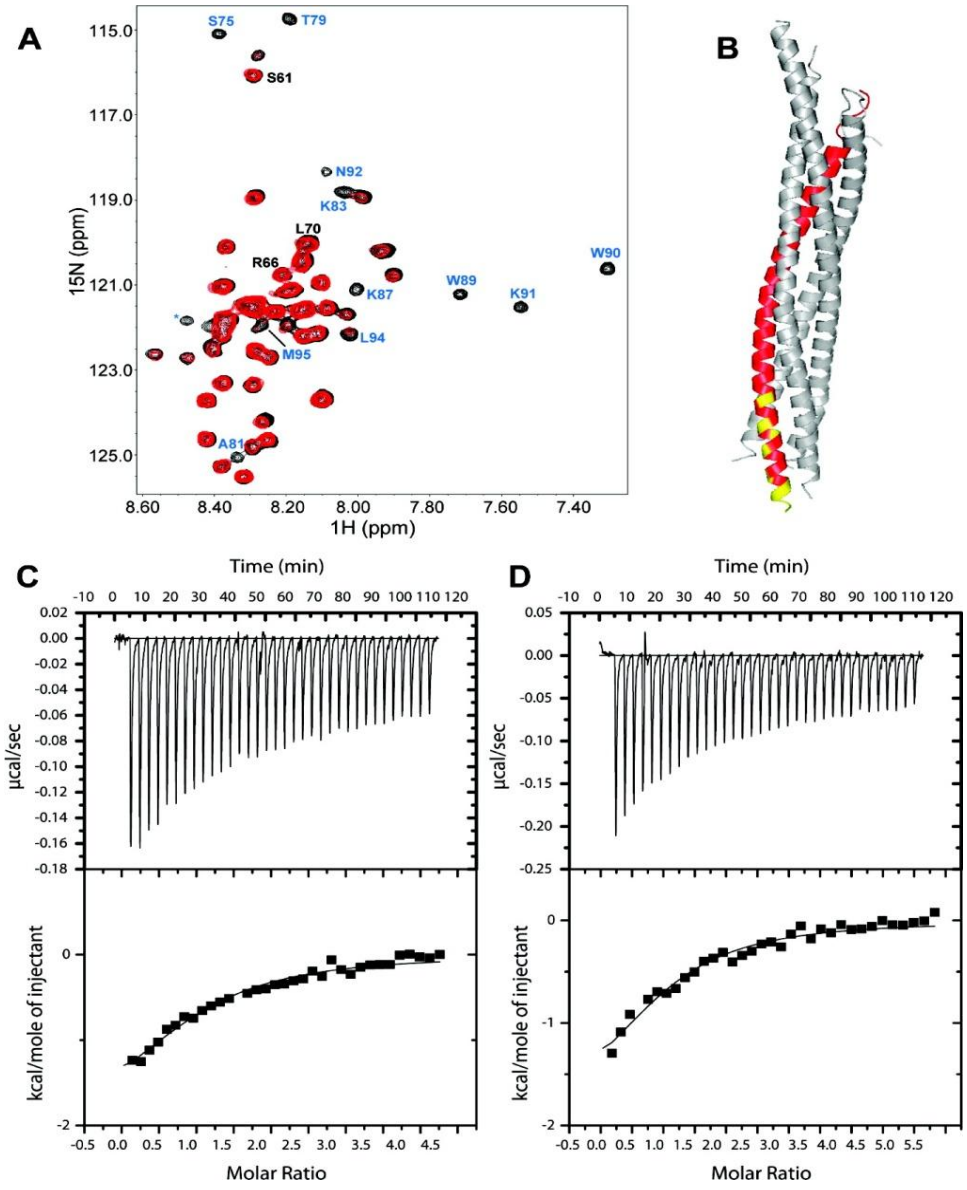
A
S75
T79
S61
N92
K83
L70
R66
K87
W89
K91
W90
L94
M95
A81
15N (ppm)
1H (ppm)
B
C
Time (min)
µcal/sec
kcal/mole of injectant
Molar Ratio
D
Time (min)
µcal/sec
kcal/mole of injectant
Molar Ratio

Figure 2.3

Figure 2.3 sMunc18-1 binds to the C-terminus of the synaptobrevin SNARE motif.

(A) 1H-15NHSQC spectra of 40 μMsynaptobrevin(29-96) in the absence (black) and presence (red) of 40 μMsMunc18-1.Well-resolved cross-peaks that were strongly broadened and correspond to residues at the C-terminus of the synaptobrevin SNARE motif are labeled in blue. Three well-resolved cross-peaks that do not exhibit such strong broadening and correspond to the region spanning residues 60-70 are labeled in black. (B) Ribbon diagram of the SNARE complex with synaptobrevin colored red; residues corresponding to the cross-peaks labeled in blue in panel A are colored yellow. (C and D) ITC analysis of binding of synaptobrevin(49-96) (C) or synaptobrevin(77-96) (D) to sMunc18-1.

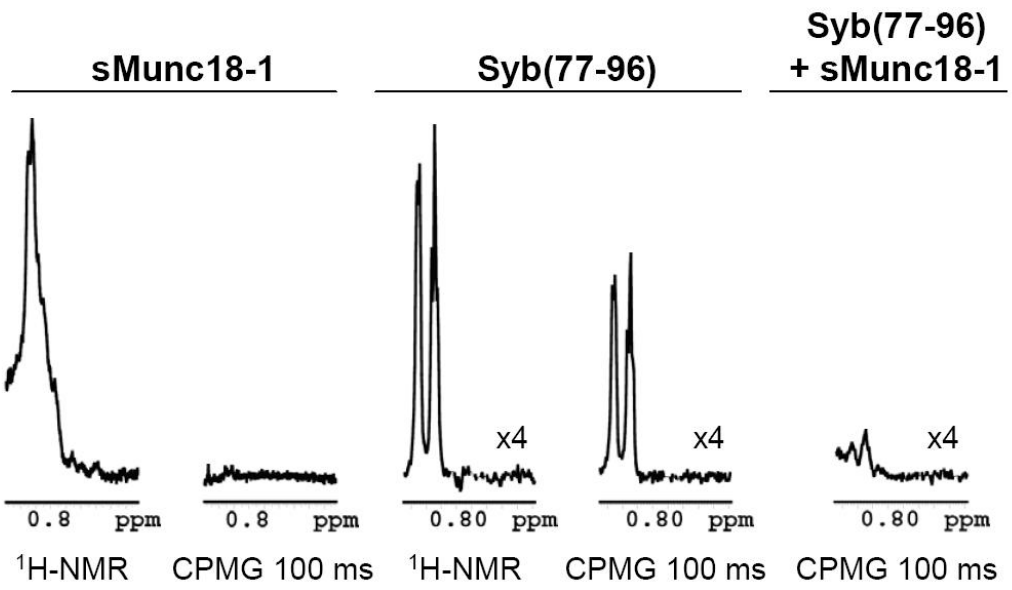

Figure 2.4 1D NMR spectra of sMunc18-1 binding to synaptobrevin 77-96.

Methyl regions of 1D ^{1}H NMR spectra without (^{1}H-NMR) and with application of a Carr Purcell Meiboom Gill (CPMG) sequence for 100 ms (CPMG 100 ms) of samples containing 50 µM sMunc18-1, or 50 µM synaptobrevin(77-96) or both. The vertical scale of the three spectra on the right was increased four-fold compared to the two spectra on the left because the peptide has much weaker signal than sMunc18-1. The CPMG sequence allows T2 relaxation during the 100 ms delay and leads to almost complete relaxation of the sMunc18-1 methyl signals because of the large size of this protein, while only a moderate reduction of the methyl signals of the synaptobrevin(77-96) peptide is observed because of its much smaller size. However, the methyl signals of the sMunc18-1/synaptobrevin(77-96) mixture are strongly decreased during the 100 ms CPMG period, showing that the peptide indeed binds to sMunc18-1.

2.3.3 Crystallization of synaptobrevin (77-96) with sMunc18-1

Since sMunc18-1 can be crystallized, I used two different methods to get the complex structure of sMunc18-1 and the synaptobrevin peptide (77-96): crystallize sMunc18-1 first and soak the peptide into the sMunc18-1 alone crystals; or mix sMunc18-1 and the peptide, then co-crystallize the mixture; and then solve the structure of the crystals from the two methods to look for peptide densities in the structure. We got the sMunc18-1 plasmid from W. Weissenhorn (Bracher *et al.* 2000). It is a His-tagged protein in the pQE vector 30, and has a maximum yield of 2 mg/L LB culture. At first, I got some thin crystals of sMunc18-1 alone (Figure 2.5A,B) in conditions including 10% PEG 1000, 0.4 M ammonium sulfate, 0.1 M sodium citrate pH 6.6 and 7.6, 20 mM DTT, 10 mM $CaCl_2$, and 6 mg/ml sMunc18-1. I tried to soak the crystals with 100 μM and 1mM peptide at 20 ℃ for 24 hours. Some crystals sustained after soaking and some did not. Those crystals that survived (Figure 2.5C,D) were sent to synchrotron to collect diffraction data. They initially diffracted to 3.2 Å, but failed to give diffraction after a while because they were too small and too thin. Later, sMunc18-1 was cloned into a pGEX-KT vector without His-tag, and it had a much higher yield (10 mg/ml). Crystallization of the proteins expressed with this new construct yielded bigger and thicker single crystals (Figure 2.6A,B) in similar conditions containing 6%-8% PEG 1000, 0.4 M ammonium sulfate, 0.1 M sodium citrate pH 6.6 and 7.6, 20 mM DTT, 10 mM $CaCl_2$, and 10 mg/ml sMunc18-1, and they diffracted to 3.5 Å in house. The nice and single crystals were soaked with 100 μM and 1mM peptide at 20 ℃ for 24 hours (Figure 2.6C,D). The best crystal diffracted to 3.4 Å in house, and a complete data set was collected. Isomorphous replacement was used to solve the structure. However, no synaptobrevin peptide densities were found. To co-crystallize sMunc18-1 and the peptide, 9.3 mg/ml sMunc18-1 and 1mM synaptobrevin peptide mixture was used for screening. Some crystals were obtained,

but they were not very nice (Figure 2.6E). After additive screen, nicer crystals were obtained (Figure 2.6F), and they diffracted to 4 Å in synchrotron. However, no peptide densities were found after solving the structure.

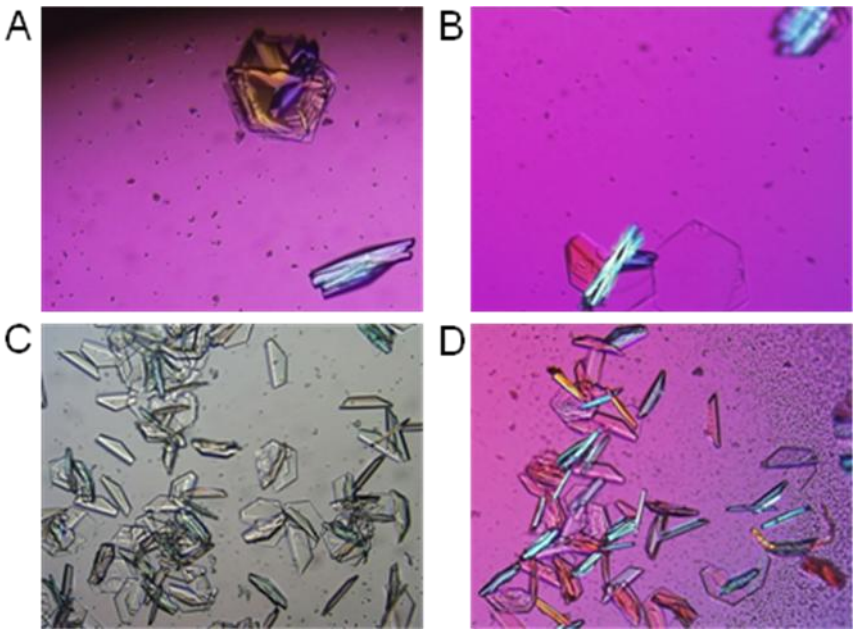

Figure 2.5 Crystallization of sMunc18-1 and sMunc18-1 with synaptobrevin peptide.

(A)(B) sMunc18-1 alone crystals in the following conditions: 10% PEG 1000, 0.4 M ammonium sulfate, 0.1 M sodium citrate pH 6.6 (A) and pH 7.6 (B), 20 mM DTT, 10 mM $CaCl_2$; (C)(D) sMunc18-1 crystals soaked with 100 μM (C) and 1mM (D) synaptobrevin peptide after 24 hours.

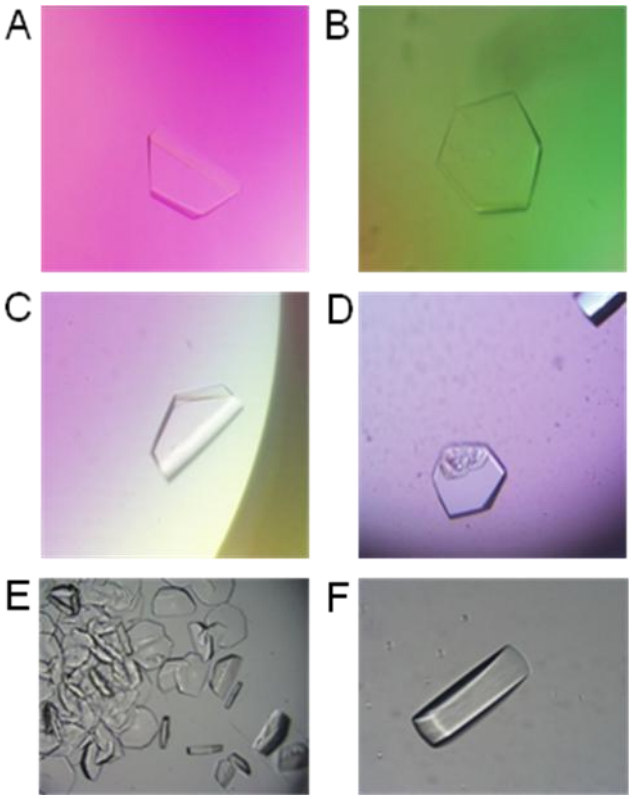

Figure 2.6 Crystallization of sMunc18-1 expressed with the new construct and sMunc18-1 with synaptobrevin peptide.

(A)(B) Crystals of sMunc18-1 alone in the following conditions: 7% PEG 1000, 0.4 M ammonium sulfate, 0.1 M sodium citrate pH 6.6 (A) and 7.6 (B), 20 mM DTT, 10 mM $CaCl_2$; (C)(D) sMunc18-1 crystals soaked with 100 μM (C) and 1mM (D) synaptobrevin peptide after 24 hours. (E) Crystals from co-crystallization of sMunc18-1 with 1mM peptide; (E) The crystal after additive screen of the mixture of sMunc18-1 and 1 mM peptide.

2.4 Discussion

SM proteins and SNAREs are the two central components of the intracellular membrane fusion machinery. The roles of SNAREs are well defined, but the main role of SM proteins is still highly unclear. This uncertainty arises in part because of the diversity of SM protein/SNARE interactions that have been identified, and in part because no definitive evidence has been presented for the various models of SM protein function that have been proposed. To explain the very strong inhibition in membrane fusion observed in the absence of SM proteins (Rizo *et al.* 2002; Verhage *et al.* 2007) , one of these models predicted that SM proteins bind to the SNARE four-helix bundle, enabling application of force to the membranes by the SNAREs (Rizo *et al.* 2006). Previous reconstitution experiments showed that Munc18-1 can strongly enhance SNARE dependent lipid mixing and suggested that this ability depends on Munc18-1/synaptobrevin interactions, but no biochemical evidence for such interactions was described (Shen *et al.* 2007). Dr. Yi Xu from the lab showed that Munc18-1 binds directly to both synaptobrevin and the SNARE four-helix bundle with an affinity in the low micromolar range. Her data suggest that these interactions involve the same cavity of Munc18-1 where the closed syntaxin-1 binds. Furthermore, Dr. Yi Xu and I together find that the C-terminus of synaptobrevin is responsible for Munc18-1 binding, placing Munc18-1 right at the site where membrane fusion occurs. These results reinforce the notion that Munc18-1, and SM proteins in general, play a direct role in membrane fusion, and suggest a model whereby a sequence of distinct Munc18-1/SNARE interactions occurs during synaptic vesicle exocytosis (Figure3.7)

Several of the models proposed for SM protein function may be at least partially correct, since SM proteins may play several roles in distinct steps, but the key unanswered question is: why are SM proteins so critical for membrane fusion? The initial finding that Munc18-1 binds to

syntaxin-1 led to the proposal that Munc18-1 forms part of the synaptic vesicle fusion machinery (Hata *et al.* 1993). This overall notion is now supported by overwhelming evidence, but the binary Munc18-1/syntaxin-1 interaction stabilizes the closed conformation of syntaxin-1 and gates entry of syntaxin-1 into SNARE complexes (Dulubova *et al.* 1999; Yang *et al.* 2000; Chen *et al.* 2008; Gerber *et al.* 2008). Nevertheless, this binary interaction might play positive roles by stabilizing both proteins in vivo (Verhage *et al.* 2000; Gerber *et al.* 2008), and by assisting in vesicle docking, since syntaxin-1 and Munc18-1 play a role in docking in chromaffin cells, while synaptobrevin does not (Gerber *et al.* 2008). Importantly, overexpression of SNAP-25 rescues the docking defect in chromaffin cells from Munc18-1 KO mice, likely by promoting formation of syntaxin-1/SNAP-25 heterodimers that bind to synaptotagmin-1, but does not rescue the secretion defect (de Wit *et al.* 2009). Hence, Munc18-1 must play an additional function downstream of docking and syntaxin-1/SNAP-25 heterodimer assembly. There is in fact evidence for participation of Munc18-1 in more than one of the steps that lead to exocytosis (Gerber *et al.* 2008; Guan *et al.* 2008; De ák *et al.* 2009).

Although Munc18-1 binding to closed syntaxin-1 hinders SNARE complex formation from an energetic point of view (Chen *et al.* 2008), Munc18-1 could still play a role in assisting SNARE complex assembly in downstream events (Dulubova *et al.* 1999; Misura *et al.* 2000; Rizo *et al.* 2008). Indeed, Munc18-1 enhances assembly of SNARE complexes between co-expressed syntaxin-1/SNAP-25 heterodimers and synaptobrevin, which might underlie the stimulation of SNARE-dependent lipid mixing in reconstitution assays and depends on binding of Munc18-1 to the syntaxin-1 N-terminus (Shen *et al.* 2007). Since the co-expressed heterodimers appear to be in an inhibited state where the Habc domain hinders full interactions between the SNARE motifs (Starai *et al.* 2008), it seems likely that Munc18-1 helps to disinhibit

this state by binding to the syntaxin-1 N-terminal region. It is unclear whether these events are related to the mechanism of neurotransmitter release in vivo, but in any case there is little doubt that interactions of Munc18-1 with the syntaxin-1 N-terminal region are important for release (Khvotchev *et al.* 2007; Deák *et al.* 2009). However, these interactions do not appear to play a role after vesicle priming (Deák *et al.* 2009). In addition, it seems unlikely that a mere role for Munc18-1 in assisting SNARE complex assembly can explain its essential nature for neurotransmitter release (Verhage *et al.* 2000), since SNARE complexes can be readily assembled in vitro. In addition, stimulation of SNARE-dependent lipid mixing by Munc18-1 appears to depend on interactions with synaptobrevin (Shen *et al.* 2007), and some evidence indicates that the SM protein Sec1p plays a key role in exocytosis downstream of SNARE complex formation (Grote *et al.* 2000).

These observations suggest that the key function of Munc18-1 and SM proteins in membrane fusion involves interactions with the SNARE four-helix bundle, as initially inferred for Sec1p (Carr *et al.* 1999) and as predicted by our previous model of how SM proteins and SNAREs form the core fusion machinery (Rizo *et al.* 2006). Some results suggested the existence of such interactions (Togneri *et al.* 2006; Dai *et al.* 2007; Dulubova *et al.* 2007; Maximov *et al.* 2009), but ITC data indicated that Munc18-1 binding to the SNARE complex involves binding to only the syntaxin-1 N-terminal region (Burkhardt *et al.* 2008), and direct binding of SM proteins to the isolated SNARE four-helix bundle has not been reported. Our results now show unambiguously that Munc18-1 indeed binds to the SNARE four-helix bundle and to the very C-terminus of the synaptobrevin SNARE motif. It seems very likely that both interactions involve the same residues, since they have similar affinities and synaptobrevin competes with the SNARE four-helix bundle for Munc18-1 binding. Dr. Yi Xu's data also

provide strong evidence that these interactions involve the cavity of Munc18-1 where closed syntaxin-1 binds, which explains the ITC data obtained with Munc18-1 and the SNARE complex (Burkhardt *et al.* 2008). These results need to be interpreted with caution, since the interactions we report have moderate affinity and their physiological relevance remains to be established. However, the finding that Munc18-1 binds to the very C-terminus of the synaptobrevin SNARE motif is very intriguing, since it places Munc18-1 right at the site of fusion and hence suggests a fundamental new view whereby Munc18-1 is intimately and directly involved in fusion. Such a role could certainly explain the critical nature of Munc18-1 and SM proteins for membrane fusion in vivo.

The original idea of how Munc18-1 could help to induce fusion (Rizo *et al.* 2006; Rodkey *et al.* 2008) was intended to provide such an explanation and was based on a simple mechanical principle: flexibility in the linker region between the SNARE motifs and TM regions could hinder transduction of the energy of SNARE complex assembly onto the membranes and allow assembled SNARE complexes to diffuse to the middle of the interrmembrane space; however, binding of a bulky protein such as Munc18-1 to assembling SNARE complexes would prevent such diffusion and would help applying torque on the two membranes to induce fusion, because Munc18-1 would push the membranes away while SNARE complexes bring them together. Note that the torque would be weakest if Munc18-1 binds to the N-terminus of the SNARE four-helix bundle and strongest if the binding site is at the C-terminus, as suggested by our data. Indeed, it seems impossible that SNARE complexes could form without fusion if Munc18-1 is bound to their C-termini (even if there is some flexibility in the linker regions). Moreover, Munc18-1 contains two highly positive surfaces surrounding the SNARE-binding cavity. These surfaces could bind to the two apposed membranes and actively help to bend them

to induce fusion (Figure 3.7), as proposed for synaptotagmin-1 (Arac *et al.* 2006). In this context, only weak binding of Munc18-1 to liposomes has been reported (Starai *et al.* 2008), but such interactions could be greatly strengthened by the intrinsic cooperativity of the system.

We proposed a model that involves three different types of interactions of Munc18-1 with the SNAREs (Figure 3.7): first the binary interaction with closed syntaxin-1; second the interaction with the N-terminal region of syntaxin-1 as syntaxin-1 opens and SNARE complexes start to form via by the help of Munc13 (Guan *et al.* 2008; Ma *et al.* 2011); and third the binding to the C-terminus of synaptobrevin. Although the affinity of Munc18-1 for synaptobrevin is moderate, and weaker than its affinity for the syntaxin-1 N-terminal regions in binding assays with isolated proteins, the transition from syntaxin-1 to synaptobrevin binding could be favored by strong cooperativity with the proposed interactions of Munc18-1 with both membranes, which would bring the membranes together and could therefore cooperate, in addition, with the pulling forces of the assembling SNARE complexes. Moreover, membranes appear to enhance binding of Munc18-1 to the SNARE four-helix bundle (Shen *et al.* 2007) and the functional importance of the synaptobrevin region that binds to Munc18-1 has been shown by the impairment in neurotransmitter release caused by mutation of two tryptophane residues in this region (Maximov *et al.* 2009), although the molecular target of this region in vivo remains to be determined. Candidates for such targets are also Munc13s, complexins and syntaptotagmin-1, factors that play key roles in neurotransmitter release and also bind to the SNARE four-helix bundle (Chen *et al.* 2002; Dai *et al.* 2007; Guan *et al.* 2008). These factors could provide additional cooperativity to the system, but they might also compete with Munc18-1 for binding to the four-helix bundle.

Clearly, our model remains highly speculative, and to better understand the mechanisms of membrane fusion and neurotransmitter release, it will be particularly important to study the interplay between the interactions among all these proteins and the lipids in the context of trans-SNARE complexes formed between two apposed membranes. The data generated by Dr. Yi Xu and the ones presented here have now yielded a hypothesis that can help guiding these very challenging studies and proposes a fundamentally new view of how Munc18-1 might cooperate with the SNAREs to induce membrane fusion.

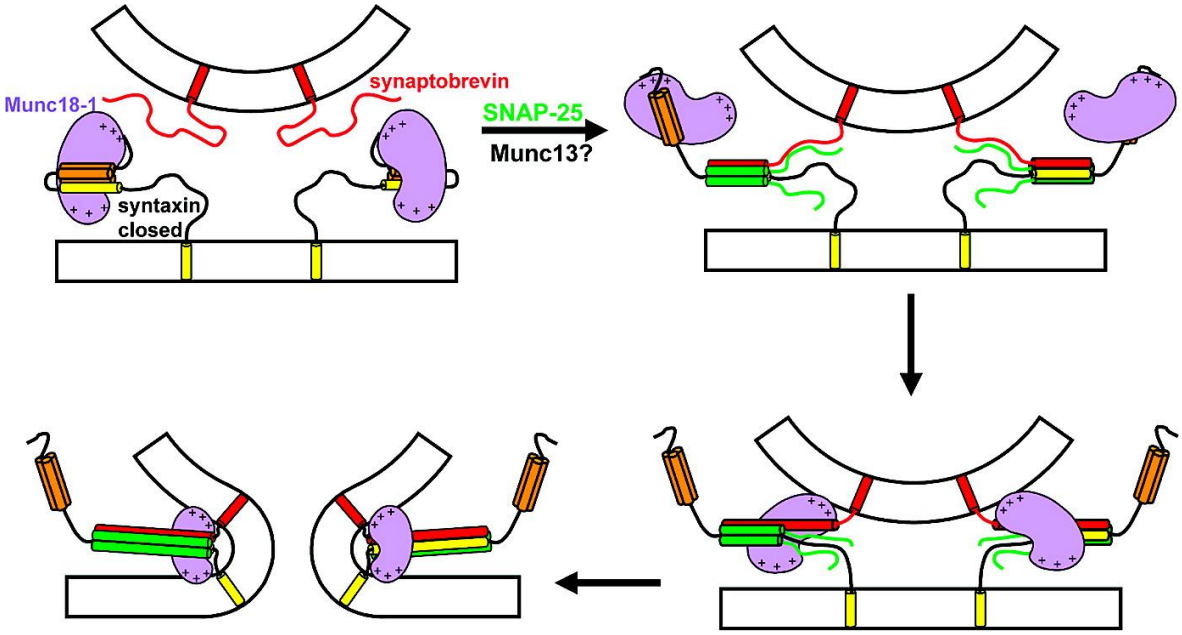

Figure 2.7

Figure 2.7 Proposed model of neurotransmitter release involving three types of Munc18-1-SNARE interactions

The model assumes that Munc18-1 (purple) is initially bound to closed syntaxin-1 (Habc domain, orange; SNARE motif, yellow) (top left panel). Partial assembly of SNARE complexes of syntaxin-1 with synaptobrevin (red) and SNAP-25 (green) occurs by an unknown mechanism that likely involves Munc13 (not shown); here we propose that Munc18-1 is bound to only the N-terminal region of syntaxin-1 at this stage (top right panel). The next step is proposed to involve the transition of Munc18-1 from the syntaxin-1 N-terminal region to the C-terminus of the synaptobrevin SNARE motif, which could be favored by cooperativity with other interactions such as Munc18-1 binding to the vesicle membrane (bottom right panel). The central aspect of this model is that membrane fusion results from the cooperative action of Munc18-1 and the SNAREs, which would be favored by the binding of Munc18-1 to synaptobrevin and could involve interactions of basic residues of Munc18-1 (indicated by the + signs) with both membranes (bottom left panel; see the text for further details). Other proteins involved in triggering release and conferring its Ca^{2+} sensitivity are not represented for the sake of simplicity, but they are expected to cooperate with Munc18-1 and the SNAREs to trigger release.

Chapter 3 Towards the structure of Munc18-1/SNARE four-helix bundle complex

3.1 Introduction

The SNAREs and Sec1/Munc18 (SM) proteins constitute the core of the intracellular membrane fusion machinery (Sudhof 2004; Verhage *et al.* 2007; Rizo *et al.* 2008). The roles of the neuronal SNAREs are well characterized. The neuronal SM protein Munc18-1 is strictly required for synaptic transmission (Verhage *et al.* 2000). As explained in the introduction of Chapter 2, research that has been carried out to investigate the functions of Munc18-1 revealed that Munc18-1 plays important roles in synaptic vesicle docking and priming. However, none of them can explain the fundamental requirement of Munc18-1 in neurotransmitter release. Moreover, the molecular mechanism of action of Munc18-1 is still unclear, especially in the Ca^{2+}-triggered membrane fusion step. Dr. Yi Xu from the lab found that Munc18-1 binds to the SNARE four-helix bundle with weak affinity (Xu *et al.* 2010). This weak interaction was reported to be responsible for Munc18-1 stimulation of SNARE-dependent in vitro liposome fusion (Shen *et al.* 2007; Shen *et al.* 2010). Hence, this weak interaction might be crucial for the key role of Munc18-1 in synaptic vesicle fusion.

Exploring the structure of Munc18-1/SNARE four-helix bundle will certainly provide important information for further characterization of the significance of this weak interaction in vivo. The structural information of the complex of Munc18-1/SNARE four-helix bundle will also help determine how Munc18-1, synaptotagmin, complexin, the SNARE complex, and other proteins cooperate with each other in Ca^{2+}-triggered synaptic vesicle fusion.

To obtain a high resolution structure of Munc18-1/SNARE four-helix bundle complex, I have been applying the methods of NMR spectroscopy, X-ray crystallography, and SAXS (small angle X-ray scattering). I did not solve the structure of this complex yet, but I have some data

showing that Munc18-1 binds to the C-terminal part of the SNARE four-helix bundle, which is adjacent to the place where membrane fusion occurs, and that Munc18-1 binding to the SNARE four-helix bundle is compatible with binding of the SNARE four-helix bundle to complexin-I, which functions in a late stage of synaptic vesicle exocytosis. These results are interesting and intriguing because it places Munc18-1 right at the site where membrane fusion occurs, suggesting that Munc18-1 might be directly involved in executing membrane fusion.

3.2 Materials and method

3.2.1 Recombinant DNA constructs

Bacteria expression vectors to express rat Munc18-1, fragments corresponding to the SNARE motifs of rat synaptobrevin-2 (29-93), synatxin-1a (191-253) and human SNAP-25B (11-82 as SNN and 141-203 as SNC), and the SNARE motifs mutants syntaxin-1a (H239C), synaptobrevin (S61C and A72C) as GST-fusion proteins were available in the lab (Dulubova *et al.* 2007; Xu *et al.* 2010). A vector to express squid Munc18-1 as a His-tagged protein was a kind gift from W. Weissenhorn (Bracher *et al.* 2000). Later, squid Munc18-1 was cloned into pGEX-KG vector as GST-fusion protein. Munc18N (1-136) and Munc18NL (1-139) were cloned into pGEX-KG vector from full length Munc18-1. Point mutants of Munc18NL (K46C and R64C) and SNC (E183C) were generated from the WT constructs using the QuickChange site-directed mutagenesis kit (Stratagene) and custom-designed primers, and were verified by sequencing.

3.2.2 Expression and purification of recombinant proteins

The expression and purification for recombinant proteins were similar to those described in Chapter 2.

3.2.3 NMR spectroscopy

^{1}H-^{15}N HSQC spectra of ^{15}N syntaxin-1a (191-253), ^{15}N SNN and ^{15}N SNC were recorded on Varian INOVA600 spectrometers at 15 ℃. 20 μM ^{15}N syntaxin-1a (191-253), ^{15}N SNN and ^{15}N SNC without and with 40 μM squid Munc18-1 in 20mM HEPES (pH 7.4) and 120 mM KCl were used in the HSQC experiments. ^{1}H-^{15}N TROSY-HSQC spectra of 85 μM ^{15}N sMunc18-1 and ^{1}H-^{13}C HMQC spectra of 11 μM ^{2}H-$^{13}C^{1}H_3$-Iso/Leu/Val labeled sMunc18-1and Munc18-1 without and with the SNARE four-helix bundle, and 30 μM ^{1}H-$^{13}C^{1}H_3$-Iso labeled sMunc18-1 without and with the SNARE four-helix bundle were recorded on Varian INOVA800 spectrometers at 32 ℃ and 25 ℃. ^{1}H-^{15}N TROSY-HSQC spectra of 40 μM ^{2}H-^{15}N labeled syntaxin-1 (191-253), synaptobrevin (29-93), SNN, and SNC assembled the SNARE four-helix bundle without and with 40 μM Munc18N, 100 μM ^{15}N labeled SNCE183C w/o DOTA-M8 assembled the SNARE four-helix bundle, and 40 μM ^{15}N Munc18NL without and with 10 μM, 20 μM, and 40 μM the SNARE four-helix bundle were recorded on Varian INOVA600 spectrometers at 25 ℃. ^{1}H-^{13}C HMQC spectra of 20 μM ^{2}H-$^{13}C^{1}H_3$-Iso/Leu/Val labeled syntaxin-1 (191-253) assembled the SNARE four-helix bundle without and with 20 μM Munc18NLK46C/R64C-DOTA-Mn^{2+}/DOTA-Gd^{3+} were recorded on Varian INOVA600 spectrometers at 25 ℃.

3.2.4 Backbone and methyl group assignments of Munc18NL

The backbone and methyl groups were assigned as described in (Chen *et al.* 2002; Chen *et al.* 2008).

3.2.5 Isothermal Titration Calorimetry (ITC) Experiments

ITC experiments were performed using a VP-ITC (MicroCal, Northhampton, MA) calorimeter at 20 ℃. The SNARE four-helix bundle or Munc18N were prepared in a buffer containing 20 mM

HEPES (PH7.4), 120 mM KCl and 1mM TCEP. 0.5 mM Munc18N was successively injected to 20 μM the SNARE four-helix bundle. The data were fitted with a nonlinear least squares routine using a single-site binding model with MicroCal Origin^{TM} software for ITC version 5.0.

3.2.6 SAXS experiments

Samples of 39 μM Munc18-1 in a buffer containing 20 mM HEPES (PH7.4), 300 mM KCl, 10% glycerol and 1mM TCEP; 120 μM the SNARE four-helix bundle in a buffer containing 20 mM HEPES (PH7.4), 120 mM KCl and 1mM TCEP; and 40 μM, 62 μM, 100 μM mixtures of Munc18-1 and the SNARE four-helix bundle in a buffer containing 20 mM HEPES (PH7.4), 120 mM KCl, 10% glycerol and 1mM TCEP were used for SAXS experiments. Data were collected in a BioSAXS-1000 instrument in Rigaku Americas Corporation, the Woodlands, TX. ATSAS2.4 was used to process all the data.

3.3 Results

3.3.1 Binding of Munc18-1 to the individual SNARE motifs.

In order to get a high resolution structure of Munc18-1/SNARE four-helix bundle complex, NMR spectroscopy and X-ray crystallography were simultaneously applied. To define the complex structure by NMR spectroscopy, binding sites in the two proteins and the relative orientation between them need to be determined. To find the binding sites in Munc18-1 and the SNARE four-helix bundle, the first thing and easiest thing to do is to investigate the bindings of Munc18-1 to the individual four SNAREs and to see whether these interactions could provide some hints for the mode of binding to the SNARE four-helix bundle.

The binding site on the synaptobrevin SNARE motif is described in Chapter 2. For the other three SNARE motifs, I performed ^{1}H-^{15}N HSQC experiments of 20 μM ^{15}N-syntaxin-1a

(191-253), SNN, SNC in the presence and absence of 40uM sMunc18-1. The spectra revealed that Munc18-1 binds to syntaxin-1 SNARE motif (202-224), but not to SNN and SNC (Figure 3.1A,B,C). A mutation on syntaxin-1 (R210E) impairs its interaction to sMunc18-1 (Figure 3.1D), which suggests that syntaxin-1 binding to sMunc18-1 is specific. However, when mapping the binding sites of syntaxin-1 (191-253) and synaptobrevin (29-96) (Figure 2.3A) onto the SNARE four-helix bundle (Figure 3.1E), the two individual binding sites are not in the same place on the SNARE four-helix bundle. The data suggest that Munc18-1 binding to the SNARE four-helix bundle is not the same as binding to the individual SNAREs, and that we need to use the SNARE four-helix bundle in the following experiments.

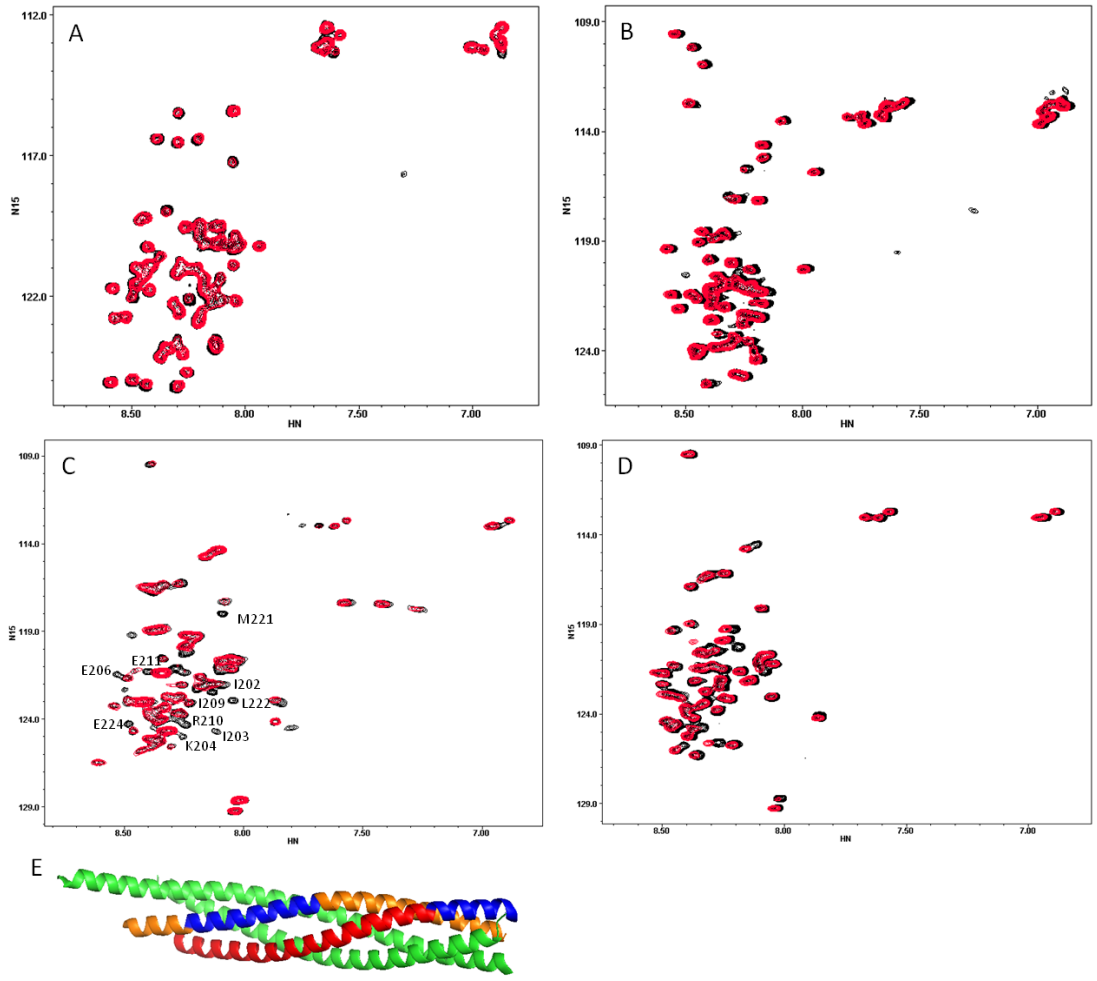

Figure 3.1 Munc18-1 binding to the individual SNAREs.

(A) ^{1}H-^{15}N HSQC spectra of 20 μM ^{15}N-SNN in the absence (black) and presence (red) of 40 μM sMunc18-1; (B) ^{1}H-^{15}N HSQC spectra of 20 μM ^{15}N-SNC in the absence (black) and presence (red) of 40 μM sMunc18-1; (C) ^{1}H-^{15}N HSQC spectra of 20 μM ^{15}N-syntaxin-1 (191-253) in the absence (black) and presence (red) of 40 μM sMunc18-1; the cross-peaks that were strongly broadened are labeled in black; (D) ^{1}H-^{15}N HSQC spectra of 20 μM ^{15}N-syntaxin-1 (191-253) R210E in the absence (black) and presence (red) of 40 μM sMunc18-1; (E) Ribbon diagram of the crystal structure of the SNARE four-helix bundle with SNN and SNC in green, synaptobrevin (29-93) in red, and syntaxin-1 (191-253) in orange; the dark blue helixes are residues broadened in (C) and Figure 2.3A.

3.3.2 To investigate the residues of Munc18-1 involved in the SNARE four-helix bundle binding.

To identify the residues of Munc18-1 involved in the SNARE four-helix bundle binding, first we need to get a good NMR spectrum of Munc18-1. I first carried out ^{1}H-^{15}N TROSY (Transverse Relaxation Optimized Spectroscopy)-HSQC experiments of 85 μM ^{15}N-labeled sMunc18-1 (squid Munc18-1) at 32 ℃. The cross-peaks in the spectrum are as crowded as expected for a 70 KDa protein (Figure 3.2A). Although there are some good dispersed peaks, the resolution is still not high enough to investigate the residues of Munc18-1 involved in binding, especially without any assignments. Deuteration of sMunc18-1 could greatly improve the resolution. However, deuteration resulted in a really low yield and a very less concentrated protein, which lowers the quality of the TROSY-HSQC experiment (Figure 3.2B). Thus, we need higher sensitivity experiments to get a good NMR spectrum. Deuteration together with ^{13}C-labeling of the methyl groups of isoleucines, valines and leucines of sMunc18-1 and Munc18-1 gave a much nicer HMQC (Heteronuclear Multiple Quantum Coherence) spectrum (Figure 3.2C,D), which can be used for the SNARE four-helix bundle binding experiments. Also, ^{13}C-labeling of the methyl groups of isoleucines of sMunc18-1 without deuteration gave a fairly good HMQC spectrum (Figure 3.2E).

^{1}H- $^{13}CH_3$ HMQC experiments of 30uM $^{13}C^{1}H_3$-Iso-sMunc18-1 in the presence and absence of 40 μM the SNARE four-helix bundle were performed. The spectra reveals specific broadenings of 3 isoleucine cross-peaks of sMunc18-1 (Figure 3.3A), which suggests that the SNARE four-helix bundle indeed interacts with Munc18-1, although it is unclear which residues are involved because we do not have the assignments of the isoleucines of sMunc18-1.

To get more changes of the cross-peaks, I labeled synaptobrevin S61C, which is close to the binding site and is used for fluorophore labeling in measuring the affinity of Munc18-1 to the SNARE four-helix bundle (Xu *et al.* 2010), with the paramagnetic probe MTSL (Figure 3.3D), which induces paramagnetic resonance enhancement (PRE) to the residues near the probe and causes broadenings of the cross-peaks corresponding to those residues. ^{1}H- $^{13}CH_3$ HMQC experiments of 11 μM ^{2}H-$^{13}C^{1}H_3$-Iso/Leu/Val-Munc18-1 in the presence and absence of 30 μM the SNARE four-helix bundle (mcc)-synaptobrevin-61C-MTSL were performed. In the mcc-synaptobrevin-61C-MTSL added spectra, the overall intensities drop because of the binding, and some cross-peaks were broadened further (Figure 3.3B). However, after adding dithionine, which is expected to kill the paramagnetic probes and reverse the changes, those broadenings were not reversed (Figure 3.3C).

These data together indicate the binding of Munc18-1 to the SNARE four-helix bundle, but the residues of Munc18-1 involved in binding are hard to define from the data for the following reasons: the affinity of the complex is low (Kd~10 μM), and Munc18-1 is not saturated; or the residue of synaptobrevin S61C is not close enough to the binding site, so the paramagnetic probes cannot induce changes of residues involved in binding. Defining the binding site in the SNARE four-helix bundle will lead us to label the probes in a better place.

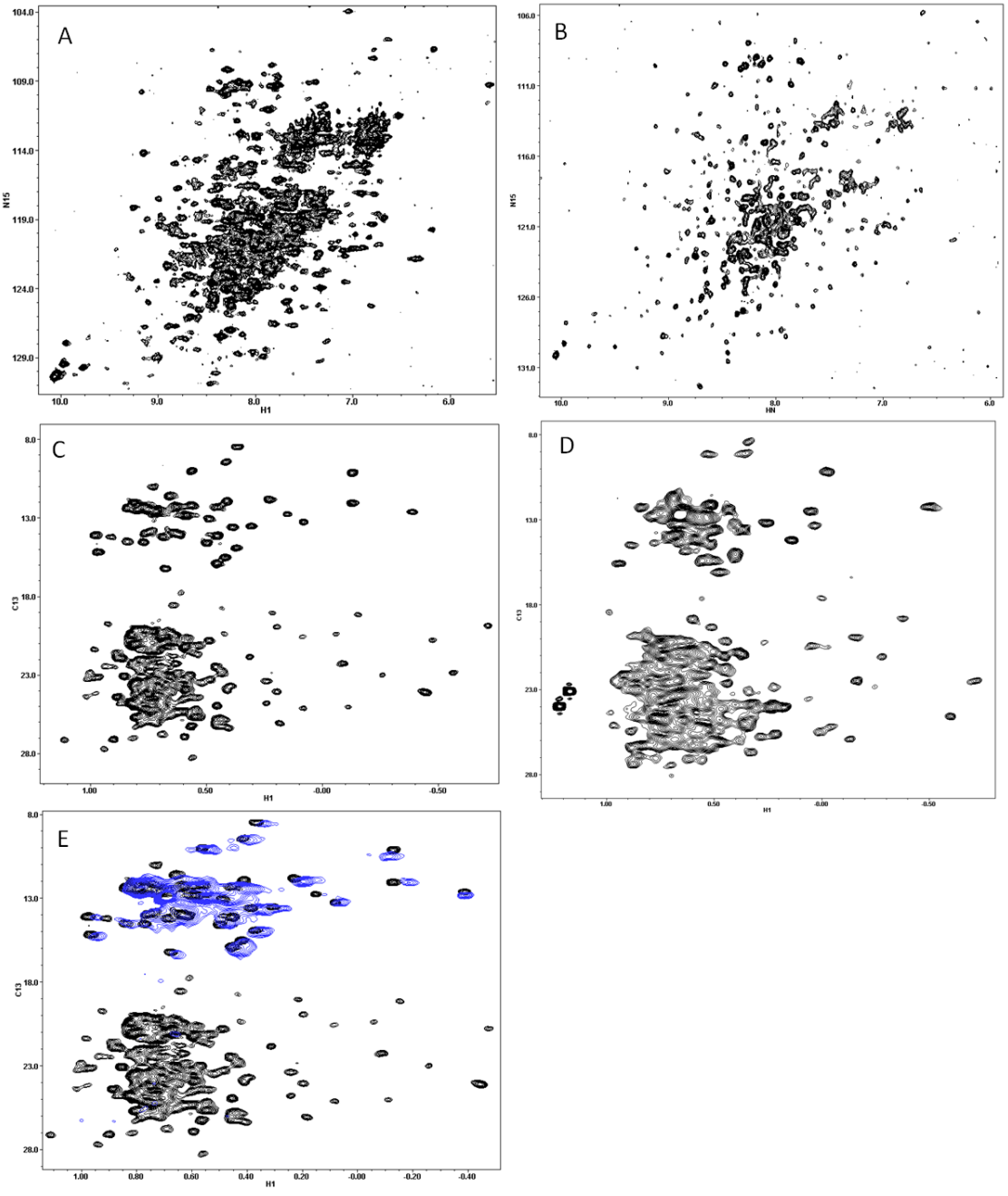

Figure 3.2

Figure 3.2 TROSY-HSQC and HMQC spectra of Munc18-1.

(A) ^{1}H-^{15}N TROSY-HSQC spectrum of 85 μM ^{15}N sMunc18-1; (B) ^{1}H-^{15}N TROSY-HSQC spectrum of 11 μM ^{2}H-$^{13}C^{1}H_3$-Iso/Leu/Val-sMunc18-1; (C) ^{1}H-$^{13}CH_3$ HMQC spectrum of 11 μM ^{2}H-$^{13}C^{1}H_3$-Iso/Leu/Val-sMunc18-1; (D) ^{1}H-$^{13}CH_3$ HMQC spectrum of 11 μM ^{2}H-$^{13}C^{1}H_3$-Iso/Leu/Val-Munc18-1; (E) comparison of ^{1}H-$^{13}CH_3$ HMQC spectra of 11 μM ^{2}H-$^{13}C^{1}H_3$-Iso/Leu/Val-Munc18-1 (black) and 30 μM $^{13}C^{1}H_3$-Iso-sMunc18-1 (blue).

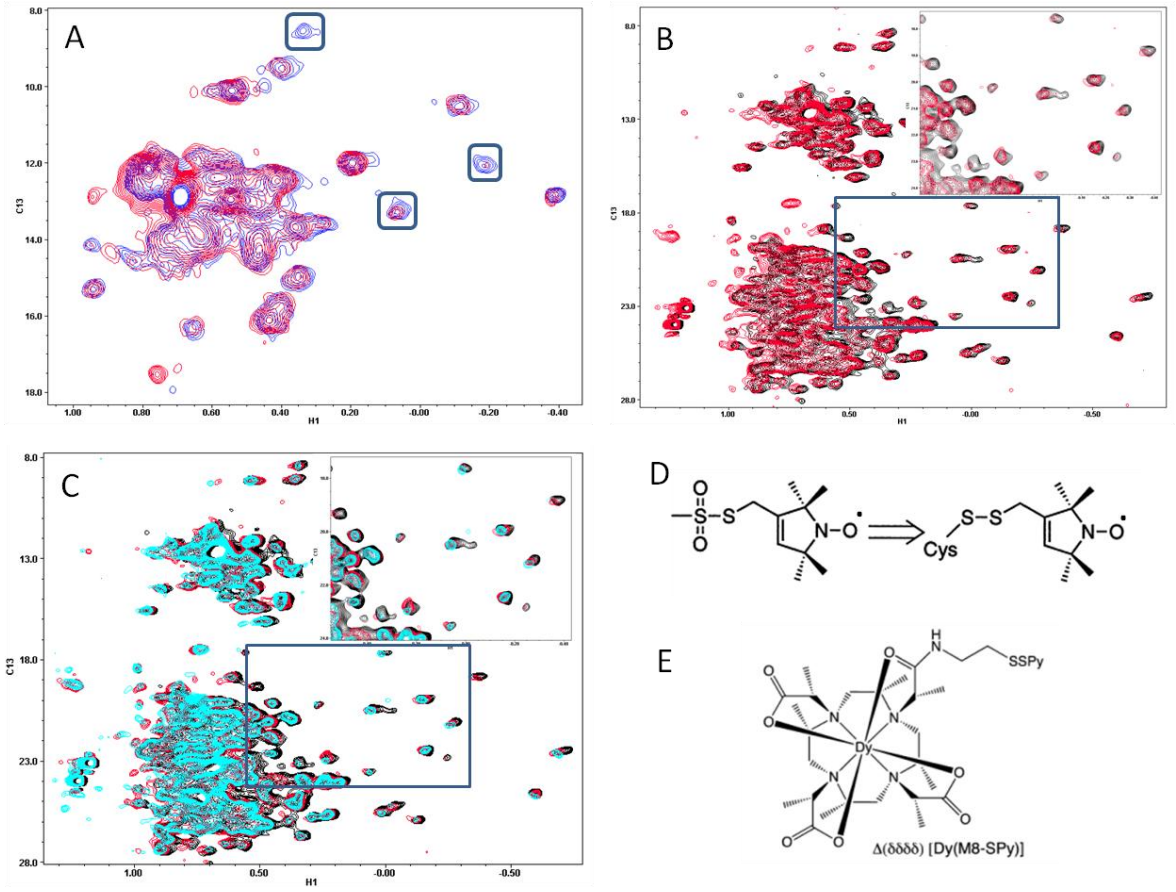

Figure 3.3 Binding of the SNARE four-helix bundle to Munc18-1 and chemical structures of MTSL and DOTA-M8-Dy^{3+}.

(A) ^{1}H-$^{13}CH_3$ HMQC spectra of 30 μM $^{13}C^{1}H_3$-Iso-sMunc18-1 in the absence (blue) and presence (red) of 40 μM the SNARE four-helix bundle; (B) ^{1}H-$^{13}CH_3$ HMQC spectra of 11 μM ^{2}H-$^{13}C^{1}H_3$-Iso/Leu/Val-Munc18-1 in the absence (black) and presence of 30 μM (red) SNARE four-helix bundle-synaptobrevin-61C-MTSL; (C) Dithionine addition (blue) to the sample in (B); in (B) and (C), the blue rectangles highlight the cross-peaks that were broadened; those cross-peaks were expanded in the windows on the upper right; (D) Chemical Structure of MTSL that attaches to a cysteine through a disulfide bond; (E) Chemical Structure of DOTA-M8-Dy^{3+}.

3.3.3 To identify the residues of the SNARE four-helix bundle involved in Munc18-1binding.

To find out the residues of the SNARE four-helix bundle involved in Munc18-1 binding, we need to label Munc18-1 with paramagnetic probes first, and then monitor the changes of the NMR spectra of the SNARE four-helix bundle upon addition of paramagnetic probe labeled Munc18-1. Experiments performed to label Munc18-1 with paramagnetic probes, such as MTSL, MTS-EDTA-Gd^{3+} (S-Methanethiosulfonylcysteaminyl]ethylenediamine-N,N,N',N'-Tetraacetic Acid-Gd^{3+}), maleimido-proxyl, and iodoacetamido-proxyl, all resulted in unfolding of Munc18-1, probably because of the intrinsic instability of Munc18-1 and the hydrophobicity of these probes that make them easy to go into Munc18-1 and unfold the protein.

One of our previous papers (Khvotchev *et al.* 2007) suggested that that Munc18-1 N-terminal domain (Munc18N) interacts with the Habc domain of syntaxin-1 in the same way as Munc18-1 interacts with syntaxin-1. The crystal structure of Munc18-1/syntaxin-1 showed that Munc18N provides large contact surface for syntaxin-1 binding especially for syntaxin-1 Habc binding (Burkhardt *et al.* 2008). Therefore, it would make sense that the way Munc18N interacts with syntaxin-1 Habc domain is similar to the way Munc18-1 interacts with syntaxin-1. These data led to the hypothesis that the mode of Munc18N binding to the SNARE four-helix bundle may represent how Munc18-1 interacts with the SNARE four-helix bundle, since the SNARE four-helix bundle binds to Munc18-1 through the central cavity where Munc18N provides a lot of surface (Dulubova *et al.* 1999). If Munc18N indeed binds to the SNARE four-helix bundle, it would greatly simplify our work since Munc18N is very small compared to Munc18-1. The structure of Munc18N/SNARE four-helix bundle would help us define the structure of Munc18-1/SNARE four-helix bundle.

^{1}H-^{15}N HSQC experiments of 40 μM ^{15}N-Munc18NL (1-139) in the absence and presence of 10 μM, 20 μM, 40 μM the SNARE four-helix bundle showed gradual and specific broadenings of several cross-peaks (Figure 3.4A), which indicates that Munc18-1 N-terminal domain indeed binds to the SNARE four-helix bundle. ITC experiments revealed an affinity of around 4 μM for this interaction, which is tighter than the complex of Munc18-1/SNARE four-helix bundle (Kd~10 μM) (Figure 3.4B). The fact that the affinity is tighter makes the project very interesting and exciting, because it could mean that Munc18-1 needs a regulator to change its conformation in order to bind better to the SNARE four-helix bundle and exert its function.

To find out the residues of the SNARE four-helix bundle involved in Munc18N binding, the four individual SNAREs were first ^{2}H-^{15}N labeled and assembled into the SNARE complex, and then Munc18N was titrated into the labeled SNARE complex. Chemical shifts changes or broadening in the TROSY-HSQC spectra of the SNARE complexes were then monitored. ^{1}H-^{15}N TROSY-HSQC experiments of 40 μM ^{2}H-^{15}N-syntaxin-1 (191-253), SNN, synaptobrevin (29-93) and SNC labeled SNARE four-helix bundle alone and in the presence of 40 μM Munc18N suggest that the C-terminal part of synaptobrevin (77-86) and syntaxin-1 (237-242) on the SNARE four helix-bundle are involved in binding to Munc18N (Figure 3.5A,B,C,D,E), although the quality of the data is not very good and the chemical shifts changes are not very big.

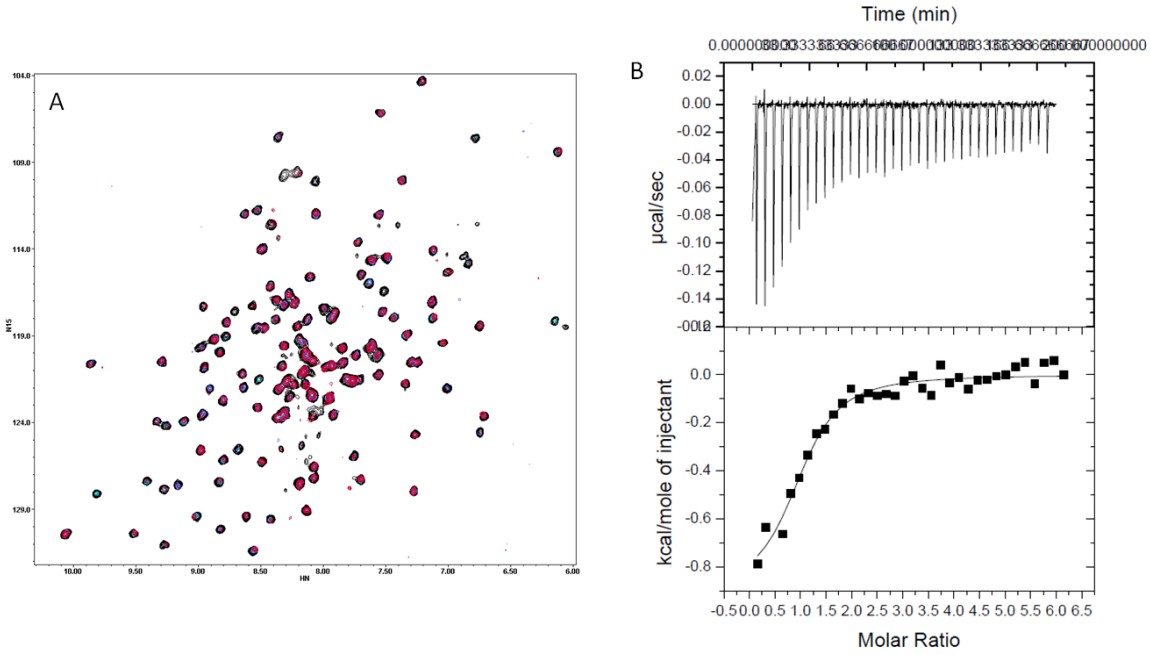

Figure 3.4 Binding of the SNARE four-helix bundle to Munc18N.

(A) ^{1}H-^{15}N TROSY-HSQC spectra of 40 µM ^{15}N Munc18NL in the absence (black) and presence of 10 µM (light blue), 20 µM (purple) and 40 µM (red) the SNARE four-helix bundle; some cross-peaks were strongly broadened; (B) ITC analysis of binding of Munc18N to the SNARE four-helix bundle; Kd=4 µM; N=1.04.

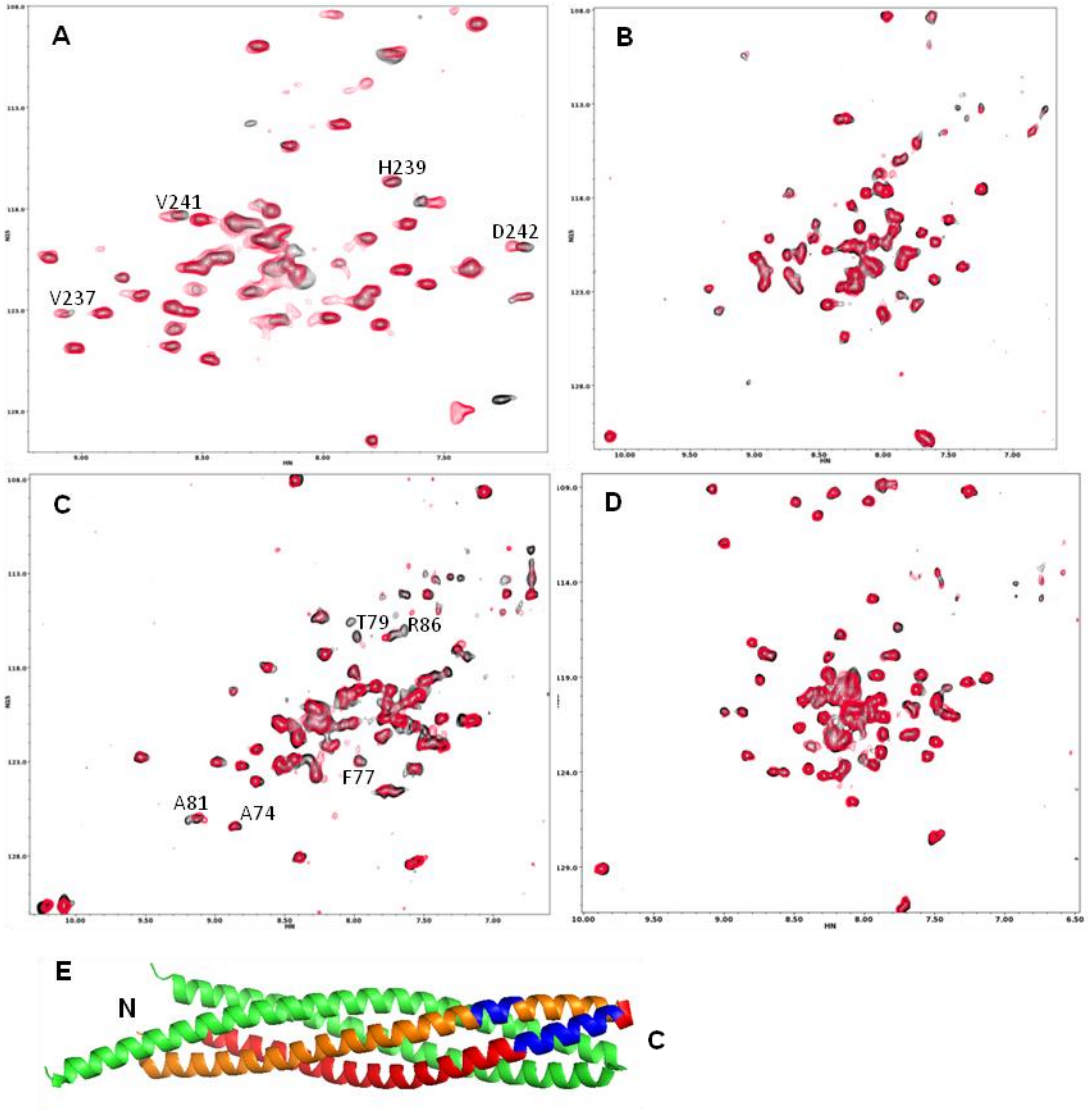

Figure 3.5

Figure 3.5 Titration of Munc18N to the ^{2}H-^{15}N labeled SNARE four-helix bundle.

(A) ^{1}H-^{15}N TROSY-HSQC spectra of 40 μM ^{15}N ^{2}H-^{15}N labeled syntaxin-1 (191-253)-SNARE four-helix bundle in the absence (black) and presence (red) of 40 μM Munc18N; the cross-peaks that were shifted are labeled in black; (B) ^{1}H-^{15}N TROSY-HSQC spectra of 40 μM ^{15}N ^{2}H-^{15}N labeled SNN-SNARE four-helix bundle in the absence (black) and presence (red) of 40 μM Munc18N; (C) ^{1}H-^{15}N TROSY-HSQC spectra of 40 μM ^{15}N ^{2}H-^{15}N labeled synaptobrevin (29-93)-SNARE four-helix bundle in the absence (black) and presence (red) of 40 μM Munc18N; the cross-peaks that were shifted are labeled in black; (D) ^{1}H-^{15}N TROSY-HSQC spectra of 40 μM ^{15}N ^{2}H-^{15}N labeled SNC-SNARE four-helix bundle in the absence (black) and presence (red) of 40 μM Munc18N; (E) Ribbon diagram of the crystal structure of the SNARE four-helix bundle with SNN and SNC in green, synaptobrevin (29-93) in red, and syntaxin-1 (191-253) in orange; the dark blue helixes are residues shifted in (A) and (C).

3.3.4 To define the binding sites in the complex of Munc18N/SNARE four-helix bundle.

To define the structure of the complex of Munc18N/SNARE four-helix bundle, we need better NMR data than the ones shown in 3.3.2 and 3.3.3. To identify the residues of Munc18N involved in binding, the backbone cross-peaks of Munc18NL were first assigned. According to the assignment, the data in Figure 3.4A showed broadenings everywhere in the structure of Munc18N, especially broadenings in the core hydrophobic region (Figure 3.6A,B,C), which suggest that there might be a slight conformational change of Munc18N when it binds to the SNARE four-helix bundle. Therefore, we need to monitor chemical shift changes rather than broadenings. I used the paramagnetic probe DOTA(1,4,7,10-tetraazacyclododecane-1,4,7,10-tetraacetic acid)-M8-Dy^{3+} (Figure 3.3E), which induces pseudo-contact chemical shift to the residues near the probe and causes chemical shift changes to the cross-peaks correspond to those residues. The SNARE four-helix bundle labeled with DOTA-M8-Dy^{3+} in a place close to the binding site would probably induce chemical shift changes in Munc18NL when it binds to Munc18NL.

I mutated glutamate 183 of SNC, which is in the C-terminal part of the SNARE four-helix bundle but not in the binding site according to Figure 3.5, to a cysteine (Figure 3.6E). ^{1}H-^{15}N-SNC-E183C was labeled with DOTA-M8-Dy^{3+} and then assembled into the SNARE four-helix bundle. TROSY-HSQC experiments of 100 μM ^{1}H-^{15}N-SNC-E183C SNARE four-helix bundle before and after DOTA-M8-Dy^{3+} labeling suggested full labeling, although the quality of the data was not very high (Figure 3.7A). ^{1}H- $^{13}CH_3$ HMQC experiments of 50 μM ^{2}H (50%)-$^{13}C^{1}H_3$-Iso/Leu/Val-Munc18NL alone and in the presence of 10 μM, 20 μM SNC-E183C-DOTA-M8-Dy^{3+} SNARE four-helix bundle, and 20 μM the SNARE four-helix bundle with 0.3 μM TCEP were performed. The results in Figure 3.7B showed that there are several cross-peaks

that shift gradually as the concentration of the SNARE four-helix bundle increases. According to the methyl group assignments, these shifted residues (V126, I127, L130) locate in a hydrohphobic pocket of Munc18N where syntaxin-1 N peptide binds (Figure 3.7C,D). However, with TCEP addition, those shifts were not reversed (Figure 3.7E). Munc18NL might be partially denaturated by the time of adding TCEP. This experiment is hard to perform because Munc18NL tends to precipitate after adding the SNARE four-helix bundle especially the ones labeled with DOTA-M8-Dy^{3+}.

To get better NMR data than those of Figure 3.5 to define the binding site in the SNARE four-helix bundle, I first labeled Munc18NL with the paramagnetic probes DOTA-Gd^{3+} and DOTA-Mn^{2+} (Figure 3.6F), which covalently binds to a cysteine and induces PRE on the residues near the probes, causing broadening of those cross-peaks, and then monitored the NMR spectra of the SNARE four-helix bundle in the absence and presence of paramagnetic probe labeled Munc18NL.

I mutated several residues of Munc18NL (K20C, K25C, K46C, R64C, S70C, T96C, R100C) to cysteines. These residues are all within 25 Å distance from the cavity and the hydrophobic pocket of Munc18-1 calculated from the crystal structure of Munc18-1/syntaxin-1 (Burkhardt *et al.* 2008)). Only K46C and R64C mutants of Munc18NL are stable in isolation, so these two were used to label with DOTA-Mn^{2+} and DOTA-Gd^{3+}. ^{1}H-^{15}N HSQC experiments of 100 μM ^{1}H-^{15}N Munc18NL K46C alone and labeled with DOTA-Mn^{2+}, and 100 μM ^{1}H-^{15}N Munc18NL R64C alone and labeled with DOTA-Gd^{3+} showed specific broadening of several cross-peaks in the spectra (Figure 3.8A,C). PRE is calculated by dividing the intensities of the cross-peaks with DOTA-Mn^{2+} or DOTA-Gd^{3+} labeling to the intensities of the corresponding cross-peaks without any labeling. Figure 3.8B and 3.8D showed the correlations between

distances to the probe and PRE caused by DOTA-Mn^{2+} and DOTA-Gd^{3+}. The correlations revealed that DOTA-Mn^{2+} and DOTA-Gd^{3+} give PRE up to 35 Å and 40 Å (Figure 3.8B,D), which are good for our experiments. ^{1}H- $^{13}CH_3$ HMQC experiments of 20 μM ^{2}H-$^{13}C^{1}H_3$-Iso/Leu/Val-syntaxin-1 (191-253) SNARE four-helix bundle alone and in the presence of 20 μM Munc18N K46C-DOTA-Mn^{2+} or Munc18N R64C-DOTA-Mn^{2+} both showed that one valine of syntaxin-1 (191-253) in the SNARE four-helix bundle was significantly affected (Figure 3.9 A,B). ^{1}H- $^{13}CH_3$ HMQC experiments of 15 μM ^{2}H-$^{13}C^{1}H_3$-Iso/Leu/Val-syntaxin-1 (191-253) SNARE four-helix bundle alone and in the presence of 15 μM Munc18NL R64C-DOTA-Gd^{3+} also showed that the same valine was affected (Figure 3.9C). Although we do not have the methyl group assignments of the SNARE four-helix bundle yet, based on the chemical shift of the valine and the structure of the SNARE four-helix bundle (Sutton *et al.* 1998), We speculate that the cross-peak corresponds to V241, which is in the C-terminal region of syntaxin-1 (Figure 3.9D). These data validate our results in 3.3.3 that the C-terminal part of the SNARE four-helix bundle is involved in Munc18N binding.

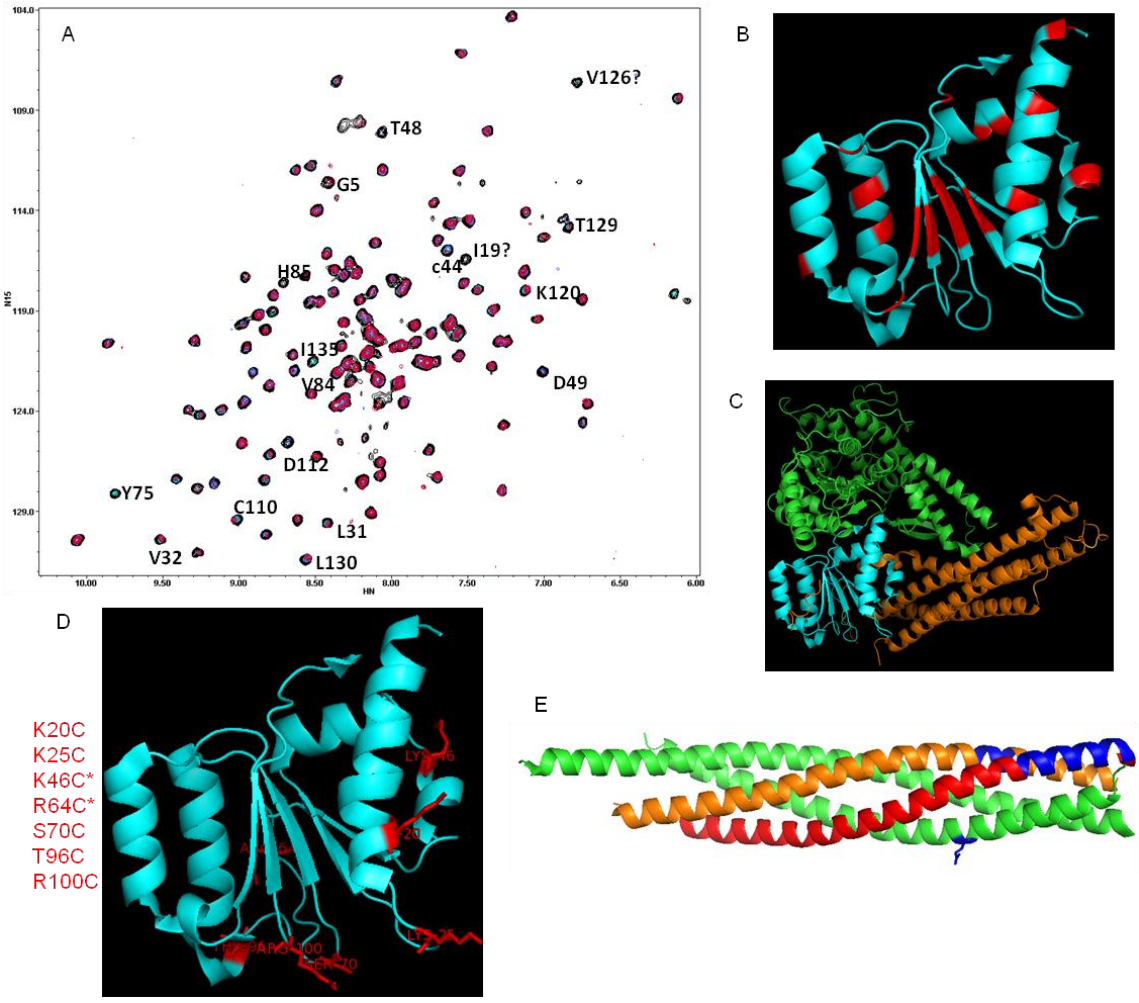
A
V126?
T48
G5
T129
I19?
c44
H85
K120
I135
V84
D49
D112
Y75
C110
L31
V32
L130
B
C
D
K20C
K25C
K46C*
R64C*
S70C
T96C
R100C
E

Figure 3.6

Figure 3.6 Potential residues of Munc18N involved in binding and paramagnetic probe labeling places of Munc18N and the SNARE four-helix bundle.

(A) ^{1}H-^{15}N TROSY-HSQC spectra of 40 μM ^{15}N Munc18NL in the absence (black) and presence of 10 μM (light blue), 20 μM (purple) and 40 μM (red) SNARE four-helix bundle; the cross-peaks that were strongly broadened are labeled in black; (B) Ribbon diagram of the structure of Munc18N in blue with residues that were broadened in (A) in red; (C) Ribbon diagram of crystal structure of Munc18-1/syntaxin-1 (2-253) complex with syntaxin-1 (2-253) in orange, Munc18-1 domain 1 in blue and domain 2 and 3 in green; (D) Ribbon diagram of the structure of Munc18N in blue with residues that were mutated to cysteins in red; the residue names are labeled on the left; the residues with star labels are stable in isolation; (E) Ribbon diagram of the crystal structure of the SNARE four-helix bundle with SNN and SNC in green, synaptobrevin (29-93) in red, and syntaxin-1 (191-253) in orange; the dark blue stick represents SNC E183; the dark blue helixes are residues involved in Munc18N binding from Figure 3.5. The structure of Munc18N here is taken from the crystal structure of Munc18-1/syntaxin-1 (Burkhardt *et al.* 2008).

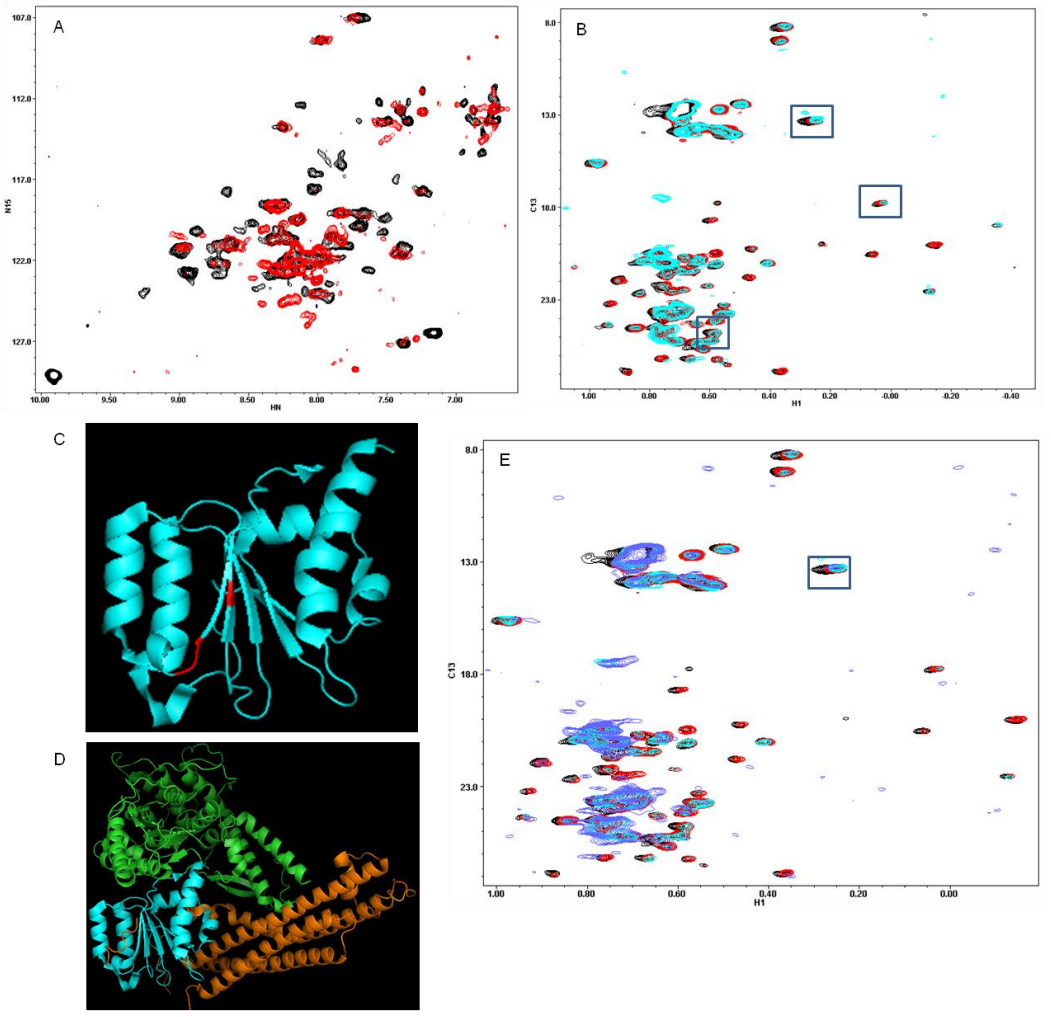

Figure 3.7

Figure 3.7 **HMQC experiments of ^{2}H-$^{13}CH_3$-Iso/Leu/Val-Munc18NL in the presence of DOTA-M8-Dy^{3+} labeled SNARE four-helix bundle**

(A) ^{1}H-^{15}N TROSY-HSQC spectra of 100 μM ^{15}N SNCE183C-SNARE four-helix bundle in the absence (black) and presence (red) of DOTA-M8 labeling; (B) ^{1}H-$^{13}CH_3$ HMQC spectra of 50 μM ^{2}H (50%)-$^{13}CH_3$-Iso/Leu/Val-Munc18NL in the absence (black) and presence of 10 μM (red), 20 μM (light blue) SNC-E183C- DOTA-M8-Dy^{3+}-SNARE four-helix bundle; the blue rectangle highlights the residues shifted; (C) Ribbon diagram of the structure of Munc18N in blue with residues (V126, I127, L130) that shifted in (B) in red; (D) Ribbon diagram of the crystal structure of Munc18-1/syntaxin-1 (2-253) complex with syntaxin-1 (2-253) in orange, Munc18-1 domain 1 in blue and domain 2 and 3 in green; (E) ^{1}H-$^{13}CH_3$ HMQC spectra of 50 μM ^{2}H (50%)-$^{13}CH_3$-Iso/Leu/Val-Munc18NL in the absence (black) and presence of 10 μM (red), 20 μM (light blue) SNC-E183C- DOTA-M8-Dy^{3+}-SNARE four-helix bundle and with 0.3 mM TCEP addition (dark blue); the blue rectangle highlights the residues shifted. The structure of Munc18N here is taken from the crystal structure of Munc18-1/syntaxin-1 (Burkhardt *et al.* 2008).

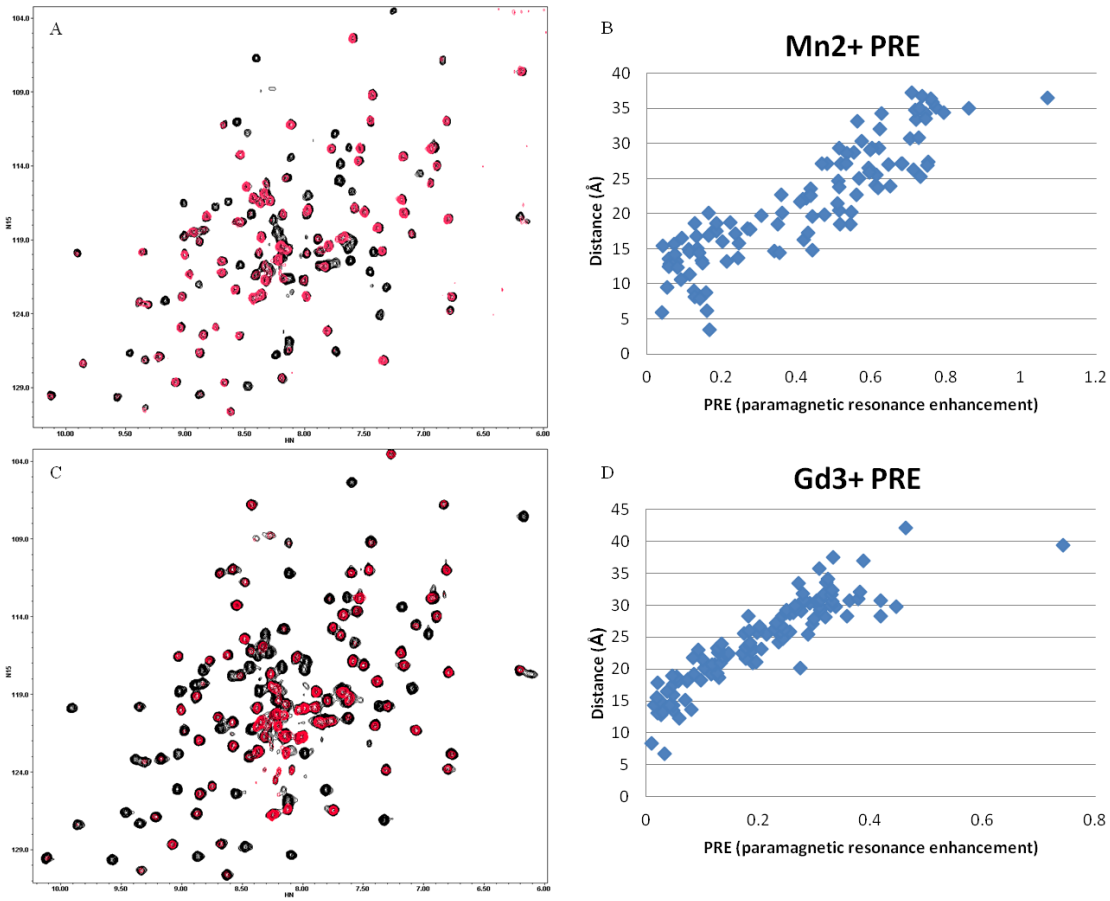

Figure 3.8 PRE of Munc18NL caused by DOTA-Mn2+/Gd3+ labeling.

(A) ^{1}H-^{15}N HSQC spectra of 100 μM ^{15}N Munc18NLK46C in the absence (black) and presence (red) of 500 μM DOTA-Mn^{2+}; many cross-peaks were significantly broadened; (B) Correlation between Mn^{2+} PRE (paramagnetic resonance enhancement) and distance to K46C; Mn^{2+} can give PRE up to 35 Å; (C) ^{1}H-^{15}N HSQC spectra of 100 μM ^{15}N Munc18NLR64C in the absence (black) and presence (red) of 500 μM DOTA-Gd^{3+}; many cross-peaks were significantly broadened; (D) Correlation between Gd^{3+} PRE and distance to R64C; Gd^{3+} can give PRE up to 40 Å.

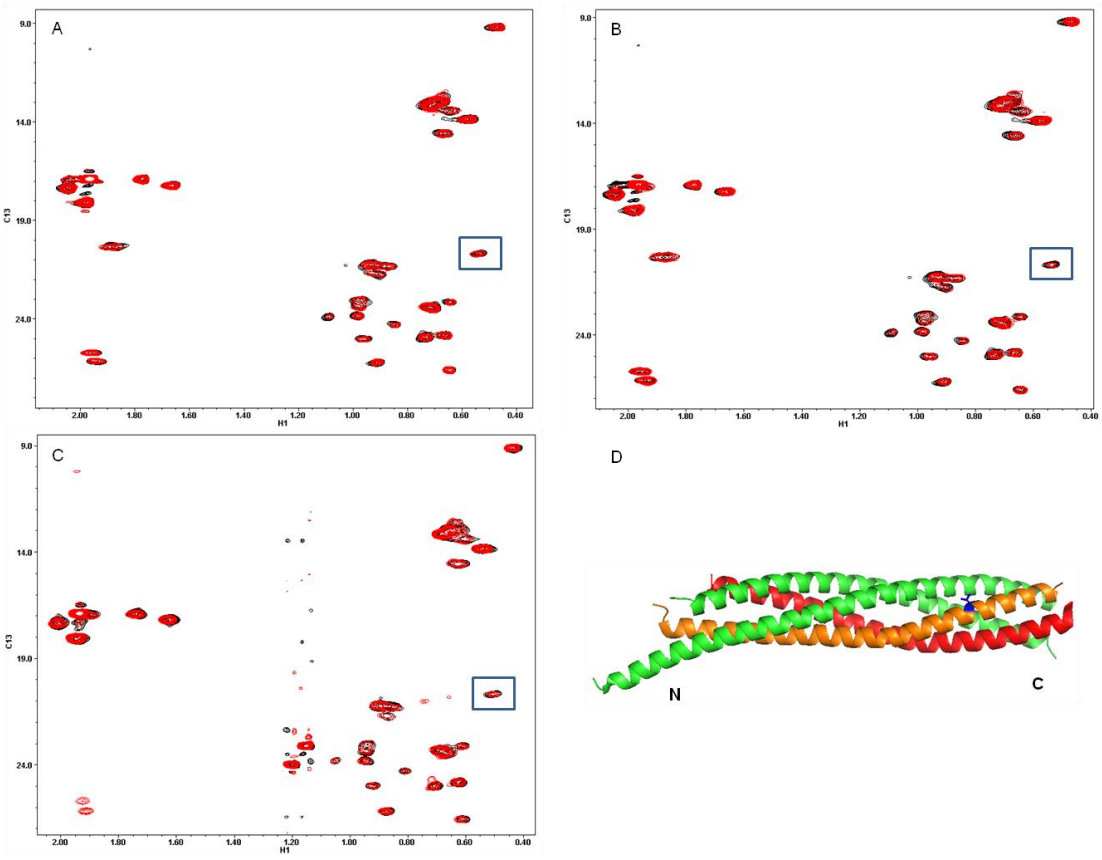

Figure 3.9 HMQC experiments of ^{2}H-$^{13}CH_3$-Iso/Leu/Val-syntaxin-1-SNARE four-helix bundle in the presence of DOTA-Mn^{2+} or DOTA-Gd^{3+} labeled Munc18NL.

(A) ^{1}H- $^{13}CH_3$ HMQC spectra of 20 μM ^{2}H-$^{13}CH_3$-Iso/Leu/Val-syntaxin-1 (191-253)-SNARE four-helix bundle in the absence (black) and presence (red) of 20 μM Munc18NLK46C-DOTA-Mn^{2+}; the blue rectangle highlights the residue that is broadened; (B) ^{1}H- $^{13}CH_3$ HMQC spectra of 20 μM ^{2}H-$^{13}CH_3$-Iso/Leu/Val-syntaxin-1 (191-253)-SNARE four-helix bundle in the absence (black) and presence (red) of 20 μM Munc18NLR64C-DOTA-Mn^{2+}; the blue rectangle highlights the residue that is significantly broadened; (C) ^{1}H-$^{13}CH_3$ HMQC spectra of 15 μM ^{2}H-$^{13}CH_3$-Iso/Leu/Val-syntaxin-1 (191-253)-SNARE four-helix bundle in the absence (black) and presence (red) of 15 μM Munc18NLR64C-DOTA-Gd^{3+}; the blue rectangle highlights the residue that is significantly broadened; (D) Ribbon diagram of the crystal structure of the SNARE four-helix bundle with SNN and SNC in green, synaptobrevin (29-93) in red, and syntaxin-1 (191-253) in orange; the dark blue stick represents Valine 241.

3.3.5 Munc18N and complexin I binding to the SNARE four-helix bundle are compatible.

The results from 3.3.3 and 3.3.4 suggest that the C-terminal part of syntaxin-1 and synaptobrevin in the SNARE four-helix bundle are involved in Munc18-1 and Munc18N binding, which raises another question: is Munc18-1 (Munc18N) binding to the SNARE four-helix bundle compatible with complexin binding to the SNARE four-helix bundle? Note that the complexin central helix binds to the SNARE four-helix bundle through the groove of syntaxin-1 and synaptobrevin (Chen *et al.* 2002). To answer this question, ^{1}H-^{15}N TROSY-HSQC experiments of 40 μM ^{1}H-^{15}N Munc18NL alone and in the presence of 20 μM SNARE four-helix bundle, 30 μM complexin I, and 20 μM SNARE four-helix bundle together with 30 μM complexin I were carried out. The spectra showed that: i) complexin I addition does not cause any changes to the intensities of cross-peaks; ii) SNARE four-helix bundle addition causes specific broadenings of some cross-peaks; iii) addition of SNARE four-helix bundle together with complexin I causes further broadenings of those cross-peaks in ii) (Figure 3.10A,B,C,D). These data suggest that Munc18N (Munc18-1) and complexin I can simultaneously bind to the SNARE four-helix bundle, which implies that Munc18-1 and complexin could both function in the fusion step of synaptic vesicle exocytosis.

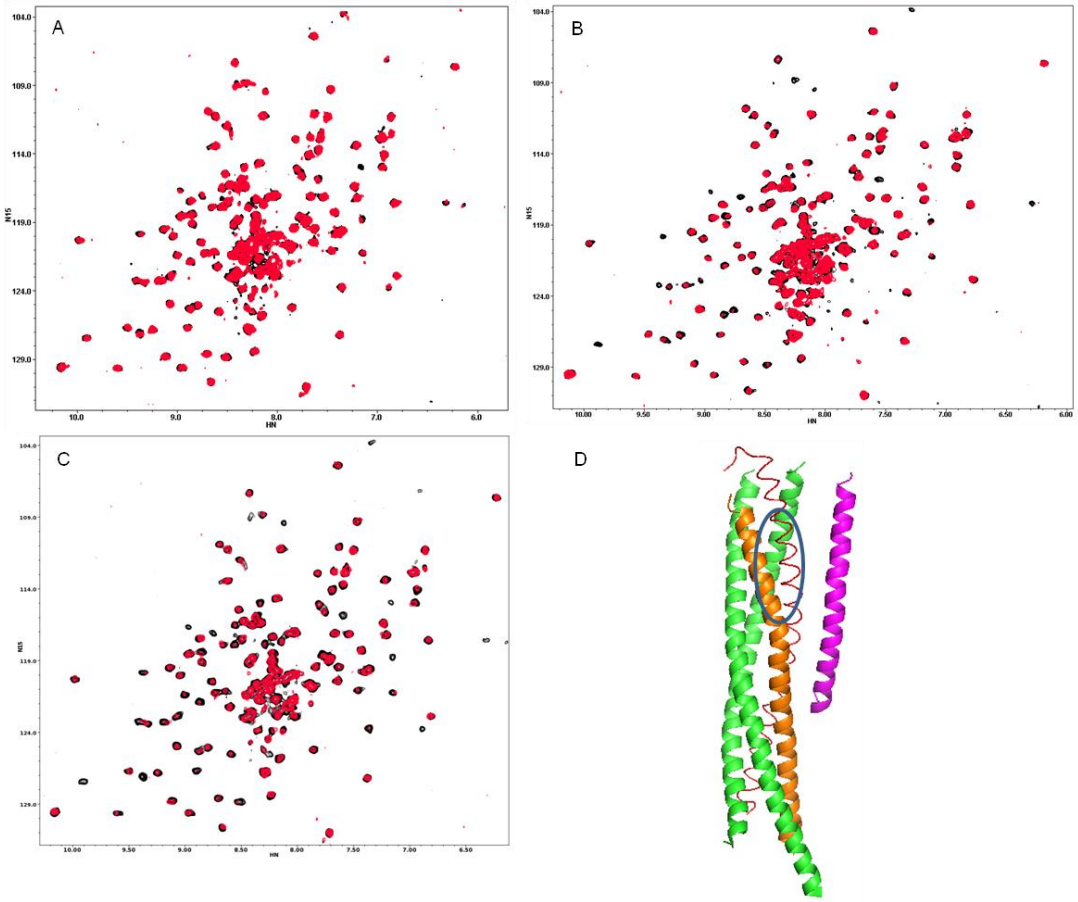

Figure 3.10 Binding of Munc18N and complexin I to the SNARE four-helix bundle.

(A) ^{1}H-^{15}N TROSY-HSQC spectra of 40 μM ^{15}N Munc18NL in the absence (black) and presence (red) of 30 μM complexin I; (B) ^{1}H-^{15}N TROSY-HSQC spectra of 40 μM ^{15}N Munc18NL in the absence (black) and presence (red) of 20 μM SNARE four-helix bundle; (C) ^{1}H-^{15}N TROSY-HSQC spectra of 40 μM ^{15}N Munc18NL in the absence (black) and presence (red) of 30 μM complexin I and 20 μM SNARE four-helix bundle; (D) Ribbon diagram of the crystal structure of the SNARE four-helix bundle and complexin I central helix with complexin I central helix in purple, SNN and SNC in green, synaptobrevin (29-93) in red, and syntaxin-1 (191-253) in orange; the blue ellipse irises out the residues involved in Munc18N binding.

3.3.6 To define the structure of the complex of Munc18-1/SNARE four-helix bundle by X-ray crystallography and SAXS.

Attempts to crystallize the complex of sMunc18-1/SNARE four-helix bundle yielded either crystals of sMunc18-1 alone or crystals of the SNARE four-helix bundle alone, probably because of the low affinity between the two proteins. SAXS (small angle X-ray scattering) could give a low resolution solution structure of the complex of Munc18-1/SNARE four-helix bundle, which in combination with the NMR results could define the complex structure.

SAXS experiments of 39 μM Munc18-1 alone, 120 μM SNARE four-helix bundle alone, and 40 μM, 62 μM, 100 μM mixtures of Munc18-1 and SNARE four-helix bundle in a 1:1 ratio were performed. The data were collected in house at Rigaku Americas Corporation, the Woodlands, TX. The quality of the data was not high but was enough to generate some preliminary results. Data analysis using ATSAS 2.4 revealed that Munc18-1 is more like a globular protein in solution (Figure 3.11A), which is consistent with crystal structure of Munc18-1 (Burkhardt *et al.* 2008). Moreover, superposition of the crystal structure and the envelope of Munc18-1 generated from SAXS data suggest that domain1 and domain 3a are probably flexible in solution, which might regulate the size of Munc18-1 cavity. The SAXS data of the SNARE four-helix bundle showed an elongated envelope, which fits well with the crystal structure of the SNARE four-helix bundle (Sutton *et al.* 1998) (Figure 3.11B). Since Munc18-1 interacts with the SNARE four-helix bundle with weak affinity (Kd is around 10 μM), the mixtures of Munc18-1/SNARE four-helix bundle contained three different species: Munc18-1, the SNARE four-helix bundle, Munc18-1/SNARE four-helix bundle complex, and different concentrations of the mixtures included different amounts of the three species (Table 3.1). Therefore, the data of the mixtures were hard to interpret. By applying some scale factors to the data of the mixtures to

subtract the data from free Munc18-1 and free SNARE four-helix bundle, we obtained one reasonable complex envelope, which can be fitted well with the crystal structures of Munc18-1 and the SNARE four-helix bundle (Figure 3.11C). The fitted complex envelope suggests that Munc18-1 interacts with one end of the SNARE four-helix bundle through the cavity, which is consistent with the NMR data that Munc18-1 binds to the C-terminal part of the SNARE four-helix bundle. However, the data need further and careful analysis and interpretation.

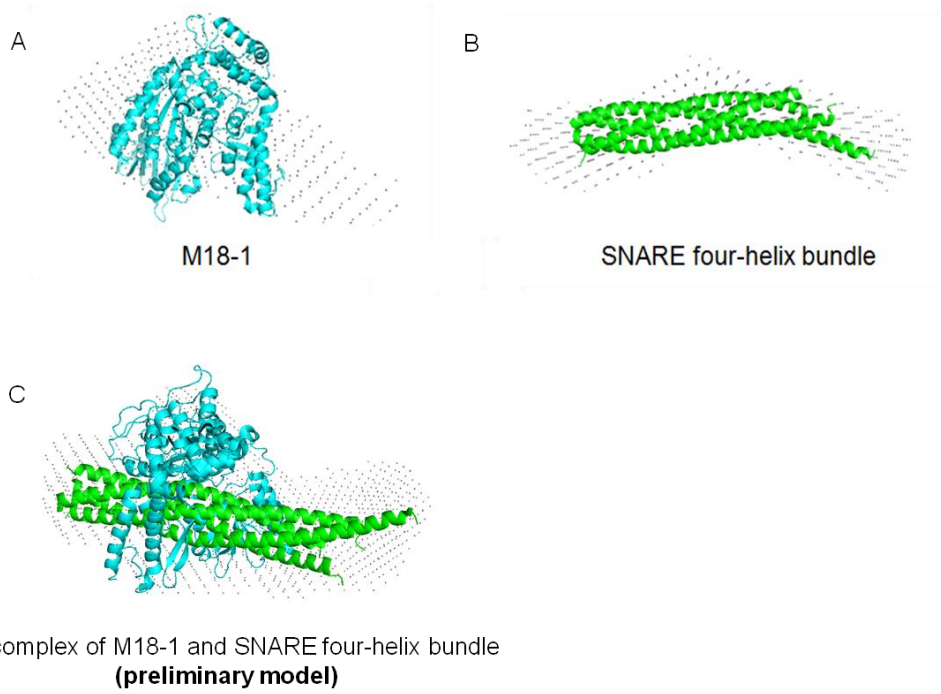

Figure 3.11 SAXS profiles of Munc18-1, the SNARE four-helix bundle, and the complex of Munc18-1/SNARE four-helix bundle.

(A) Structural envelope of Munc18-1 generated by ATSAS2.4 from SAXS data in grey dots and ribbon diagram of the crystal structure of Munc18-1 in blue; (B) Structural envelope of the SNARE four-helix bundle generated by ATSAS2.4 from SAXS data in grey dots and ribbon diagram of the crystal structure of the SNARE four-helix bundle in blue; (C) Structural envelope of the mixture of Munc18-1/SNARE four-helix bundle generated by ATSAS2.4 from SAXS data in grey dots and ribbon diagram of the crystal structures of Munc18-1 and the SNARE four-helix bundle in blue.

Mixture of Munc18-1 and the SNARE four-helix bundle (1:1) concentration (μM)	Complex of Munc18-1/SNARE four-helix bundle concentration (μM)	Complex of Munc18-1/SNARE four-helix bundle percentage (%)	Free Munc18-1 concentration (μM)	Free SNARE four-helix bundle concentration (μM)
40	24	60	16	16
62	42	68	20	20
100	73	73	27	27

Table 3.1 Different amounts of Munc18-1, the SNARE four-helix bundle, and the complex of Munc18-1/SNARE four-helix bundle in the mixtures of Munc18-1 and the SNARE four-helix bundle.

The concentrations of free Munc18-1, free SNARE four-helix bundle, and the complex of Munc18-1/SNARE four-helix bundle were calculated from Kd (assume Kd=10 μM) and the concentrations of the mixtures of the two proteins. If A represents Munc18-1, B represents the SNARE four-helix bundle, AB represents the complex of Munc18-1/SNARE four-helix bundle. $AB \rightleftharpoons A + B$, $Kd=[A]_{free}[B]_{free}/[AB]=10$ μM. The percentages of the complex of Munc18-1/SNARE four-helix bundle are calculated by dividing the concentrations of this complex to the concentrations of the mixtures of the two proteins.

3.4 Discussion

Despite intensive studies of SM proteins in the recent years, their key roles are largely unclear. Our model (Figure 2.7) together with in vitro reconstitutions (Shen *et al.* 2007; Shen *et al.* 2010) suggest that Munc18-1 might be directly involved in membrane fusion and that interaction of Munc18-1 with the SNARE four-helix bundle might be key to uncover its crucial role in neurotransmitter release. To investigate whether this interaction is physiologically relevant, the best way is to understand the complex structure first, perform mutagenesis to disrupt their interaction, and then test the impairments of neurotransmitter release of these mutants in vivo. However, the interaction between Munc18-1 and the SNARE four-helix bundle is weak, so it is technically hard to solve the complex structure.

By applying ITC and NMR spectroscopy, I was able to get some data that suggest that Munc18N binds to the SNARE four-helix bundle tighter than Munc18-1, and that the C-terminal part of the SNARE four-helix bundle is involved in binding, especially synaptobrevin and syntaxin-1. NMR data also showed that Munc18N and complexin simultaneously bind to the SNARE four-helix bundle. SAXS data suggest that Munc18-1 binds to one end of the SNARE four-helix bundle, and that in solution the relative orientation between domain 1 and domain 3a of Munc18-1 is flexible, which implies that there might be an allosteric regulation of Munc18-1 in vivo.

The finding that Munc18N binds tighter than Munc18-1 full length protein to the SNARE four-helix bundle is very interesting. Data from our previous paper (Xu *et al.* 2010) suggest that the binding of Munc18-1/SNARE four-helix bundle involves the Munc18-1 cavity. Munc18N provides a major contact surface of the cavity but not all, so it would make sense that Munc18N interacts with the SNARE four-helix bundle weaker than full length Munc18-1. However, the

result is opposite to our hypothesis, which implies that Munc18-1 needs a conformation change in order to bind better to the SNARE four-helix bundle. This finding is consistent with SAXS data that the relative orientation between domain 1 and domain 3a of Munc18-1 is flexible in solution. Our data suggest a view that in vivo Munc18-1 might require an activator or a modification to regulate its conformation so as to exert its critical function in fusion. In addition, our results showed that Munc18N binds to the C-terminal part of syntaxin-1 and synaptobrevin on the SNARE four-helix bundle, which is consistent with the SAXS result that Munc18-1 full length protein binds to one end of the SNARE four-helix bundle. These results are intriguing because they really place Munc18-1 right at the site where membrane fusion occurs, which suggest that Munc18-1 might be directly involved in membrane fusion. Such a role together with the allosteric regulation could certainly explain the critical nature of Munc18-1 and SM proteins for membrane fusion in vivo.

The results that the C-terminal part of syntaxin-1 and synaptobrevin are involved in Munc18N binding raise one question: does Munc18N (Munc18-1) and complexin bind together to the SNARE four-helix bundle? The complexin central helix binds to the SNARE four-helix bundle through the groove of syntaxin-1 and synaptobrevin (Chen *et al.* 2002), and complexin plays important roles in late stage of neurotransmitter release. If complexin and Munc18-1 cannot simultaneously bind to the SNARE four-helix bundle, it would argue against our hypothesis that Munc18-1 is directly involved in fusion through interaction to the SNARE four-helix bundle. Our NMR results suggest that these three proteins bind together, which supports our hypothesis.

Our data presented here are not very conclusive and they need further validation because of several problems: i) Munc18-1 is a big molecule (70Kd) and it is destabilized when deuterated;

ii) The interaction between Munc18/SNARE four-helix bundle complex is weak; iii) Munc18N is intrinsically unstable in isolation and undergoes some conformational change when it binds to the SNARE four-helix bundle. These problems make it really hard to get good data by NMR spectroscopy and to solve the structure of the complex. In this case of weak interaction, SAXS and X-ray crystallography are not very ideal methods to tackle the problem, although I did not try a lot in both methods. Further investigations need to be carried out to overcome the difficulties, to validate the data presented here, and eventually to solve the complex structure and to perform in vivo studies to uncover the key role of Munc18-1 in neurotransmitter release.

Chapter 4 Reconstitution of the vital functions of Munc18-1 and Munc13 in neurotransmitter release

4.1 Introduction

The release of neurotransmitters by Ca^{2+}-triggered synaptic vesicle exocytosis is crucial for neural function. The machinery that controls this process contains proteins that have homologues in most types of intracellular membrane traffic and underlie a conserved mechanism of membrane fusion, including N-ethylmaleimide sensitive factor (NSF), soluble NSF adaptor proteins (SNAPs), the neuronal SNAP receptors (SNAREs) synaptobrevin, syntaxin-1 and SNAP-25, and the Sec1/Munc18 (SM) protein Munc18-1 [reviewed in (Brunger 2005; Jahn *et al.* 2006; Rizo *et al.* 2008; Sudhof *et al.* 2009)]. The SNAREs form a tight four-helix bundle called SNARE complex that brings the synaptic vesicle and plasma membranes together (Sollner *et al.* 1993; Hanson *et al.* 1997; Poirier *et al.* 1998; Sutton *et al.* 1998), which is key for fusion. NSF/SNAPs disassemble the SNARE complex (Sollner *et al.* 1993) to recycle the SNAREs for another round of fusion (Banerjee *et al.* 1996; Mayer *et al.* 1996). Munc18-1 binds to a self-inhibited 'closed' conformation of syntaxin-1, an interaction that gates entry of syntaxin-1 into SNARE complexes and is not conserved in some other systems (Carr *et al.* 1999; Dulubova *et al.* 1999; Misura *et al.* 2000; Sudhof 2004; Gerber *et al.* 2008). In addition, Munc18-1 binds to SNARE complexes and likely cooperates with the SNAREs in membrane fusion by an as yet unclear mechanism (Dulubova *et al.* 2007; Shen *et al.* 2007). Synaptic vesicle fusion also depends critically on factors that are specialized for the exquisite regulation of neurotransmitter release. Particularly important are the Ca^{2+} sensor synaptotagmin-1 (Fernandez-Chacon *et al.* 2001) and the large active zone proteins Munc13s, which play an essential role through their MUN domain (Basu *et al.* 2005; Madison *et al.* 2005; Stevens *et al.* 2005) and modulate release through other domains [e.g. (Rhee *et al.* 2002; Shin *et al.* 2010)]. The Munc13 MUN domain

catalyzes the opening of syntaxin-1 (Ma *et al.* 2011) and is related to tethering factors from other membrane traffic systems, suggesting that the MUN domain may in addition have a universal function in docking and/or fusion (Pei *et al.* 2009; Li *et al.* 2011).

Despite these advances, a coherent model that can explain the importance of all these eight central components of the release machinery has not emerged yet. A particularly fundamental question is why Munc18-1 and Munc13s are so crucial for exocytosis in vivo (Wu *et al.* 1998; Aravamudan *et al.* 1999; Augustin *et al.* 1999; Richmond *et al.* 1999), which is emphasized by the total abrogation of neurotransmitter release observed in the absence of Munc18-1 or Munc13-1/2 [the strongest phenotypes observed so far with the high resolution of electrophysiology in mammalian synapses (Verhage *et al.* 2000; Varoqueaux *et al.* 2002)]. Attempts to reconstitute synaptic vesicle fusion with purified components have provided seminal insights into the mechanism of release, but they have not answered this vital question.

Reconstitution studies showed that the neuronal SNAREs alone can induce lipid mixing between liposomes (Weber *et al.* 1998), and that this activity can be enhanced by Munc18-1 (Shen *et al.* 2007; Rodkey *et al.* 2008; Diao *et al.* 2010), by synaptotagmin-1 (Tucker *et al.* 2004), and by Munc13-4 (Boswell *et al.* 2012) or the related protein CAPS (James *et al.* 2009), which also contains a MUN domain. Moreover, evidence for content mixing was provided in reconstitutions with neuronal SNAREs alone (Nickel *et al.* 1999; van den Bogaart *et al.* 2010) and together with synaptotagmin-1 (Kyoung *et al.* 2011) or CAPS (James *et al.* 2009). However, the combined effects of all these factors have not been studied, in contrast to the more comprehensive reconstitutions performed in other membrane traffic systems (Mima *et al.* 2008; Ohya *et al.* 2009; Stroupe *et al.* 2009). Particularly intriguing among the results obtained with the neuronal proteins is the observation that the activity of the SNAREs in reconstitution assays is

dramatically stimulated by synaptotagmin-1 in the presence of Ca^{2+} and that some features of such stimulation correlate with physiological observations (Stein *et al.* 2007; Chicka *et al.* 2008; Xue *et al.* 2008; Lee *et al.* 2010; Kyoung *et al.* 2011; van den Bogaart *et al.* 2011). At the same time, these findings are puzzling because they were obtained without Munc18-1 and Munc13s, and hence contrast with the crucial importance of these proteins for neurotransmitter release.

It is also worth noting that most of these studies did not include NSF and SNAPs, and used reconstituted syntaxin-1/SNAP-25 heterodimers (often referred to as t-SNARE complexes), assuming that these heterodimers are obligatory intermediates in the membrane fusion pathway. However, early data showed that NSF/SNAPs inhibit the activity of the SNAREs in inducing lipid mixing because they disassemble the syntaxin-1/SNAP-25 heterodimers (Weber *et al.* 2000). Moreover, it is plausible that the correct starting point is the binary syntaxin-1/Munc18-1 complex, since syntaxin-1 and Munc18-1 stabilize each other in vivo (Verhage *et al.* 2000; Gerber *et al.* 2008), and may travel together to the plasma membrane (Medine *et al.* 2007). Interestingly, in reconstitutions started with syntaxin-1, Munc18-1 had inhibitory and stimulatory effects of Munc18-1 on lipid mixing that may reflect at least in part the multiple roles of this protein (Schollmeier *et al.* 2011), but the effects of other factors were not studied.

In the research presented here, we sought to develop a model of synaptic vesicle fusion that integrates the functions of the neuronal SNAREs, Munc18-1, Munc13s, NSF, SNAPs and synaptotagmin-1, expecting that such a model could explain why Munc18-1 and Munc13s are so crucial for neurotransmitter release and could thus bridge the large gap existing between the available reconstitution and physiological data. We show that Munc18-1 binding to syntaxin-1 displaces SNAP-25 from syntaxin-1/SNAP-25 heterodimers, which is aided by NSF/α-SNAP on membranes. We reconstituted co-expressed syntaxin-1/Munc18-1 into proteoliposomes and

observed efficient lipid and content mixing with synaptobrevin proteoliposomes that requires Ca^{2+}, SNAP-25, and core fragments of Munc13-1 and synaptotagmin-1. We also found that the efficient lipid mixing between liposomes containing syntaxin-1/SNAP-25 heterodimers and synaptobrevin-liposomes occurring in the presence of Ca^{2+}/synaptotagmin-1 is strongly inhibited by NSF/α-SNAP, but is activated upon further addition of Munc18-1 and Munc13-1. These results suggest that our system reconstitutes basic steps of synaptic vesicle fusion in a manner that requires Munc18-1 and Munc13-1, as observed in vivo, and that in addition incorporates the three neuronal SNAREs, NSF, α-SNAP, synaptotagmin-1 and Ca^{2+}. We propose a model whereby syntaxin-1/heterodimers are disassembled by NSF/SNAPs and synaptic vesicle fusion starts with closed syntaxin-1 bound to Munc18-1, which orchestrates SNARE complex assembly together with Munc13s through a pathway that is not inhibited by NSF/α-SNAP and allows the exquisite regulation of neurotransmitter release.

4.2 Materials and methods

4.2.1 Recombinant DNA constructs

Bacteria expression vectors to express full-length rat synaptobrevin and its cytoplasmic domain (residues 29-93), full length rat syntaxin-1A and its cytoplasmic domain (2-253), human SNAP-25B full-length (with its four cysteins mutated to serines), the SNARE motifs of human SNAP-25B (SNN, residues 11-82; and SNC, residues 141-203), full-length rat Munc18-1, full-length squid Munc18-1, rat Munc13-1 MUN domain (residues 859-1407,EF,1453-1531), rat Munc13-1 fragment C1C2BMUN (residues 529-1407,EF,1453-1531), co-expressed Munc18-1/syntaxin-1, co-expressed syntaxin-1/SNAP-25, NSF, α-SNAP, and the rat synaptotagmin-1 C2AB fragment (residues 140-421) were available in the lab. Note that the MUN domain and

C1C2BMUN contained a partial deletion in a long loop that promotes aggregation [see (Rizo *et al.* 2008; Ma *et al.* 2011)].

4.2.2 Expression and purification of recombinant proteins

4.2.2.1 Expression and purification of C1C2BMUN

To generate a vector to express the C1C2BMUN fragment of rat Munc13-1 with the same loop deletion as the MUN domain (residues 529-1407, EF, 1453-1531), we cloned a DNA sequence encoding Munc13-1(529-1531) into the pFastBacTMHT B vector (invitrogen), which contains a polyhedron promoter (for hight-level expression of recombinant protein in insect cell) before the start codon and encodes an N-terminal TEV cleavable His_6 tag. The loop deletion was then performed using QickChange (Stratagene). The construct was used to generate a baculovirus using the Bac-to-Bac system (Invitrogen). Insect cells (sf9) were infected with the baculovirus, harvested about 68-72 hours post-infection, and resuspended in lysis buffer (50 mM Tris 8.0, 250 mM Nacl, 10 mM imidazole). Cells were lysed through one freeze and thaw circle. The cell lysate was centrifuged at 18,000 rpm for 45 minutes, and the clear supernatant was incubated with Ni2+-NTA agarose at 4 ℃ for 2 hours. The beads were washed with: i) lysis buffer; ii) lysis buffer containing 1% Triton-100; iii) lysis buffer containing 1 M NaCl; and iv) lysis buffer. The protein was eluted with 200 mM imidazole and the His_6-tag was removed by incubation with TEV protease at 4 ℃ overnight. The protein was further purified by ion exchange chromatography and gel filtration, and was concentrated to 9 mg/ml for storage in 10 mM Tris buffer (pH 8.0) containing 10% glycerol and 250 mM NaCl.

4.2.2.2 Expression and purification of NSF and α-SNAP

NSF and α-SNAP were cloned from a pQE9 vector into a pGEX-KG vector. Both proteins were expressed in BL21 E.Coli cells in LB media. NSF was induced with 0.4 mM IPTG at 20 ℃ for 20 hrs. α-SNAP was induced with 0.4 mM IPTG at 25 ℃ for 18 hrs. Cells were re-suspended in a buffer containing 50 mM HEPES pH7.6, 400 mM KCl, 10% glycerol (v/v), and 2 mM DTT. The cells were lysed with an Avestin cell disruptor and the lysate was clarified by centrifugation at 20,000 rpm for 30 minutes. The supernatant was incubated with Glutathione Sepharose 4B (GE Healthcare) at 4 ℃ overnight. The bound proteins were washed with PBS, PBS with 1% Triton X-100, and then PBS with 500 mM NaCl. The GST-tag was cleaved from the proteins by thrombin cleavage at 4 ℃ overnight on the beads. The proteins were further purified by sizeexclusion chromatography using a Superdex 75 (for α-SNAP) or Superdex 200 (for NSF) column in a buffer containing 20 mM HEPES pH7.6, 150 mM KCl, 10% glycerol (v/v), 1 mM DTT. For NSF purification, all buffers contain 0.5 mM ATP.

4.2.2.3 Co-expression and purification of Munc18-1 and full-length syntaxin-1

A pET-DUET vector (Novagen) to co-express N-terminally His_6-tagged full-length rat Munc18-1 and full-length rat syntaxin-1A in BL21 E. coli cells was constructed using standard recombinant DNA methods. Cells were grown in LB media and induced with 0.4 mM IPTG at an optical density A600=1.0 for 18 hrs at 23 ℃. Cells were harvested and lysed with an Avestin cell disruptor in buffer containing 50 mM Tris pH 8.0, 300 mM KCl, 10% glycerol, 1% TX-100 and 0.3 mM TCEP. The cell lysate was centrifuged at 20,000 rpm for 30 minutes. The supernatant was incubated with Ni^{2+} - nitrilotriacetic acid (NTA) Agarose (QIAGEN) at room temperature for 1 hr. The bound proteins were first washed with buffer containing 50 mM Tris pH 8.0, 300 mM KCl, 10% glycerol (v/v), 0.5% TX-100 and 0.3 mM TCEP, and then washed

with the same buffer containing 20 mM imidazole and 1% CHAPS instead of 0.5% TX-100. The bound proteins were eluted in the same buffer containing 250 mM imidazole and 1% CHAPS. The eluted proteins were purified by size-exclusion chromatography using a superdex 200 10/300 column in a buffer containing 20 mM Tris pH8.0, 150 mM KCl, 10% glycerol (v/v), 1% CHAPS, and 0.5 mM TCEP.

4.2.2.4 Co-expression and purification of full-length syntaxin-1 and SNAP25

Recombinant rat full-length syntaxin and human SNAP25B were co-expressed and purified basically as described (Misura *et al.* 2000), but with some modifications. BL21 E. Coli cells were grown in Terrific Broth media. Cells were induced with 0.4 mM IPTG to an optical density A600=1.0 for 20 hrs at 25 ℃. Cells were lysed with an Avestin cell disruptor in buffer A (50 mM Tris pH 8.0, 500 mM NaCl, 5% glycerol, 1% Triton X-100, 20 mM imidazole, and 10 mM 2-Mercaptoethanol). Cell lysate was clarified by centrifugation at 20,000 rpm for 30 minutes. The supernatant was incubated with Ni^{2+}-NTA Agarose (QIAGEN) at room temperature for 1 hr. The bound proteins were first washed with buffer A, then washed with buffer B (50 mM Tris pH 8.0, 200 mM NaCl, 1% w/v octyl-β-D-glucopyranoside (β-OG), 5% glycerol (v/v), and 50 mM imidazole), and then eluted with buffer B containing 250 mM imidazole instead of 50 mM imidazole. The eluted proteins were further purified by ion exchange chromatography on Mono Q with buffers containing β-OG.

4.2.2.5 Expression and purification of other recombinant proteins

The expression and purification of other recombinant proteins were similar to those described in previous chapter. Isotopic labeling to obtain ^{2}H-Ile-$^{13}CH_3$-syntaxin-1 was performed using well-established procedures (Tugarinov *et al.* 2004).

4.2.3 NMR spectroscopy

^{1}H-^{13}C HMQC spectra were acquired at 25 ^{o}C on a Varian INOVA800 spectrometer. Samples contained 12-20 μM ^{2}H-Ile-$^{13}CH_3$-syntaxin-1 alone or with different additions (Munc18-1, sMunc18-1 and/or SNAP-25 were added in a 20% excess). Samples were dissolved in 20 mM Tris pH 8.0, 150 mM NaCl, 2 mM TCEP, using D2O as the solvent. Spectra were acquired with a 2.3 hour total acquisition time.

4.2.4 Lipid mixing assay using syntaxin-1/Munc18-1 liposomes

All lipids were purchased from Avanti Polar Lipid. Donor (synaptobrevin) liposomes contained 60% POPC, 17% POPE, 20% DOPS, 1.5% NBD-PE and 1.5% Rhodamine-PE. Acceptor (syntaxin-1/Munc18-1) liposomes contained 58% POPC, 20% POPE, 18% DOPS, 2% PIP2 and 2% DAG. Lipid mixtures were dried in glass tubes with nitrogen gas and under vacuum overnight. Lipid films were re-suspended in buffer buffer C (25 mM HEPES, pH 7.4, 150 mM KCl, 1 mM DTT, 10% glycerol (v/v)) and vortexed for at least 5 min. The re-suspended lipid films were frozen and thawed five times, and then extruded through a 50 nm polycarbonate filter with an Avanti extruder for at least 29 times. Purified proteins in buffer containing 1% CHAPS were added slowly to liposomes (5 mM lipids) to make the final concentration of CHAPS to 0.4%. The P/L ratio ranged from 1:500 to 1:1000 for the synaptobrevin liposomes, and from 1:1000 to 1:2000 for the syntaxin-1/Munc18-1 liposomes. The liposome protein mixtures were incubated at room temperature for 40 minutes and then dialyzed extensively with 1g/L Bio-beads SM2 (Bio-Rad) 3 times in 20 mM HEPES, pH 7.4, 150 mM KCl, 1 mM DTT, 10% glycerol (v/v) at 4 ℃. For lipid mixing assays, donor liposomes (0.25 mM lipids) were mixed with acceptor liposomes (0.5 mM lipids) in the presence of 1 μM C1C2BMUN, 5 μM SNAP-25, 2 μM C2AB fragment and/or 0.5 mM Ca2+ (as indicated in the figures) in a total

volume of 80 µl. NBD fluorescence emission at 538 nm (excitation 460 nm) was monitored with a PTI Spectrofluorometer. All experiments were performed at 30 ℃. At the end of each reaction, 1% w/v β-OG was added to solubilize the liposomes. Because of considerable variability in the fluorescence intensity observed upon detergent addition, which may arise from partial precipitation, we find that we obtain more consistent results by first converting the time traces to F1/F0, where F1 is the observed fluorescence intensity and F0 is the initial intensity, and then we average the F1/F0 value observed upon detergent addition for an entire set of experiments. This average is then used to normalize all the traces to express the data as % of maximum fluorescence.

4.2.5 Lipid mixing assay using syntaxin-1/SNAP-25 liposomes

Donor (synaptobrevin) liposomes and acceptor (syntaxin-1/SNAP25) liposomes contained the same lipid compositions described above. Lipid mixtures were dried in glass tubes with nitrogen gas and under vacuum overnight. Lipid films were re-suspended and dissolved in buffer C with 1.2% β-OG. Purified proteins in buffer containing 1% β-OG were added to liposomes (5 mM lipids) to make the P/L ratio 1:600. The mixtures were incubated at room temperature for 40 minutes and dialyzed extensively with 1g/L Bio-beads SM2 (Bio-Rad) 3 times in buffer C. For lipid mixing assays, donor liposomes (0.25 mM) were mixed with acceptor liposomes (0.5 mM) with different additions in a total volume of 80 µl. For experiments with NSF/α-SNAP, acceptor liposomes were first incubated with 0.1 µM NSF, 0.5 µM α-SNAP, 5 mM $MgCl_2$ and 2 mM ATP at 37 ℃ for 20minutes, and then mixed with donor liposomes with different additions, which included 0.5 µM Munc18-1, 1 µM C1C2BMUN, 2 µM C2AB fragment, 0.5 mM Ca^{2+}, and excess SNAP-25 as indicated in the figures. All experiments were

performed at 37 ℃. At the end of each reaction, 1% w/v β-OG was added to solubilize the liposomes, and the data were analyzed as described above.

4.2.6 Content mixing assay

Donor (synaptobrevin) liposomes contained 44.5% POPC, 20% POPE, 12% DOPS, 20% cholesterol, 3.5% DiD (Invitrogen). Lipid mixtures were dried in glass tubes with nitrogen gas and under vacuum overnight. Lipid films were re-suspended and dissolved in buffer C containing 1% w/v β-OG and 40mM sulforhodamine B (Acros Organics). Purified full-length synaptobrevin in buffer containing 1% w/v β-OG was added to the lipid mixtures to make the final concentration of lipids 5 mM and the P/L ratio 1:500. The protein lipid mixtures were diluted 4 times (keeping the sulforhodamine concentration at 40 mM) to allow liposome formation, and then were incubated at room temperature for 40 minutes. The liposomes were purified with a Superose 6 column. The first 1 ml sample coming out in the void volume was collected and dialyzed in 150 ml detergent free buffer (20 mM HEPES pH 7.4, 150 mM KCl, 1 mM DTT) containing 10 g of Amberlite XAD2 3 times at 4 ^{o}C (2 times 2 hrs and one time overnight). The resulting lipid concentration was determined by UV. Acceptor (syntaxin-1/Munc18-1) liposomes were prepared with the same method described for the lipid mixing assays. Lipid mixing and content mixing were monitored as described for the lipid mixing assays by measuring dequenching of DiD (excited at 650 nm, emission at 675 nm) and sulforhodamine B (excited at 565 nm, emission at 587 nm).

4.2.7 Liposome co-floatation assays

Proteoliposomes containing syntaxin-1/Munc18-1 complex were prepared as described below with a protein/lipid (P/L) ratio of 1:1000. Solutions containing 4 mM lipids (4 μM

syntaxin-1/Munc18-1 complex) were incubated with 10 μM SNAP-25 at room temperature for 1 hr. The proteoliposomes and bound proteins were isolated by floatation on a Histodenz density gradient (40%:35%:30%) as described (Guan *et al.* 2008). Samples from the top of the gradient (35 μl) were taken and analyzed by SDS-PAGE and Coomassie blue staining. For experiments with reconstituted full-length syntaxin-1, proteoliposomes containing PC:PE:PS:PIP2 (60:18:20:2) at a P/L ratio of 1:500 were prepared as previously described for a syntaxin-1(183-288) fragment (Chen *et al.* 2006). The syntaxin-1 proteoliposomes were then dialyzed with 1g/L Bio-beads SM2 (Bio-Rad) 3 times in 25 mM HEPES pH 7.3, 150 mM KCl, 10% glycerol (v/v) at 4 ℃ overnight to remove the detergent. The syntaxin-1 liposomes were incubated with SNAP-25 at 4 ℃ for 2h and contained 3 μM syntaxin-1 and 6 μM SNAP-25 after addition of different reagents, which included 5 μM Munc18-1, 0.5 μM NSF, 1 μM α-SNAP, 2 mM ATP, 5 mM $MgCl_2$ or 5 mM EDTA. After incubation at 37 ℃ for 1 hr, the proteoliposomes were isolated by floatation on a Histodenz density gradient (40%:35%:30%) and samples at the top (35 μl) were taken and analyzed by SDS-PAGE and Coomassie blue staining.

4.3 Results

4.3.1 Munc18-1 displaces SNAP-25 from syntaxin-1 in solution

This work stems from our previous efforts to understand the critical role of Munc13-1 in neurotransmitter release and its relation to Munc18-1 and SNARE function. Dr. Cong Ma from the lab showed that Munc13-1 MUN domain dramatically accelerates the transition from the closed syntaxin-1/Munc18-1 complex to the SNARE complex (Ma *et al.* 2011). Since many models of neurotransmitter release assume that syntaxin-1/SNAP-25 heterodimers are obligatory intermediates that are formed downstream of the syntaxin-1/Munc18-1 complex, Dr. Cong Ma investigated whether the MUN domain can also accelerate the transition from the latter complex

to the former. For this purpose, he used NMR spectroscopy, taking advantage of the power of ^{1}H-^{13}C heteronuclear multiple quantum coherence (HMQC) spectra to distinguish between different states of syntaxin-1 cytoplasmic region (residues 2-253) specifically ^{1}H,^{13}C-labeled at Ile methyl groups (^{2}H-Ile-$^{13}CH_3$-syntaxin-1) (Ma *et al.* 2011). Thus, multiple changes were observed when ^{1}H-^{13}C HMQC spectra were acquired on samples of ^{2}H-Ile-$^{13}CH_3$-syntaxin-1 alone, assembled in the SNARE complex, or bound to Munc18-1 or SNAP-25 (Figures 4.1A-C).

He acquired consecutive 2-hr ^{1}H-^{13}C HMQC spectra of ^{2}H-Ile-$^{13}CH_3$-syntaxin-1 bound to Munc18-1 after addition of the N- and C-terminal SNARE motifs of SNAP-25 (SNN and SNC, respectively) to test whether SNN and SNC can displace Munc18-1 from syntaxin-1. However, no spectral changes were observed after long incubations whether a fragment spanning the Munc13-1 MUN was present (Figure 4.1D) or absent (Figure 4.1I). This result contrasts with the efficient formation of the SNARE complex observed in analogous experiments performed in the presence of synaptobrevin and the MUN domain (Ma *et al.* 2011), suggesting that synaptobrevin (in addition to SNAP-25) is required to open the conformation of syntaxin-1 bound to Munc18-1.

To test whether the opposite reaction can occur, i.e. whether Munc18-1 can displace SNAP-25 from syntaxin-1, he used squid Munc18-1 (sMunc18-1), since it is more soluble in isolation and forms similar complexes with the mammalian SNAREs as rat Munc18-1 (Xu *et al.* 2010), as confirmed in part by the similarity of the ^{1}H-^{13}C HMQC spectra of ^{2}H-Ile-$^{13}CH_3$-syntaxin-1 bound to rat Munc18-1 or sMunc18-1 (Figures 4.1A,E). Importantly, ^{1}H-^{13}C HMQC spectra of ^{2}H-Ile-$^{13}CH_3$-syntaxin-1 bound to SNAP-25 showed gradual changes upon addition of sMunc18-1 that revealed quantitative formation of the closed syntaxin-1/sMunc18-1 complex after several hours (Figures 4.1F,G). To confirm this result by a different method, he used FRET assays starting with complexes between the SNAP-25 SNARE motifs and syntaxin-1(2-253) that

were labeled with a donor fluorescent probe on SNC and an acceptor fluorescent probe on syntaxin-1 to yield efficient FRET. Addition of Munc18-1 caused a gradual increase in donor fluorescence that can be attributed to loss of FRET because of displacement of SNAP-25 from syntaxin-1 by Munc18-1, whereas addition of MUN domain instead of Munc18-1 did not cause any changes, showing the specificity of the reaction (Figure 4.1H). Interestingly, the fluorescence increase caused by Munc18-1 was enhanced in the presence of MUN domain, suggesting that the MUN domain accelerates the reversal from the syntaxin-1/SNAP-25 complex to the syntaxin-1/Munc18-1 complex. Together with his previous results showing a MUN-domain-induced acceleration of SNARE complex assembly starting from syntaxin-1/Munc18-1 (Ma *et al.* 2011), these results suggest that the MUN domain acts as a catalyst of both opening and closing of syntaxin-1.

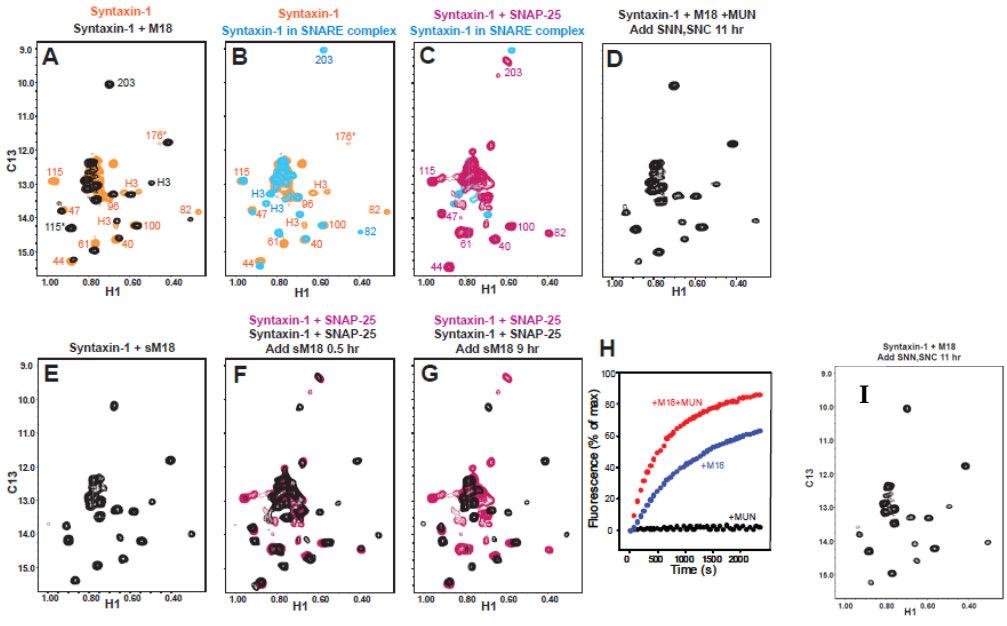
Syntaxin-1
Syntaxin-1 + M18
A
Syntaxin-1
Syntaxin-1 in SNARE complex
B
Syntaxin-1 + SNAP-25
Syntaxin-1 in SNARE complex
C
Syntaxin-1 + M18 +MUN
Add SNN,SNC 11 hr
D
Syntaxin-1 + sM18
E
Syntaxin-1 + SNAP-25
Syntaxin-1 + SNAP-25
Add sM18 0.5 hr
F
Syntaxin-1 + SNAP-25
Syntaxin-1 + SNAP-25
Add sM18 9 hr
G
H
+M18+MUN
+M18
+MUN
Fluorescence (% of max)
Time (s)
Syntaxin-1 + M18
Add SNN,SNC 11 hr
I
C13
H1

Figure 4.1

Figure 4.1 Munc18-1 displaces SNAP-25 from syntaxin-1 in solution.

(**A-G**) ^{1}H-^{13}C HMQC spectra of ^{2}H-Ile-$^{13}CH_3$-syntaxin-1 alone (orange) or bound to Munc18-1 (black) (**A**); alone (orange) or forming the SNARE complex with the synaptobrevin and SNAP-25 SNARE motifs (blue) (**B**); forming the SNARE complex (blue) or bound to SNAP-25 (magenta) (**C**); bound to Munc18-1 after incubation with the SNAP-25 SNARE motifs (SNN and SNC) for 11 hr in the presence of the Munc13-1 MUN domain (black) (**D**); bound to sMunc18-1 (**E**); bound to SNAP-25 (magenta) or bound to SNAP-25 after incubation with sMunc18-1 for 0.5 hr (black) (**F**); and bound to SNAP-25 (magenta) or bound to SNAP-25 after incubation with sMunc18-1 for 9 hr (black) (**G**). Note that after 9 hr the spectrum is analogous to that in panel **E**, showing that 2H-Ile-13CH3-syntaxin- 1 was released from SNAP-25 and bound to sMunc18-1, and that only partial displacement was observed in the spectrum acquired after 0.5 hr incubation with sMunc18-1 (black in panel **F**). The cross-peak assignments that are available for isolated syntaxin-1 (Dulubova *et al.* 1999; Chen *et al.* 2008) are indicated in orange in **A,B**. Cross-peaks that move considerably upon formation of the syntaxin-1/Munc18-1 complex or the SNARE complex are indicated in black in **A** or in blue in **B**, respectively. H3 identifies cross-peaks that are known to belong to the SNARE motif but do not have residue-specific assignment; * indicates tentative assignments. (**H**) The Munc13-1 MUN domain accelerates the transition from the syntaxin-1/SNAP-25 complex to the syntaxin-1/Munc18-1 complex. Syntaxin-1 cytoplasmic region (residues 2-253) labeled with rhodamine at residue 249 was incubated with SNN and SNC that was labeled with BODIPY at residue 187. The BODIPY fluorescence, which decreases upon formation of the syntaxin-1/SNN/SNC complex due to efficient FRET with the rhodamine label on syntaxin-1, was monitored and the sample was incubated until the BODIPY fluorescence reached a plateau that indicated completion of the reaction. Munc18-1, Munc13-1 MUN domain or both were added and then we monitored the increase in BODIPY fluorescence resulting from loss of FRET as syntaxin-1 binds to Munc18-1 and SNN/SNC are released. The three curves were normalized to the extrapolated maximum fluorescence in the presence of Munc18-1 and MUN domain. (I) The SNAP-25 SNARE motifs cannot displace Munc18-1 from syntaxin-1. The diagram shows a ^{1}H-^{13}C HMQC spectrum of ^{2}H-Ile-$^{13}CH_3$-syntaxin-1 bound to Munc18-1 after incubation with the SNAP-25 SNARE motifs (SNN and SNC) for 11 hr (black).

4.3.2 NSF/α-SNAP facilitate displacement of SNAP-25 from syntaxin-1 by Munc18-1 on membranes

Dr. Cong Ma's results show that the cytoplasmic region of syntaxin-1 has a much higher affinity for Munc18-1 than for SNAP-25 in solution. To test whether this conclusion applies also to full length syntaxin-1 reconstituted into membranes, he first co-expressed full-length syntaxin-1 and Munc18-1, and reconstituted their complex into proteoliposomes. Co-floatation assays with these proteoliposomes revealed no binding of SNAP-25 (Figure 4.2A), indicating that SNAP-25 cannot displace Munc18-1 to form heterodimers with membrane-anchored syntaxin-1. In my experiments with proteoliposomes containing only syntaxin-1, I did observe co-floatation of SNAP-25, revealing efficient binding to syntaxin-1 (Figure 4.2B, left lane). Addition of Munc18-1 resulted in its co-floatation with the proteoliposomes and only a small decrease in the bound SNAP-25 (Figure 4.2B). This result suggests that most of SNAP-25 remained bound to syntaxin-1 and that Munc18-1 co-floated with the liposomes because it can bind to the syntaxin-1 N-terminal region of the syntaxin-1/SNAP-25 heterodimers (Dulubova *et al.* 2007; Shen *et al.* 2007; Guan *et al.* 2008).

The finding that syntaxin-1/SNAP-25 heterodimers have a tendency to aggregate in detergent solution (Figure 4.2C,D) suggested that release of SNAP-25 by Munc18-1 in these assays might be hindered by aggregation of the syntaxin-1/SNAP-25 heterodimers on the membrane. Since there is evidence that NSF/α-SNAP not only act on SNARE complexes but can also disassemble syntaxin-1/SNAP-25 heterodimers in solution and on membranes (Hanson *et al.* 1995; Weber *et al.* 2000), I tested their effect in the co-floatation assays. Importantly, addition of Munc18-1, NSF/α-SNAP and Mg^{2+}-ATP completely released SNAP-25 from the proteoliposomes while Munc18-1 remain bound, but such release was not observed in the

presence of EDTA and/or absence of Munc18-1 (Figure 4.2B). The natural explanation for these results is that NSF/α-SNAP disassemble the syntaxin-1/SNAP-25 heterodimers, which requires ATP hydrolysis, and such disassembly allows Munc18-1 to ‘capture’ the syntaxin-1 closed conformation, thus preventing the re-binding of the released SNAP-25 to syntaxin-1.

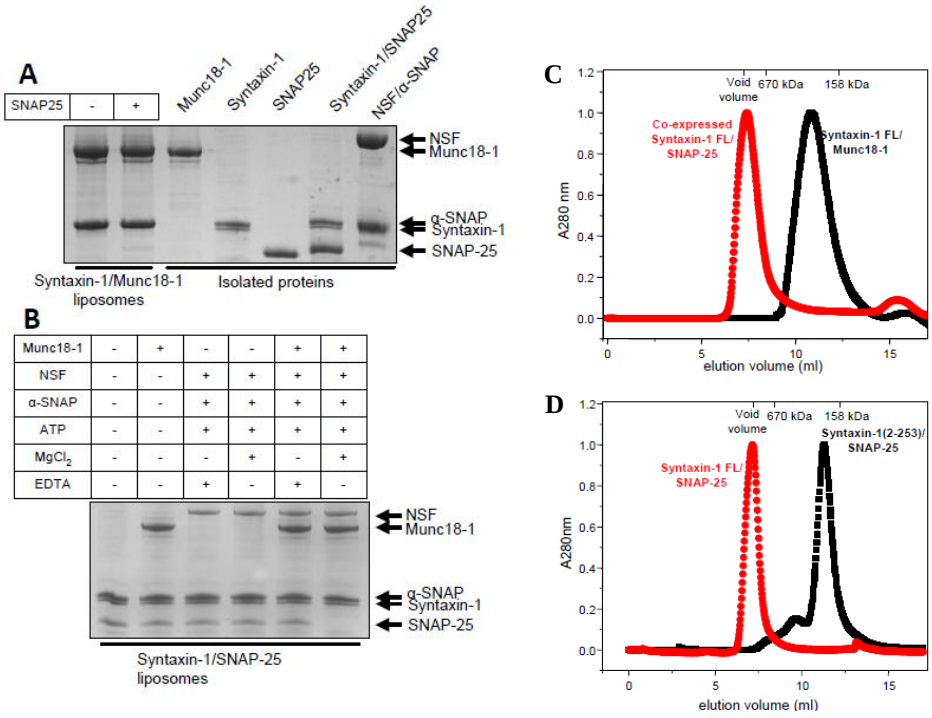
A
SNAP25
-
+
Munc18-1
Syntaxin-1
SNAP25
Syntaxin-1/SNAP25
NSF/α-SNAP
NSF
Munc18-1
α-SNAP
Syntaxin-1
SNAP-25
Syntaxin-1/Munc18-1 liposomes
Isolated proteins
B
Munc18-1
NSF
α-SNAP
ATP
MgCl2
EDTA
NSF
Munc18-1
α-SNAP
Syntaxin-1
SNAP-25
Syntaxin-1/SNAP-25 liposomes
C
Void volume
670 kDa
158 kDa
Co-expressed Syntaxin-1 FL/ SNAP-25
Syntaxin-1 FL/ Munc18-1
A280 nm
elution volume (ml)
D
Void volume
670 kDa
158 kDa
Syntaxin-1(2-253)/ SNAP-25
Syntaxin-1 FL/ SNAP-25
A280nm
elution volume (ml)

Figure 4.2

Figure 4.2 NSF/α-SNAP facilitate displacement of SNAP-25 from syntaxin-1 by Munc18-1, and syntaxin-1/SNAP-25 complexes readily aggregate.

(**A**) Proteoliposomes containing co-expressed syntaxin-1/Munc18-1 complex were incubated with SNAP-25 or buffer and co-floatation assays were performed. The top fraction was analyzed by SDS-PAGE and Coomassie Blue staining (left two lanes). The five lanes on the right show loading controls with soluble proteins for the co-floatation assays in this panel and in panel **B**. (**B**) Proteoliposomes containing syntaxin-1 were incubated with Munc18-1, SNAP-25, NSF, α-SNAP, ATP, Mg2+ and/or EDTA as indicated. Co-floatation assays were then performed and the results analyzed by SDS-PAGE and Coomassie Blue staining. (**C,D**) Gel filtration profiles on Superdex 200 of co-expressed full-length (FL) syntaxin-1 and SNAP-25 complex (red) or FL syntaxin-1 and Munc18-1 complex (black) (**C**), and of FL syntaxin-1/SNAP-25 complex (red) or syntaxin-1(2-253)/SNAP-25 complex (D) formed with separately expressed proteins. The void volume and the elution volumes of molecular weight standards are indicated at the top. Note that the buffer used for chromatography contained 1% CHAPS and, as a result of solvation with detergent micelles and the elongated nature of the complexes, monomeric complexes elute considerably earlier than expected from their molecular weights. Nevertheless, the elution of the FL syntaxin-1/SNAP-25 complexes with the void volume clearly shows the formation of aggregates. In all chromatograms, the UV absorbance at 280 nm was normalized to the maximum value.

4.3.3 Reconstitution of a strict Munc13 requirement for lipid mixing

The above results suggest that the syntaxin-1/Munc18-1 complex may constitute the true starting point for neurotransmitter release in vivo, rather than syntaxin-1/SNAP-25 heterodimers. This postulate might explain the critical importance of Munc13s for neurotransmitter release, since they mediate the transition from the syntaxin-1/Munc18-1 complex to the SNARE complex (Ma *et al.* 2011). Thus, we decided to investigate whether basic features of synaptic vesicle fusion, in particular the strict requirement for Munc13s, can be reproduced in reconstitution experiments started with syntaxin-1/Munc18-1 proteoliposomes.

For the experiments described below we used a Munc13-1 fragment that includes the MUN domain and its preceding C1 and C2B domains (residues 529-1531; referred to as C1C2BMUN). These domains mediate binding to diacylglycerol (DAG) (Rhee *et al.* 2002) and phosphatidylinositol- 4,5-bisphosphate (PIP2) (Shin *et al.* 2010), respectively. To perform some basic characterization of the C1C2BMUN fragment, Dr. Cong Ma tested whether it can accelerate the transition from the syntaxin-1/Munc18-1 complex to the SNARE complex using a FRET assay (Ma *et al.* 2011), and found that the C1C2BMUN fragment has a similar activity as the MUN domain in promoting this transition in solution (Figure 4.3A). We also tested whether the C1C2BMUN fragment binds DAG and PIP2 using liposome co-floatation assays. These experiments showed that both DAG and PIP2 enhance binding of the C1C2BMUN fragment to liposomes, and that there is a clear synergy between both types of lipids in promoting such binding (Figure 4.3B).

To test whether syntaxin-1/Munc18-1 complexes can provide an appropriate starting point for synaptic vesicle fusion, we first used standard lipid mixing assays that monitor dequenching of NBD fluorescence when the lipids of synaptobrevin donor liposomes containing

NBD- and rhodamine-labeled lipids dilute into unlabeled acceptor liposomes, similar to the original reconstitutions with SNAREs alone (Weber *et al.* 1998) but using acceptor proteolipomes that contained syntaxin-1/Munc18-1 complex instead of syntaxin-1/heterodimers (Figure 4.4A). Throughout this work, we used low protein-to-lipid ratios (ranging from 1:500 to 1:2000) and relatively low concentrations of soluble proteins, and we routinely checked that the observed increases in NBD fluorescence intensity reflected true dequenching rather than light scattering caused by liposome clustering [see (Xu *et al.* 2011)]. Unless otherwise specified, the syntaxin-1/Munc18-1 liposomes included DAG and PIP2 to facilitate binding of C1C2BMUN.

To have a quantitative idea of the results obtained under different conditions, we used the NBD fluorescence intensity after 1000 s of reaction (expressed as % from the maximum fluorescence observed upon detergent addition) as a compromise measurement that reflects in part the initial slope and in part the level of completion of the reaction at longer times. The values observed under identical conditions in experiments repeated with the same liposome preparations were then averaged.

When we mixed donor liposomes containing synaptobrevin with the acceptor syntaxin-1/Munc18-1-liposomes, no significant lipid mixing was observed even after addition of SNAP-25 (Figure 4.4B,D). We did observe some (albeit inefficient) lipid mixing when SNAP-25 was added together with C12BMUN either in the presence or absence of Ca^{2+}, and the rate of lipid mixing was dramatically increased when we included a synaptotagmin-1 fragment containing its two C2 domains (C2AB fragment) in addition to SNAP-25, C1C2BMUN and Ca^{2+} (Figure 4.4B,D). Control experiments showed that no lipid mixing occurs in the absence of SNAP-25 or C1C2BMUN and that the synaptobrevin cytoplasmic domain (Sybcd) inhibits the reaction, demonstrating that lipid mixing is SNARE-dependent and strictly requires the Munc13-1

C1C2BMUN fragment (Figures 4.4C,D). This strict requirement is particularly rewarding because it mirrors the essential nature of Munc13s for neurotransmitter release.

To further explore the factors that influence the lipid mixing observed in the presence of SNAP-25, C1C2BMUN and C2AB fragment, I performed a Ca^{2+} titration and found that the efficiency of lipid mixing exhibits a high cooperativity with Ca^{2+}, with a Hill coefficient of 5.9 and half-maximal rate occurring at 250 μM Ca^{2+} (Figure 4.4E,F). These Ca^{2+} concentrations are somewhat higher than those required for neurotransmitter release at the Calyx of Held but comparable to those estimated for other systems, and the Ca^{2+} cooperativity resembles that of neurotransmitter release, which occurs with a Hill coefficient of 5 (Meinrenken *et al.* 2003; Schneggenburger *et al.* 2005). We also examined how the observed lipid mixing depends on DAG and PIP2, agents that underlie the stimulation of neurotransmitter release during presynaptic plasticity processes mediated by the Munc13 C1 and C2B domains. Removal of either DAG or PIP2 led to a considerable decrease in the rate of lipid mixing, which was accentuated when both DAG and PIP2 were absent (Figure 4.4G,H). These results suggest that these two types of lipids play a synergistic role in attracting C1C2BMUN to the membrane, thus enhancing its activity on the syntaxin-1/Munc18-1 complex to mediate SNARE complex formation.

Finally, to establish an additional correlation with physiological data, we tested the effects of a point mutation in Munc18-1 (E66A) that decreases neurotransmitter release in neurons by about 50% (Deak *et al.* 2009). Reassuringly, this mutation led to a comparable decrease in the lipid mixing observed in our reconstitution assays (Figures 4.4I,J). We would like to emphasize that the syntaxin-1/Munc18-1 liposomes used to test the effects of removing DAG or PIP2, as well as the effects of the Munc18-1 E66A mutation, were prepared side-by-side with

liposomes containing WT syntaxin-1/Munc18-1 and contained similar amounts of both proteins (Figure 4.3C), ruling out the possibility that the differences observed arise from different amounts of reconstituted proteins.

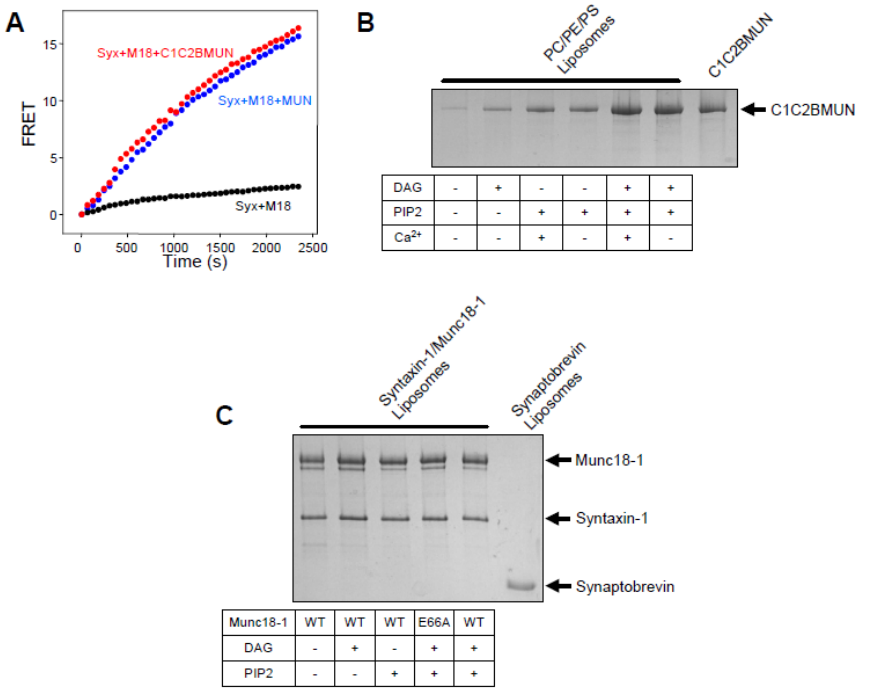

Figure 4.3 Characterization of the Munc13-1 C1C2BMUN fragment and reconstituted proteoliposomes.

(**A**) Time dependence of FRET between a BODIPY fluorescence donor probe place on residue 61 of the synaptobrevin SNARE motif and a rhodamine acceptor probe placed on residue 249 of syntaxin-1(2-253) as they form the SNARE complex with the SNARE motifs of SNAP-25. Reactions were performed as described in (Ma *et al.* 2011)and started with the labeled syntaxin-1(2-253) bound to Munc18-1 in the absence or presence of Munc13-1 MUN domain or C1C2BMUN fragment as indicated. Both fragments led to a similar acceleration of SNARE complex formation. (**B**) Co-floatation assays showing the binding of Munc13-1 C1C2BMUN fragment to liposomes containing PC, PE and PS, and containing or lacking DAG or PIP2 as indicated. Experiments with PIP2 were performed in the presence or absence of Ca^{2+}, revealing some Ca^{2+}-dependent enhancement of binding that is expected to be mediated by the C2B domain (Shin *et al.* 2010). (**C**) SDS-PAGE analysis, monitored by Coomassie Blue staining, of the syntaxin-1/Munc18-1-liposomes and the synaptobrevin-liposomes used in the reconstitution experiments of Figures 4.2,4.4.

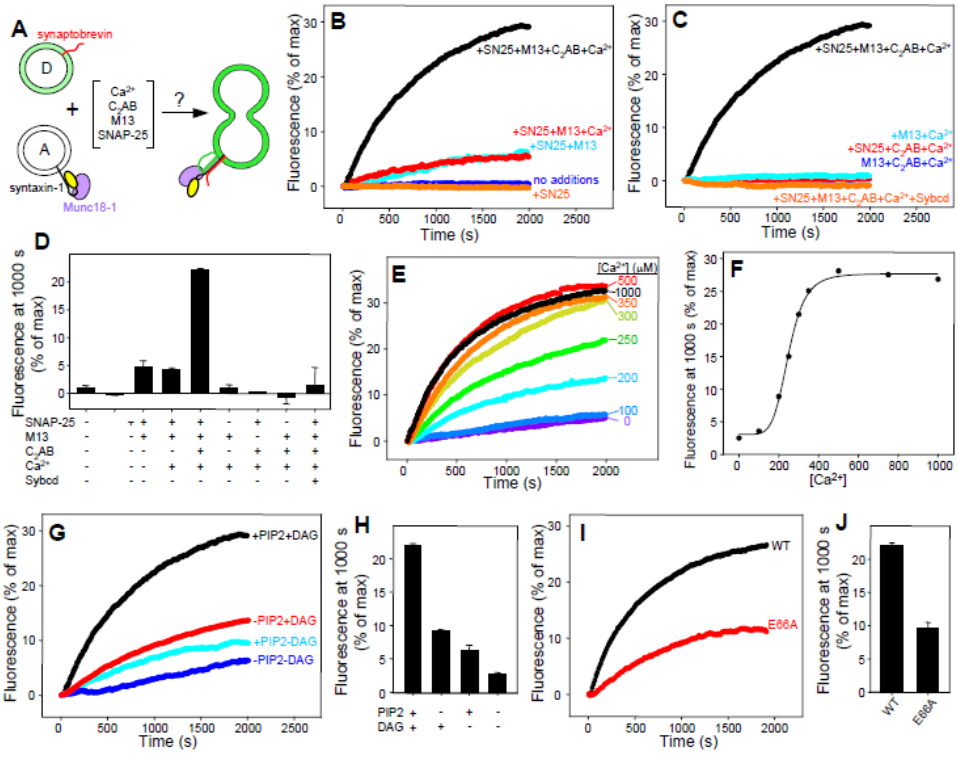
A
synaptobrevin
D
A
syntaxin-1
Munc18-1
Ca2+
C2AB
M13
SNAP-25
?
B
+SN25+M13+C2AB+Ca2+
+SN25+M13+Ca2+
+SN25+M13
no additions
+SN25
Fluorescence (% of max)
Time (s)
C
+SN25+M13+C2AB+Ca2+
+M13+Ca2+
+SN25+C2AB+Ca2+
M13+C2AB+Ca2+
+SN25+M13+C2AB+Ca2+Sybcd
Fluorescence (% of max)
Time (s)
D
Fluorescence at 1000 s (% of max)
SNAP-25
M13
C2AB
Ca2+
Sybcd
E
[Ca2+] (μM)
500
1000
350
300
250
200
100
0
Fluorescence (% of max)
Time (s)
F
Fluorescence at 1000 s (% of max)
[Ca2+]
G
+PIP2+DAG
-PIP2+DAG
+PIP2-DAG
-PIP2-DAG
Fluorescence (% of max)
Time (s)
H
Fluorescence at 1000 s (% of max)
PIP2
DAG
I
WT
E66A
Fluorescence (% of max)
Time (s)
J
Fluorescence at 1000 s (% of max)
WT
E66A

Figure 4.4

Figure 4.4 Requirement of Munc13 for lipid mixing of syntaxin-1/Munc18-1-liposomes with synaptobrevin-liposomes.

(**A**) Diagram summarizing the lipid mixing experiments, which were performed with acceptor liposomes containing syntaxin-1/Munc18-1, donor liposomes containing synaptobrevin and NBD-lipids quenched by rhodamine-lipids, and addition of various reagents. Lipid mixing is expected to result in increased NBD fluorescence. (**B,C**) Traces showing the lipid mixing observed in the presence of SNAP-25, Munc13-1 C1C2BMUN (M13), synaptotagmin-1 C2AB fragment (C2AB), synaptobrevin cytoplasmic domain (Sybcd) and/or 0.5 mM Ca^{2+} in various combinations. The y axis represents NBD fluorescence normalized to the maximum fluorescence observed upon detergent addition. (**D**) Quantification of the results obtained in the experiments of (**B,C**). (**E**) Lipid mixing observed in the presence of SNAP-25, C1C2BMUN and C2AB fragment as a function of Ca^{2+} concentration. (**F**) Plot of the normalized NBD fluorescence intensity at 1000 s as a function of Ca^{2+} observed in (**E**). Curve fitting of the data (solid line) fielded a Hill coefficient of 5.9 and half-maximal rate at 250 μM Ca^{2+}. (**G,H**) Fluorescence traces showing the dependence of the lipid mixing observed on the presence of DAG and/or PIP2 in the acceptor syntaxin-1/Munc18-1 liposomes (**G**), and quantification of the results (**H**). (**I,J**) Traces comparing lipid mixing obtained with acceptor liposomes that contained syntaxin-1 bound to WT or E66A mutant Munc18-1 (**I**) and quantification of the results (**J**). In (**D**, **H** and **J**), bars represent averages of the normalized NBD fluorescence observed after 1000 s in repeated experiments performed under the same conditions. Error bars represent standard deviations.

4.3.4 Lipid mixing is accompanied by content mixing

To demonstrate liposome fusion, it is important to show not only lipid mixing but also content mixing. These experiments have commonly been hindered by the tendency of small molecules to leak from SNARE-containing proteoliposomes [e.g. see (Dennison *et al.* 2006; Diao *et al.* 2010; Zucchi *et al.* 2011)]. However, synaptobrevin-liposomes with encapsulated sulforhodamine were recently reported to have very slow leakage rates that allowed monitoring of content mixing from dequenching of sulforhodamine upon fusion with acceptor liposomes (Kyoung *et al.* 2011). In our hands, a small amount of leakiness of sulforhodamine trapped into synaptobrevin-liposomes was observed when standard methods were used to prepare the proteoliposomes, and addition of C1C2BMUN exacerbated the leakiness (Figure 4.5A), likely because of sensitivity to residual detergent. However, I was able to minimize this problem through extensive dialysis of the liposomes against buffer with detergent-absorbing beads in small volumes (see Experimental Procedures), resulting in a very slow degree of leakiness that can be readily subtracted from signal increases due to content mixing (Figure 4.5B).

We adapted the sulforhodamine fluorescence de-quenching method to monitor content mixing in our bulk assays, including self-quenched DiD lipids in the donor liposomes to allow simultaneous monitoring of lipid mixing as described for the single-vesicle assays (Kyoung *et al.* 2011) (Figure 4.6A). In these experiments, two clearly distinct outcomes are expected if true content mixing occurs or the content of the donor vesicles is released due to lysis. Thus, since our NBD fluorescence de-quenching assays indicate that donor vesicles undergo an average of 1.5 to 2 rounds of fusion based on a standard conversion method (Parlati *et al.* 1999), content release upon vesicle lysis should lead to a monotonous increase in sulforhodamine fluorescence intensity that would saturate close to the maximal signal observed upon detergent addition. In

contrast, bona-fide content mixing should result in increases in sulforhodamine fluorescence intensity that saturate at lower intensities and follow a similar time course as lipid mixing, perhaps with some delay.

When we mixed the synaptobrevin donor liposomes with acceptor liposomes containing syntaxin-1/Munc18-1 complex, we observed efficient sulforhodamine fluorescence de-quenching upon addition of SNAP-25, C1C2BMUN and C2AB fragment/ Ca^{2+} (Figure 4.6B,C). Control experiments showed that SNAP-25, C1C2BMUN and the C2AB fragment are each essential for the de-quenching (Figure 4.6B,C). The lipid mixing measured simultaneously during these experiments from the DiD fluorescence dequenching (Figure 4.6D,E) paralleled the data obtained with the NBD fluorescence de-quenching assay (Figures 4.4B-D) and were similar to the sulforhodamine de-quenching results, although in the absence of C2AB fragment there is a small amount of lipid mixing but not sulforhodamine de-quenching. Importantly, the time course of the sulforhodamine fluorescence de-quenching in the presence of SNAP-25, C1C2BMUN and C2AB fragment/ Ca^{2+} closely followed the time course observed for lipid mixing through DiD fluorescence de-quenching (see the comparison in Figure 4.6F). These results show that content mixing accompanies lipid mixing in these experiments and hence that our system reconstitutes membrane fusion with the three neuronal SNAREs, Munc18-1 and core fragments of Munc13-1 and synaptotagmin-1, although we cannot rule out that some degree of leakiness may occur during fusion.

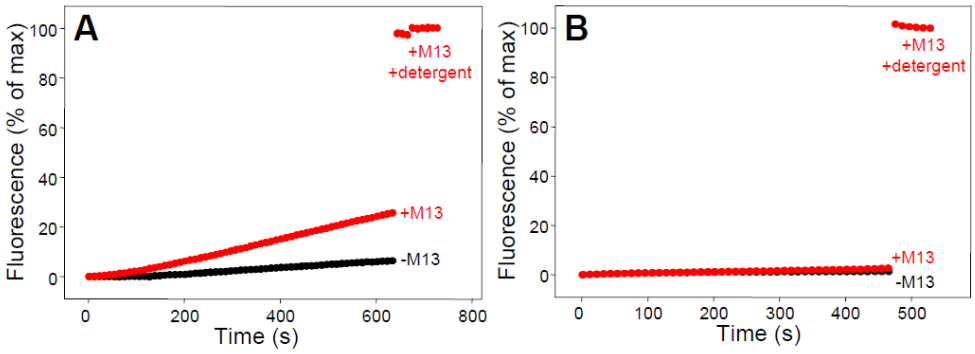

Figure 4.5 Analysis of donor liposome leakiness.

(**A,B**) The sulforhodamine fluorescence intensity of synaptobrevin-donor liposomes was monitored as a function of time in the absence or presence of Munc13-1 C1C2BMUN fragment. In (**A**), the liposomes were prepared by standard methods as described (Kyoung *et al.* 2011).In (**B**), the same procedure was followed except that dialysis was performed against BioBeads (BioRad) in small volumes to remove the detergent more efficiently.

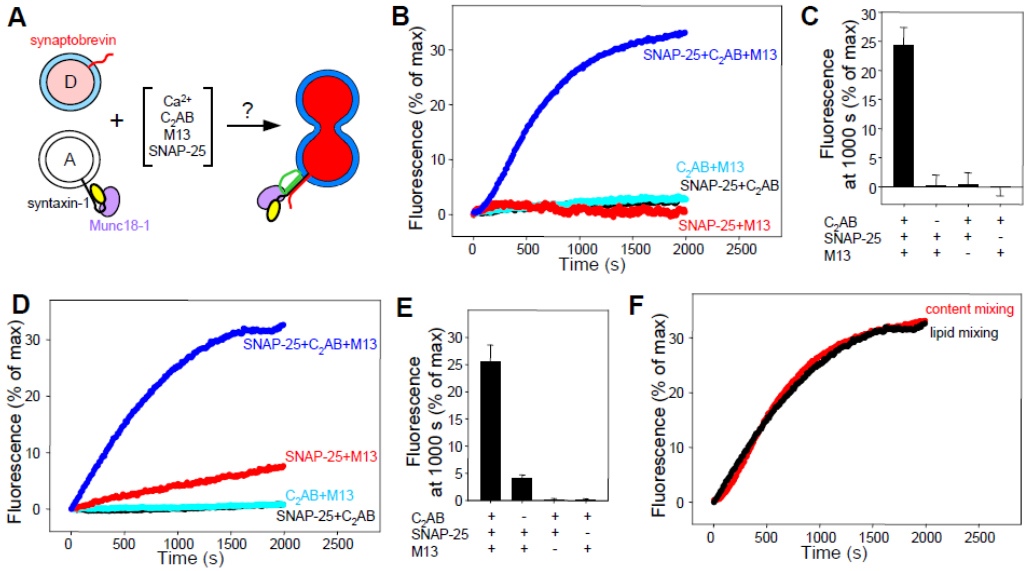

Figure 4.6 Reconstitution of membrane fusion with syntaxin-1/Munc18-1-liposomes and synaptobrevin-liposomes.

(**A**) Diagram summarizing the simultaneous lipid mixing and content mixing experiments, which were performed with acceptor liposomes containing syntaxin-1/Munc18-1, donor liposomes containing synaptobrevin and addition of various reagents. The donor liposomes contained encapsulated self-quenched sulforhodamine and self-quenched DiD lipids for simultaneous monitoring of content and lipid mixing due to dilution of the probes upon fusion. (**B**) Traces showing the content mixing observed in the presence of SNAP-25, Munc13-1 C1C2BMUN (M13) and/or synaptotagmin-1 C2AB fragment (C2AB) in various combinations. All experiments were performed in the presence of 0.5 mM Ca^{2+}. The y axis represents sulforhodamine fluorescence normalized to the maximum fluorescence observed upon detergent addition. (**C**) Quantification of the results obtained in the experiments of (**B**). (**D,E**) Traces of the lipid mixing observed from DiD fluorescence de-quenching in the same experiments (**D**) and quantification of the results (**E**). (**F**) Superposition of content mixing and lipid mixing traces observed in the presence of SNAP-25, C1C2BMUN, C2AB fragment and 0.5 mM Ca^{2+}.

4.3.5 Munc18-1- and Munc13-1-dependent lipid mixing in the presence of NSF/α-SNAP

While membrane fusion in our reconstitution experiments exhibits a strict requirement for Munc13-1, and uses Munc18-1 as an intrinsic component of the acceptor liposomes, our results still do not explain why Munc18-1 and Munc13-1 are so crucial for neurotransmitter release in vivo, since efficient lipid mixing and content mixing can also be obtained with SNAREs and syntaptotagmin-1 in the absence of Munc18-1 and Munc13-1 (see Introduction). However, almost all reconstitution studies of synaptic vesicle fusion described so far started with syntaxin-1/SNAP-25 heterodimers and did not incorporate NSF/SNAPs, which play fundamental roles in all SNARE-dependent forms of intracellular membrane traffic. One study that did incorporate NSF/α-SNAP showed that these factors inhibit lipid mixing, likely because they disassemble the syntaxin-1/SNAP-25 heterodimers (Weber *et al.* 2000). Since our biochemical results showed that Munc18-1 displaces SNAP-25 from syntaxin-1 and that NSF/α-SNAP facilitate this displacement on a membrane (Figures 4.1 and 4.2), we hypothesized that fusion might be activated by Munc18-1 and Munc13-1 even in the presence of NSF/α-SNAP because Munc18-1 can ‘capture’ the syntaxin-1 released from the syntaxin-1/SNAP-25 heterodimers and lead to membrane fusion with the help of Munc13-1 (Figures 4.4 and 4.6).

To test our hypothesis, we used the NBD fluorescence de-quenching assay as in the experiments of Figure 4.4 but starting with acceptor liposomes that contained reconstituted syntaxin-1/SNAP-25 heterodimers (Figure 4.7A). In one set of experiments, the heterodimers were formed from separately expressed proteins. As expected, when the acceptor liposomes were mixed with synaptobrevin-containing donor liposomes in the presence of Ca^{2+} and C2AB fragment, highly efficient lipid mixing was observed (Figure 4.7B,C). The amount of lipid mixing was not substantially altered by addition of Munc18-1 and C1C2BMUN, or by addition

of NSF/α-SNAP in the absence of ATP, but lipid mixing was almost completely abolished by NSF/α-SNAP in the presence of ATP (Figure 4.7B,C). Interestingly, some lipid mixing was observed when Munc18-1 and C1C2BMUN were added together with NSF/α-SNAP and ATP (Figure 4.7B,C), suggesting that that Munc18-1 and C1C2BMUN can activate fusion through a pathway that is resistant to NSF/α-SNAP, as predicted by our hypothesis.

We reasoned that, since the concentration of free SNAP-25 should favor the formation of SNARE complexes without affecting the rate of syntaxin-1/SNAP-25 heterodimer dissociation by NSF/α-SNAP, an excess of SNAP-25 might assist in the activation of the lipid mixing by Munc18-1 and C1C2BMUN. Indeed, a titration with SNAP-25 showed increased efficiency of the lipid mixing activated by Munc18-1 and C1C2BMUN, which saturated at an excess SNAP-25 concentration of 2 μM (Figure 4.7D). Importantly, the 2 μM excess SNAP-25 did not affect the overall lipid mixing observed upon addition of only C2AB fragment and Ca^{2+} (compare black symbols in Figures 4.7B,E), and NSF/α-SNAP still inhibited lipid mixing strongly in the presence of excess SNAP-25 and the absence of Munc18-1 and C1C2BMUN (Figures 4.7E,F). With the 2 μM excess SNAP-25, Munc18-1 and C1C2BMUN stimulated lipid mixing to levels comparable to those observed in the absence of NSF/α-SNAP (compare orange and black curves in Figure 4.7E); Munc18-1 alone (but not C12C2BMUN alone) appeared to provide a small amount of activation (Figure 4.7E, cyan and blue symbols; see also Figure 4.7F).

We repeated the same set of experiments using acceptor liposomes with reconstituted syntaxin-1/SNAP-25 heterodimers that were co-expressed, since it was originally reported that co-expression of syntaxin-1/SNAP-25 was necessary for lipid mixing induced by the neuronal SNAREs (Weber *et al.* 1998). Under our conditions, the efficiency of lipid mixing between these liposomes and synaptobrevin-containing donor liposomes in the presence of Ca^{2+} and C2AB

fragment (Figure 4.8A,B) was similar to those observed with the separately expressed syntaxin-1 and SNAP-25 (Figure 4.7B,C). Moreover, we again observed strong inhibition of lipid mixing by NSF/α-SNAP in the presence of ATP, and activation of lipid mixing upon further addition of Munc18-1, C1C2BMUN and excess SNAP-25 (Figure 4.8). Hence, the interplay between NSF/α-SNAP and Munc18-1/Munc13-1 does not depend on the method of expression of syntaxin-1 and SNAP-25. Overall, these results suggest that inclusion of NSF/α-SNAP is key to unmask the crucial importance of Munc18-1 and Munc13-1 for membrane fusion in these reconstituted systems.

To see whether we can get the same conclusions in the absence of synaptotagmin-1 C2AB fragment, I performed lipid mixing assays as in the experiments of Figure 4.7. As expected, when syntaxin-1/SNAP-25-containing acceptor liposomes were mixed with synaptobrevin-containig liposomes in the absence of C2AB, a small amount of lipid mixing was observed (Figure 4.9A,B,C). Addition of C1C2BMUN/Ca^{2+} did not alter the amount of lipid mixing (Figure 4.9A,C). Addition of Munc18-1 slightly enhanced the amount of lipid mixing, while addition of both Munc18-1 and C1C2BMUN/Ca^{2+} increased amount of lipid mixing to a larger amount (Figure 4.9A,C), suggesting that Munc18-1 and C1C2BMUN cooperate in stimulating SNARE-dependent lipid mixing. Lipid mixing was almost completely abolished by addition of NSF/α-SNAP/ATP in the absence or presence of Munc18-1 or C1C2BMUN (Figure 4.9A,B,C). Munc18-1 and C1C2BMUN together activated lipid mixing in the presence of NSF/α-SNAP/ATP (Figure 4.9B,C), suggesting that in the absence of C2AB, Munc18-1 and Munc13 still activate fusion that is inhibited by NSF/α-SNAP/ATP.

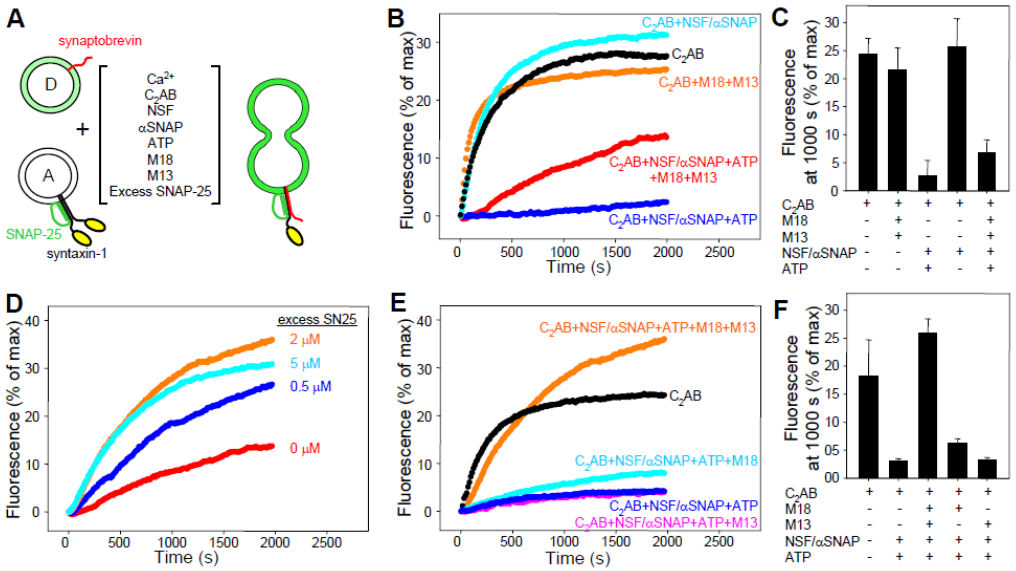

Figure 4.7 NSF/α-SNAP inhibit lipid mixing between syntaxin-1/SNAP-25-liposomes and synaptobrevin-liposomes, and Munc18-1/Munc13-1 activate lipid mixing.

(**A**) Diagram summarizing the lipid mixing experiments, which were performed with acceptor liposomes containing syntaxin-1/SNAP-25 (separately expressed), donor liposomes containing synaptobrevin and NBD-lipids quenched by rhodamine-lipids, and addition of various reagents. (**B**) Traces showing the lipid mixing observed in the presence of Munc18-1 (M18), Munc13-1 C1C2BMUN (M13), synaptotagmin-1 C2AB fragment (C2AB), NSF, α-SNAP and/or Mg^{2+}-ATP in various combinations. All experiments were performed in the presence of 0.5 mM Ca2+. The y axis represents NBD fluorescence normalized to the maximum fluorescence observed upon detergent addition. (**C**) Quantification of the results obtained in the experiments of (**B**). (**D**) Lipid mixing observed in the presence of Munc18-1, C1C2BMUN, C2AB fragment, NSF, α-SNAP, Mg^{2+}-ATP and 0.5 mM Ca^{2+} as function of added SNAP-25 excess. (**E**) Lipid mixing experiments performed as in (**B**) with various additions, all in the presence of 2 μM SNAP-25 excess. (**F**) Quantification of the results of panel (**E**).

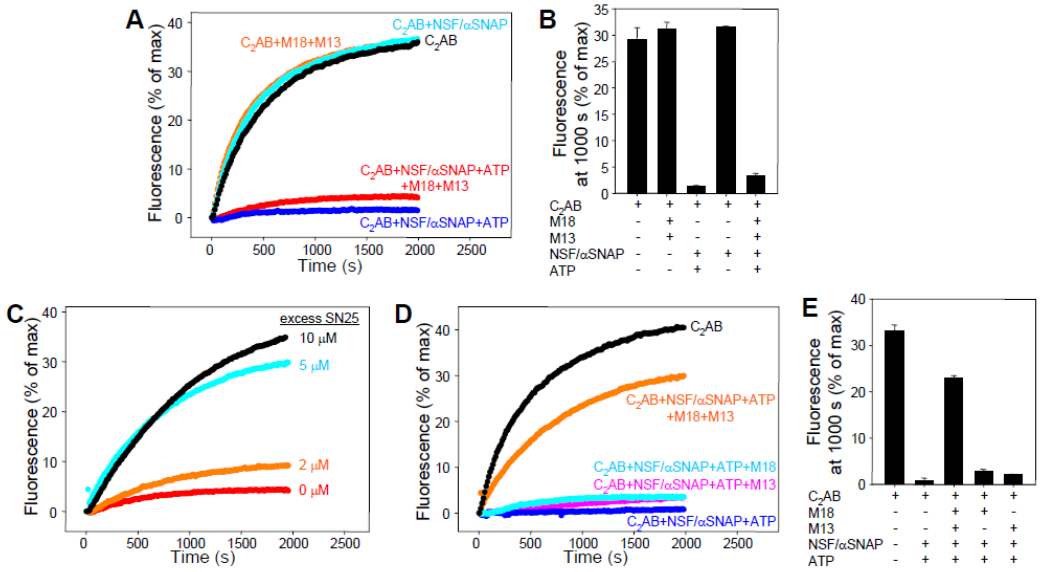

Figure 4.8 NSF/α-SNAP inhibit lipid mixing between co-expressed syntaxin-1/SNAP-25-liposomes and synaptobrevin-liposomes, and Munc18-1/Munc13-1 activate lipid mixing.

The experiments were performed as in Figure 4.7, except that the reconstituted syntaxin-1 and SNAP-25 were co-expressed. (A) Traces showing the lipid mixing observed in the presence of Munc18-1 (M18), Munc13-1 C1C2BMUN (M13), synaptotagmin-1 C2AB fragment (C2AB), NSF, α-SNAP and/or Mg^{2+}-ATP in various combinations. All experiments were performed in the presence of 0.5 mM Ca^{2+}. The y axis represents NBD fluorescence normalized to the maximum fluorescence observed upon detergent addition. (**B**) Quantification of the results obtained in the experiments of (**A**). (**C**) Lipid mixing observed in the presence of Munc18-1, C1C2BMUN, C2AB fragment, NSF, α-SNAP, Mg^{2+}-ATP and 0.5 mM Ca^{2+} as function of added SNAP-25 excess. (**D**) Lipid mixing experiments performed as in (**A**) with various additions, all in the presence of 5 μM SNAP-25 excess. (**E**) Quantification of the results of panel (**D**).

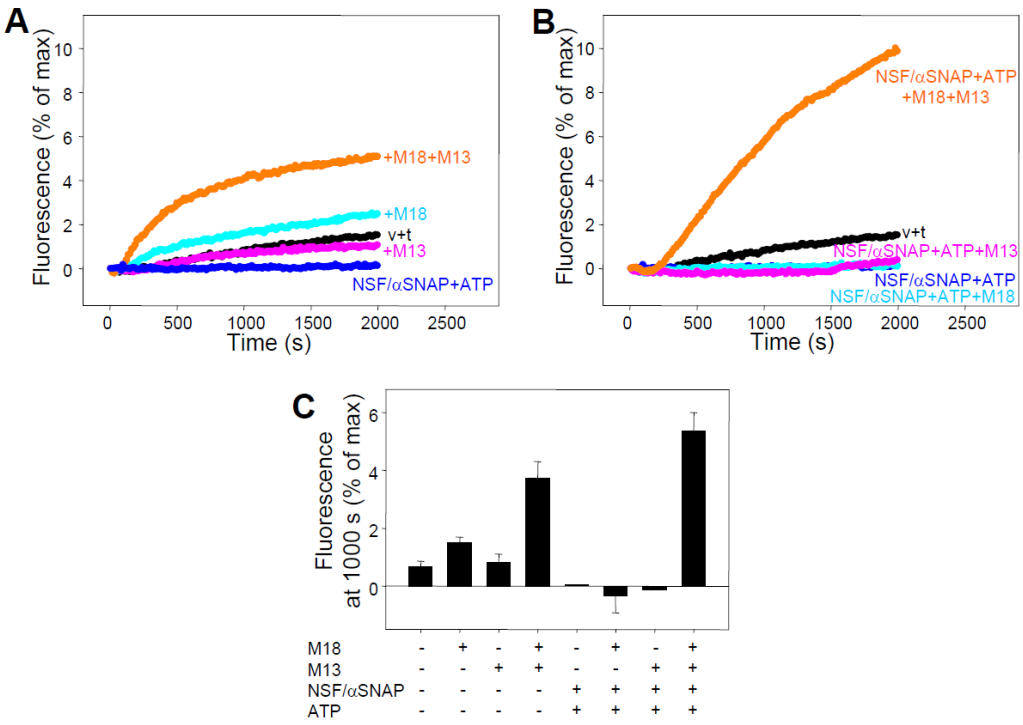
A
Fluorescence (% of max)
Time (s)
+M18+M13
+M18
v+t
+M13
NSF/αSNAP+ATP
B
Fluorescence (% of max)
Time (s)
NSF/αSNAP+ATP
+M18+M13
v+t
NSF/αSNAP+ATP+M13
NSF/αSNAP+ATP
NSF/αSNAP+ATP+M18
C
Fluorescence
at 1000 s (% of max)
M18
M13
NSF/αSNAP
ATP

Figure 4.9

Figure 4.9 NSF-α-SNAP inhibit lipid mixing between syntaxin-1-SNAP-25-liposomes and synaptobrevin-liposomes, and Munc18-1-Munc13-1 activate lipid mixing in the absence of synaptotagmin-1.

(**A**,**B**) Traces showing the lipid mixing observed between acceptor liposomes containing syntaxin-1-SNAP-25 heterodimers (separately expressed proteins) and synaptobrevin donor liposomes containing NBD-lipids quenched by rhodamine-lipids in the presence of Munc18-1 (M18), Munc13-1 C1C2BMUN (M13), NSF, α-SNAP and/or Mg^{2+}-ATP in various combinations (v+t indicates the lipid mixing observed with no additions). All samples contained an excess of 2 μM SNAP-25. Samples containing C1C2BMUN also included 0.5 mM Ca^{2+}. The y axis represents NBD fluorescence normalized to the maximum fluorescence observed upon detergent addition. (**C**) Quantification of the results obtained in the experiments of (**A**,**B**). Error bars represent standard deviations. In **A**, the black trace (v+t) shows that lipid mixing between the synaptobrevin-liposomes and the syntaxin-1-SNAP-25 liposomes was inefficient under the conditions of our experiments, that Munc18-1 enhanced lipid mixing moderately, and that Munc18-1 together the Munc13-1 C1C2BMUN fragment stimulated lipid mixing more strongly, revealing a synergy between them. NSF-α-SNAP completely abolished the lipid mixing induced by the SNAREs alone. Panel **B** shows that Munc18-1 alone or the Munc13-1 C1C2BMUN fragment alone could not overcome the inhibition caused by NSF-α-SNAP, but together they dramatically activated lipid mixing. These results show that Munc18-1 and Munc13-1 can also stimulate lipid mixing in an NSF-α-SNAP-resistant manner in the absence of the synaptotagmin-1 C_2AB fragment, although the overall lipid mixing is less efficient because of the lack of the activity of the Ca^{2+} sensor (note the different scale of the y axis in panels **A**-**C** compared to those in Figure 4.7).

4.4 Discussion

Multiple seminal contributions over the past three decades have identified the major proteins that control neurotransmitter release, have shown that some of these proteins belong to families with general roles in intracellular membrane fusion, have provided key insights into their functions, and have revealed their three-dimensional structures. And yet, it has been difficult to integrate all this knowledge into a coherent model of synaptic vesicle fusion that explains all the most key findings. Perhaps most worrisome was the huge gap that emerged between physiological data showing that Munc18-1 and Munc13s are crucial for neurotransmitter release and in vitro reconstitution results revealing highly efficient membrane fusion without these proteins (see Introduction). The results presented here now bridge this gap, showing that multiple basic features of synaptic vesicle fusion, including critical roles for Munc18-1 and Munc13s, can be reproduced when these two proteins and the other six major components of the release machinery (syntaxin-1, synaptobrevin, SNAP-25, synaptotagmin-1, NSF and α-SNAP) are included in the reconstitution system. Our results, together with the available data, lead naturally to a model of synaptic vesicle fusion that readily explains the key physiological importance of each one of these eight proteins (Figure 4.10). This model postulates that: i) the syntaxin-1/Munc18- 1 complex constitutes the starting point for synaptic vesicle fusion; ii) Munc13 opens syntaxin-1 and, together with Munc18-1, forms a template to bring the three SNAREs together and initiate SNARE complex assembly; iii) the resulting Munc18-1/Munc13/SNARE assembly is resistant to disassembly by NSF/SNAPs and underlies the primed state that enables fast membrane fusion through the action of synaptotagmin-1/Ca^{2+}; iv) syntaxin-1/SNAP-25 heterodimers constitute ‘off-pathway’ complexes that are disassembled by

NSF/SNAPs, and the released syntaxin-1 is captured in its closed conformation by Munc18-1, leading to the productive pathway for membrane fusion.

Elucidating the basis for the key functions of Munc18-1 and other SM proteins is perhaps the most fundamental question that needs to be answered to understand the mechanism of neurotransmitter release and intracellular membrane fusion in general (Sudhof *et al.* 2011). Addressing this question at the synapse also necessitates an understanding of the role of Munc13s given the similarly drastic phenotypes observed in the absence of Munc18-1 or Munc13s (Verhage *et al.* 2000; Varoqueaux *et al.* 2002). The recent finding of sequence and structural similarity between the Munc13 MUN domain and subunits of tethering factors that function in diverse membrane compartments (e.g. exocyst, GARP, Cog and Dsl1) indicated that Munc13s have a general function that is shared with these factors (Pei *et al.* 2009; Li *et al.* 2011). However, these tethering factors form part of large complexes with multiple subunits, and tethering complexes from other membrane compartments that do not exhibit sequence homology with Munc13s, such as HOPS and TRAPP, also contain multiple subunits. Hence, it was highly unclear whether Munc13s by themselves could play similar roles as these tethering complexes.

Our results now uncover a clear similarity with reconstitutions of yeast vacuolar fusion, where the HOPS complex orchestrates formation of trans-SNARE complexes (Mima *et al.* 2008) and protects them from disassembly by Sec18p/Sec17p (Xu *et al.* 2010), the yeast homologues of NSF/SNAPs. Although vacuolar fusion does not require synaptotagmin-1/ Ca^{2+} and some of the details of the interplay between HOPS and Sec18p/Sec17p (Mima *et al.* 2008) differ from the interplay between Munc18-1/Munc13 and NSF/α-SNAP described here, our data strongly suggest that Munc18-1 and Munc13 must coordinate trans-SNARE complex assembly in an NSF/α-SNAP-resistant manner to promote membrane fusion. It is rather remarkable that this

same task can be executed both by Munc18-1/Munc13 and by HOPS since, although HOPS includes the SM protein Vps33p, it contains five additional large subunits unrelated to Munc13. Considering these differences in architecture and the fact that synaptic exocytosis and yeast vacuolar fusion are distantly related forms of membrane traffic, this similarity suggests that a major general function of SM proteins and their associated factors is indeed the orchestration of SNARE complex assembly in an NSF/SNAP-resistant manner. This notion does not preclude other functions proposed for SM proteins and their co-factors, including the possibility that they cooperate with the SNAREs in exerting force on the membranes to induce fusion much more efficiently than SNAREs alone (Rizo *et al.* 2006; Dulubova *et al.* 2007).

The findings that NSF/α-SNAP disassemble syntaxin-1/SNAP-25 heterodimers [Figure 4.2 and (Weber *et al.* 2000)] and that Secp18p/Sec17p also act on vacuolar t-SNARE complexes (Mima *et al.* 2008) suggest that the function of NSF/SNAPs is not limited to disassembling SNARE complexes to recycle the SNAREs for another round of fusion. It is plausible that the activity of NSF/SNAPs on syntaxin-1/SNAP-25 heterodimers and homologous complexes may be an 'accident' reminiscent of its 'true' function on the SNARE complex. However, if syntaxin-1/SNAP-25 heterodimers were bona-fide starting points for synaptic vesicle fusion, it seems that their disassembly by NSF/SNAPs would involve a futile waste of energy. Hence, the activity of NSF/SNAPs on syntaxin-1/SNAP-25 heterodimers is likely to serve an important function. In this context, sequences that form long coiled coils have a natural promiscuity, which is particularly emphasized by the tendency of the syntaxin-1 SNARE motif to bind to many proteins (Jahn *et al.* 2006), to form a tetramer (Misura *et al.* 2001), and to associate with SNAP-25 in different forms (Misura *et al.* 2001), including 2:1 complexes where synaptobrevin is replaced by a second syntaxin-1 unit (Zhang *et al.* 2002). Moreover, oligomeric t-SNARE

complexes can be formed through bridging by the two SNARE motifs of SNAP-25 (Figure 4.10). Hence, syntaxin-1/SNAP-25 heterodimers constitute a heterogeneous mixture of complexes that probably provide a poor starting point for an exquisitely regulated process such as neurotransmitter release.

We propose that direct displacement of SNAP-25 from syntaxin-1 by Munc18-1, and disassembly of syntaxin-1/SNAP-25 heterodimers by NSF/SNAPs followed by capture of syntaxin-1 by Munc18-1, provide two means toward the correct pathway for fusion, with a well defined starting point (the syntaxin-1/Munc18-1 complex) that is amenable to tight regulation. This proposal implies that the acceptor complex for synaptobrevin is not a syntaxin-1/SNAP-25 heterodimer but rather a complex of Munc18-1, Munc13-1 and syntaxin-1. Binding of SNAP-25 and synaptobrevin to this acceptor complex may occur concomitantly or sequentially but, regardless of the mechanism, our data [(Figures 4.1,4.2) and (Ma *et al.* 2011)] suggest that both SNAREs are required to favor the transition from closed to open syntaxin-1. It is also worth noting that specific protein-protein interactions in presynaptic active zones may also favor this pathway over the potential formation of trans-SNARE complexes containing only syntaxin-1, SNAP-25 and synaptobrevin, including for instance the formation of tripartite complexes of Munc13-1 with RIMs and Rab3s (Dulubova *et al.* 2005).

Based on the seminal work on yeast vacuolar fusion (Mima *et al.* 2008; Stroupe *et al.* 2009), the common features of synaptic vesicle fusion described here, and increasing evidence for interactions of SNAREs with tethering factors [e.g. (Sivaram *et al.* 2005; Tripathi *et al.* 2009)], it is tempting to speculate that the acceptor complexes for v-SNAREs may generally be formed by t-SNAREs, SM proteins and tethering factors, rather than by t-SNAREs alone. At the same time, the diversity in the architecture of tethering complexes suggests that, even if they

share a common function in orchestrating SNARE complex assembly, they may accomplish this function by different mechanisms that respond to different regulatory requirements. For instance, the closed conformation of syntaxin-1 is not adopted by the vacuolar syntaxin Vam3p (Dulubova *et al.* 2001), and the Munc18-1/syntaxin-1 complex appears to be a specialization of regulated secretion (Carr *et al.* 1999; Dulubova *et al.* 1999). Correspondingly, the Munc13 MUN domain may have a general role in coordinating SNARE complex assembly and a specific role in opening syntaxin-1. This latter role appears to be catalytic in nature, since the MUN domain not only accelerates the transition from the syntaxin-1/Munc18-1 complex to the SNARE complex (Ma *et al.* 2011) but also the transition from syntaxin-1/SNAP-25 heterodimers to the syntaxin-1/Munc18-1 complex (Figure 4.1H). Hence, Munc13s can provide an additional means to facilitate disruption of syntaxin-1/SNAP-25 heterodimers in favor of the syntaxin-1/Munc18-1 complex.

Can we conclude that our system represents a bona-fide reconstitution of synaptic vesicle fusion? More research will be necessary to fully answer this question, but it is reassuring that our experiments were performed under mild conditions, with relatively low protein concentrations and protein-to-lipid ratios, and reproduce multiple basic features of neurotransmitter release, including a key function for Munc18-1, Munc13-1 and the other six proteins used. Moreover, the effects of the Munc18-1 E66A mutation on lipid mixing (Figure 4.4I,J) correlate well with the functional effects of this mutation in neurons (Deak *et al.* 2009), and our experiments reveal a high cooperativity with Ca^{2+} that mirrors that of neurotransmitter release (Meinrenken *et al.* 2003; Schneggenburger *et al.* 2005). The Ca^{2+} concentrations required for fusion in our experiments are somewhat higher than those that trigger release, but this is not surprising given the natural limitations of our reconstituted system. For instance, the use of reconstituted fulllength

synaptotagmin-1 may improve this behavior, although the C2AB fragment contains the key Ca^{2+}-binding domains of synaptotagmin-1 and is sufficient to dramatically enhance SNAREdependent lipid mixing due to its ability to bridge membranes (Xue *et al.* 2008; Hui *et al.* 2011). Likely a more important issue that hinders the fusion efficiency in our experiments is the absence of a defined mechanism for vesicle docking, which depends on proteins such as RIMs/unc10 and Rab3s (Weimer *et al.* 2006; Gracheva *et al.* 2008), and enables the high speed of release. Addressing this issue is hampered by our limited understanding of the mechanism of docking, but it will be interesting to extend our studies to single-vesicle fusion assays, which allow measurement of the rates of individual fusion events after docking [e.g. (Lee *et al.* 2010; Kyoung *et al.* 2011)]. We also note that our experiments did not include other proteins with important roles in neurotransmitter release such as complexins. Nevertheless, despite these limitations, the fundamental results obtained with this system can now be used as a basis for further studies of the functions of these proteins with a variety of approaches.

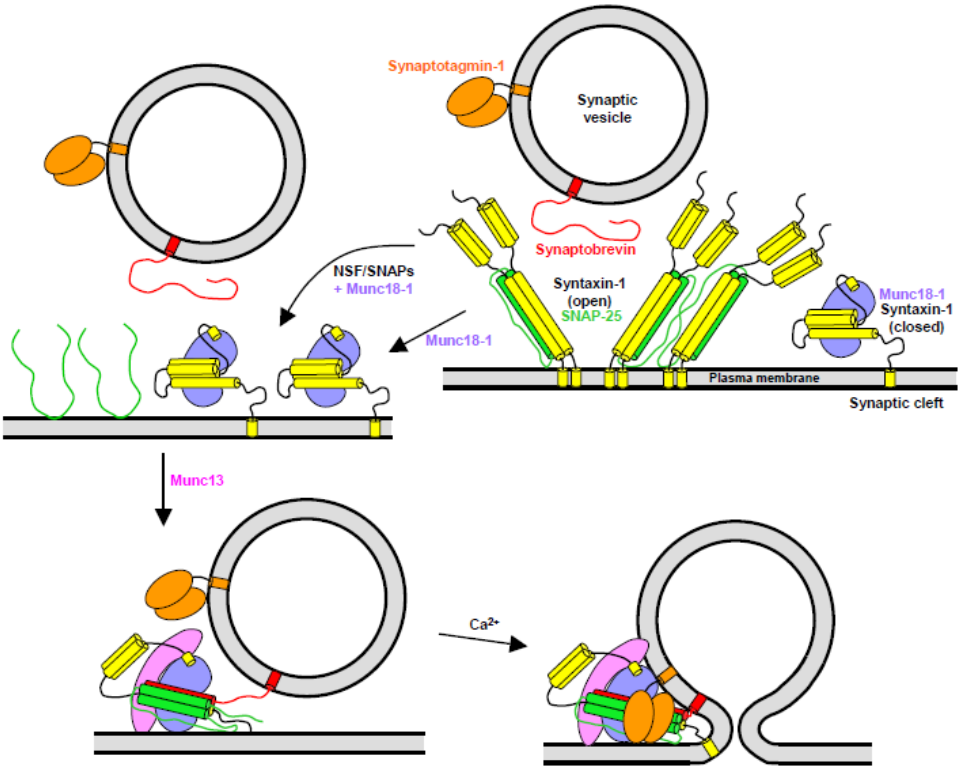
Synaptotagmin-1
Synaptic vesicle
Synaptobrevin
NSF/SNAPs
+ Munc18-1
Syntaxin-1
(open)
SNAP-25
Munc18-1
Munc18-1
Syntaxin-1
(closed)
Plasma membrane
Synaptic cleft
Munc13
Ca2+

Figure 4.10

Figure 4.10 Model of synaptic vesicle fusion intergrating the function of the eight major components of the release machinery

The key feature of this model, compared to previous models, is that the closed syntaxin-1/Munc18-1 complex is predicted to be the starting point for the pathway that leads to membrane fusion with the help of Munc13s, without transiting through heterodimers of open syntaxin-1 with SNAP-25. These heterodimers are likely heterogeneous, including among others syntaxin-1/SNAP-25 complexes with 2:1 or 4:2 stoichiometry (upper right panel), as well as larger complexes bridged by SNAP-25 (not shown); syntaxin-1 oligomers are also likely to exist. The model postulates that the syntaxin-1/SNAP-25 heterodimers are converted to syntaxin-1/Munc18-1 complexes directly by replacement of SNAP-25 with Munc18-1, or indirectly through disassembly by NSF/SNAPs and capture of the released closed syntaxin-1 by Munc18-1 (upper left). In this model, Munc13s help to open syntaxin-1 and to orchestrate trans-SNARE complex assembly together with Munc18-1, perhaps transiting through an intermediate that serves as the acceptor complex for SNAP-25 and synaptobrevin, leading to a partially assembled SNARE complex that remains bound to Munc18-1 and Munc13-1 (lower left). This state, which may correspond to that of primed synaptic vesicles and cannot be disassembled by NSF/SNAPs, serves as the substrate for synaptotagmin-1/Ca^{2+} to trigger fast synaptic vesicle fusion (lower right). The arrangement of Munc18-1, Munc13-1 and synaptotagmin-1 with respect to the SNARE complex is unknown, but is drawn to suggest the possibility that the three proteins may bind simultaneously to the SNARE complex and may also help to bridge the two membranes to help inducing fusion. The interaction of synaptotagmin-1 with the SNARE complex may occur before Ca^{2+} influx (not shown in the lower left panel for simplicity). Most of the experiments presented in this study to support this model were performed with a synaptotagmin-1 fragment containing its two C2 domains (C2AB fragment) and a Munc13-1 fragment containing its C1, C2B and MUN domains (C1C2BMUN).

Chapter 5 Summary and Future Directions

Munc18-1 is considered part of the fusion machinery for synaptic transmission. Several functions of Munc18-1 have been discovered through knocking it out or expressing its mutants of in neurons, but its key role has not been found yet. Most importantly, its mode of action is still largely unknown. This dissertation provides insights into the roles of Munc18-1 in neurotransmitter release, especially Chapter 4.

Chapter 4 demonstrates that: i) in the presence of NSF and α-SNAP, Munc18-1 interacts with syntaxin-1 or breaks the syntaxin-1/SNAP-25 complex and replace SNAP-25 to hold syntaxin-1 in a closed conformation; ii) the priming factor Munc13, opens syntaxin-1 that is held by Munc18-1, and then Munc18-1and Munc13 guide the synaptic vesicle fusion through a tightly regulated pathway that depends on SNARE-complex and synaptotagmin, and is NSF and α-SNAP resistant (Figure 4.10). This is the first convincing evidence showing the molecular mechanism of action of Munc18-1 in synaptic vesicle exocytosis, despite extensive studies of this protein in the past decade. However, there are still questions to ask about this protein. i) Is Munc18-1 directly involved in membrane fusion itself after SNARE complex formation? Our model leaves the possibility open that Munc18-1 might also have a separate effect on the Ca^{2+}-triggered membrane fusion step. Chapters 2 and 3 showed that Munc18-1 interacts with the SNARE motifs of synaptobrevin and syntaxin-1 respectively, and that Munc18-1 interacts with the C-terminal part of synaptobrevin and syntaxin-1 on the SNARE four-helix bundle, which is right adjacent to the place where membrane fusion occurs. Moreover, the interaction of Munc18-1 with the SNARE four-helix bundle is compatible with binding of the SNARE four-helix bundle to complexin-I, which functions in a late stage of synaptic vesicle exocytosis. These data suggest

that Munc18-1 might be directly involved in membrane fusion itself. A high resolution structure of the complex of Munc18-1/SNARE four-helix bundle will be needed for further in vivo investigation to provide answers to this question. Moreover, capturing the intermediate steps of synaptic vesicle fusion by Cryo-EM and identifying Munc18-1 in those intermediate fusion steps would also be great evidence to prove that Munc18-1 is directly involved in the Ca^{2+}-triggered membrane fusion step. ii) Does Munc18-1 cooperate with Munc13 to play a direct role in the membrane fusion step? The results in Figure 4.9 showed that Munc18-1 cooperates with Munc13 in stimulation of SNARE-dependent lipid mixing in the absence of synaptotagmin, although the amount of stimulation is small. In vivo investigation suggests that Munc13 might have a role downstream of priming. It is hard to provide direct evidence that Munc18-1 and Munc13 are involved in Ca^{2+}-triggered membrane fusion step so far. Studying Munc18-1 and Munc13 together might be easier to uncover their roles in the fusion step. Cryo-EM would be a great method to identify whether these two proteins are together in the fusion intermediates, which would provide important information for further in vitro cooperativity studies. iii) Does the glass-hour shape fusion pore proposed by the stalk model (Figure 1.4) really exist? Is it regulated by Munc18-1 or Munc18-1 together with Munc13-1? Recent cryo-EM studies of intermediates of SNARE-mediated vesicle fusion (Hernandez *et al.* 2012) showed that fusion proceeds through membrane contact, membrane flattening, membrane merging, and fusion pore formation from one end, which is very different from the stalk model. Does Munc18-1 regulated or Munc18-1 and Munc13 regulated membrane fusion proceed through the stalk model? Cryo-EM to capture the intermediates of Munc18-1 and Munc13 regulated membrane fusion, and comparison of these intermediates with those observed with the SNARE alone would provide answers. iv) Structurally, how are Munc18-1, Munc13, complexin, and synaptotagmin arranged on the

SNARE four-helix bundle? These proteins all bind to the SNARE four-helix bundle, and most probably they all participate in the membrane fusion step. Understanding their spatial arrangement is also important for understanding the whole system. In vitro studies of the structures of the complexes will be needed. v) Do Munc18-1 homologs function in the same way in other intracellular membrane fusion events? This question remains to be tested in other systems. The answers to questions i, ii and iii will shed lights on the answer to question iv.

BIBLIOGRAPHY

Arac, D., X. Chen, H. A. Khant, J. Ubach, S. J. Ludtke, M. Kikkawa, A. E. Johnson, W. Chiu, T. C. Südhof and J. Rizo (2006). "Close membrane-membrane proximity induced by Ca(2+)-dependent multivalent binding of synaptotagmin-1 to phospholipids." Nat Struct Mol Biol **13**(3): 209-217.

Arac, D., X. Chen, H. A. Khant, J. Ubach, S. J. Ludtke, M. Kikkawa, A. E. Johnson, W. Chiu, T. C. Sudhof and J. Rizo (2006). "Close membrane-membrane proximity induced by Ca(2+)-dependent multivalent binding of synaptotagmin-1 to phospholipids." Nat Struct Mol Biol **13**(3): 209-217.

Aravamudan, B., T. Fergestad, W. S. Davis, C. K. Rodesch and K. Broadie (1999). "Drosophila UNC-13 is essential for synaptic transmission." Nat Neurosci **2**(11): 965-971.

Arunachalam, L., L. Han, N. G. Tassew, Y. He, L. Wang, L. Xie, Y. Fujita, E. Kwan, B. Davletov, P. P. Monnier, H. Y. Gaisano and S. Sugita (2008). "Munc18-1 is critical for plasma membrane localization of syntaxin1 but not of SNAP-25 in PC12 cells." Mol Biol Cell **19**(2): 722-734.

Augustin, I., A. Betz, C. Herrmann, T. Jo and N. Brose (1999). "Differential expression of two novel Munc13 proteins in rat brain." Biochem J **337 (Pt 3)**: 363-371.

Augustin, I., C. Rosenmund, T. C. Sudhof and N. Brose (1999). "Munc13-1 is essential for fusion competence of glutamatergic synaptic vesicles." Nature **400**(6743): 457-461.

Bai, J. and E. R. Chapman (2004). "The C2 domains of synaptotagmin--partners in exocytosis." Trends Biochem Sci **29**(3): 143-151.

Banerjee, A., V. A. Barry, B. R. DasGupta and T. F. Martin (1996). "N-Ethylmaleimide-sensitive factor acts at a prefusion ATP-dependent step in Ca2+-activated exocytosis." J Biol Chem **271**(34): 20223-20226.

Basanez, G., F. M. Goni and A. Alonso (1998). "Effect of single chain lipids on phospholipase C-promoted vesicle fusion. A test for the stalk hypothesis of membrane fusion." Biochemistry **37**(11): 3901-3908.

Basu, J., N. Shen, I. Dulubova, J. Lu, R. Guan, O. Guryev, N. V. Grishin, C. Rosenmund and J. Rizo (2005). "A minimal domain responsible for Munc13 activity." Nat Struct Mol Biol **12**(11): 1017-1018.

Bennett, M. K., N. Calakos and R. H. Scheller (1992). "Syntaxin: a synaptic protein implicated in docking of synaptic vesicles at presynaptic active zones." Science **257**(5067): 255-259.

Bennett, M. K. and R. H. Scheller (1993). "The molecular machinery for secretion is conserved from yeast to neurons." Proc Natl Acad Sci U S A **90**(7): 2559-2563.

Betz, A., M. Okamoto, F. Benseler and N. Brose (1997). "Direct interaction of the rat unc-13 homologue Munc13-1 with the N terminus of syntaxin." J Biol Chem **272**(4): 2520-2526.

Boswell, K. L., D. J. James, J. M. Esquibel, S. Bruinsma, R. Shirakawa, H. Horiuchi and T. F. Martin (2012). "Munc13-4 reconstitutes calcium-dependent SNARE-mediated membrane fusion." J Cell Biol **197**(2): 301-312.

Bowen, M. E., K. Weninger, J. Ernst, S. Chu and A. T. Brunger (2005). "Single-molecule studies of synaptotagmin and complexin binding to the SNARE complex." Biophys J **89**(1): 690-702.

Bracher, A., T. Dresbach, H. Betz and W. Weissenhorn (2000). "Crystallization and preliminary X-ray analysis of squid neuronal Sec1." Acta Crystallogr D Biol Crystallogr **56**(Pt 4): 501-503.

Bracher, A., A. Perrakis, T. Dresbach, H. Betz and W. Weissenhorn (2000). "The X-ray crystal structure of neuronal Sec1 from squid sheds new light on the role of this protein in exocytosis." Structure **8**(7): 685-694.

Bracher, A. and W. Weissenhorn (2001). "Crystal structures of neuronal squid Sec1 implicate inter-domain hinge movement in the release of t-SNAREs." J Mol Biol **306**(1): 7-13.

Bracher, A. and W. Weissenhorn (2002). "Structural basis for the Golgi membrane recruitment of Sly1p by Sed5p." EMBO J **21**(22): 6114-6124.

Brenner, S. (1974). "The genetics of Caenorhabditis elegans." Genetics **77**(1): 71-94.

Brose, N. (2008). "For better or for worse: complexins regulate SNARE function and vesicle fusion." Traffic **9**(9): 1403-1413.

Brose, N., K. Hofmann, Y. Hata and T. C. Sudhof (1995). "Mammalian homologues of Caenorhabditis elegans unc-13 gene define novel family of C2-domain proteins." J Biol Chem **270**(42): 25273-25280.

Brose, N., A. G. Petrenko, T. C. Sudhof and R. Jahn (1992). "Synaptotagmin: a calcium sensor on the synaptic vesicle surface." Science **256**(5059): 1021-1025.

Brunger, A. T. (2005). "Structure and function of SNARE and SNARE-interacting proteins." Q Rev Biophys **38**(1): 1-47.

Burkhardt, P., D. A. Hattendorf, W. I. Weis and D. Fasshauer (2008). "Munc18a controls SNARE assembly through its interaction with the syntaxin N-peptide." EMBO J **27**(7): 923-933.

Carpp, L. N., L. F. Ciufo, S. G. Shanks, A. Boyd and N. J. Bryant (2006). "The Sec1p/Munc18 protein Vps45p binds its cognate SNARE proteins via two distinct modes." J Cell Biol **173**(6): 927-936.

Carr, C. M., E. Grote, M. Munson, F. M. Hughson and P. J. Novick (1999). "Sec1p binds to SNARE complexes and concentrates at sites of secretion." J Cell Biol **146**(2): 333-344.

Carr, C. M. and J. Rizo (2010). "At the junction of SNARE and SM protein function." Curr Opin Cell Biol **22**(4): 488-495.

Chapman, E. R., S. An, N. Barton and R. Jahn (1994). "SNAP-25, a t-SNARE which binds to both syntaxin and synaptobrevin via domains that may form coiled coils." J Biol Chem **269**(44): 27427-27432.

Chapman, E. R., P. I. Hanson, S. An and R. Jahn (1995). "Ca2+ regulates the interaction between synaptotagmin and syntaxin 1." J Biol Chem **270**(40): 23667-23671.

Chen, X., D. Arac, T. M. Wang, C. J. Gilpin, J. Zimmerberg and J. Rizo (2006). "SNARE-mediated lipid mixing depends on the physical state of the vesicles." Biophys J **90**(6): 2062-2074.

Chen, X., J. Lu, I. Dulubova and J. Rizo (2008). "NMR analysis of the closed conformation of syntaxin-1." Journal of biomolecular NMR **41**(1): 43-54.

Chen, X., J. Lu, I. Dulubova and J. Rizo (2008). "NMR analysis of the closed conformation of syntaxin-1." J Biomol NMR **41**(1): 43-54.

Chen, X., D. Tomchick, E. Kovrigin, D. Ara , M. Machius, T. Südhof and J. Rizo (2002). "Three-dimensional structure of the complexin/SNARE complex." Neuron **33**(3): 397-409.

Chen, X., D. R. Tomchick, E. Kovrigin, D. Arac, M. Machius, T. C. Sudhof and J. Rizo (2002). "Three-dimensional structure of the complexin/SNARE complex." Neuron **33**(3): 397-409.

Chen, Y. A., S. J. Scales and R. H. Scheller (2001). "Sequential SNARE assembly underlies priming and triggering of exocytosis." Neuron **30**(1): 161-170.

Chernomordik, L. (1996). "Non-bilayer lipids and biological fusion intermediates." Chem Phys Lipids **81**(2): 203-213.

Chernomordik, L. V., G. B. Melikyan and Y. A. Chizmadzhev (1987). "Biomembrane fusion: a new concept derived from model studies using two interacting planar lipid bilayers." Biochim Biophys Acta **906**(3): 309-352.

Chicka, M. C., E. Hui, H. Liu and E. R. Chapman (2008). "Synaptotagmin arrests the SNARE complex before triggering fast, efficient membrane fusion in response to Ca2+." Nat Struct Mol Biol **15**(8): 827-835.

Clary, D. O. and J. E. Rothman (1990). "Purification of three related peripheral membrane proteins needed for vesicular transport." J Biol Chem **265**(17): 10109-10117.

Dai, H., N. Shen, D. Arac and J. Rizo (2007). "A quaternary SNARE-synaptotagmin-Ca2+-phospholipid complex in neurotransmitter release." J Mol Biol **367**(3): 848-863.

Deák, F., Y. Xu, W. Chang, I. Dulubova, M. Khvotchev, X. Liu, T. Südhof and J. Rizo (2009). "Munc18-1 binding to the neuronal SNARE complex controls synaptic vesicle priming." The Journal of cell biology **184**(5): 751.

de Wit, H., A. Walter, I. Milosevic, A. Gulyás-Kovács, D. Riedel, J. Sørensen and M. Verhage (2009). "Synaptotagmin-1 docks secretory vesicles to syntaxin-1/SNAP-25 acceptor complexes." Cell **138**(5): 935-946.

Deak, F., Y. Xu, W. P. Chang, I. Dulubova, M. Khvotchev, X. Liu, T. C. Sudhof and J. Rizo (2009). "Munc18-1 binding to the neuronal SNARE complex controls synaptic vesicle priming." J Cell Biol **184**(5): 751-764.

Dennison, S. M., M. E. Bowen, A. T. Brunger and B. R. Lentz (2006). "Neuronal SNAREs do not trigger fusion between synthetic membranes but do promote PEG-mediated membrane fusion." Biophys J **90**(5): 1661-1675.

Diao, J., Z. Su, Y. Ishitsuka, B. Lu, K. S. Lee, Y. Lai, Y. K. Shin and T. Ha (2010). "A single-vesicle content mixing assay for SNARE-mediated membrane fusion." Nat Commun **1**: 54.

Diao, J., Z. Su, X. Lu, T. Y. Yoon, Y. K. Shin and T. Ha (2010). "Single-Vesicle Fusion Assay Reveals Munc18-1 Binding to the SNARE Core Is Sufficient for Stimulating Membrane Fusion." ACS Chem Neurosci **1**(3): 168-174.

Dulubova, I., M. Khvotchev, S. Liu, I. Huryeva, T. C. Südhof and J. Rizo (2007). "Munc18-1 binds directly to the neuronal SNARE complex." Proc Natl Acad Sci U S A **104**(8): 2697-2702.

Dulubova, I., M. Khvotchev, S. Liu, I. Huryeva, T. C. Sudhof and J. Rizo (2007). "Munc18-1 binds directly to the neuronal SNARE complex." Proc Natl Acad Sci U S A **104**(8): 2697-2702.

Dulubova, I., X. Lou, J. Lu, I. Huryeva, A. Alam, R. Schneggenburger, T. C. Sudhof and J. Rizo (2005). "A Munc13/RIM/Rab3 tripartite complex: from priming to plasticity?" EMBO J **24**(16): 2839-2850.

Dulubova, I., S. Sugita, S. Hill, M. Hosaka, I. Fernandez, T. C. Südhof and J. Rizo (1999). "A conformational switch in syntaxin during exocytosis: role of munc18." EMBO J **18**(16): 4372-4382.

Dulubova, I., S. Sugita, S. Hill, M. Hosaka, I. Fernandez, T. C. Sudhof and J. Rizo (1999). "A conformational switch in syntaxin during exocytosis: role of munc18." EMBO J **18**(16): 4372-4382.

Dulubova, I., T. Yamaguchi, Y. Wang, T. C. Sudhof and J. Rizo (2001). "Vam3p structure reveals conserved and divergent properties of syntaxins." Nat Struct Biol **8**(3): 258-264.

Fasshauer, D., D. Bruns, B. Shen, R. Jahn and A. T. Brunger (1997). "A structural change occurs upon binding of syntaxin to SNAP-25." J Biol Chem **272**(7): 4582-4590.

Fasshauer, D. and M. Margittai (2004). "A transient N-terminal interaction of SNAP-25 and syntaxin nucleates SNARE assembly." J Biol Chem **279**(9): 7613-7621.

Fasshauer, D., R. B. Sutton, A. T. Brunger and R. Jahn (1998). "Conserved structural features of the synaptic fusion complex: SNARE proteins reclassified as Q- and R-SNAREs." Proc Natl Acad Sci U S A **95**(26): 15781-15786.

Fernandez-Chacon, R., A. Konigstorfer, S. H. Gerber, J. Garcia, M. F. Matos, C. F. Stevens, N. Brose, J. Rizo, C. Rosenmund and T. C. Sudhof (2001). "Synaptotagmin I functions as a calcium regulator of release probability." Nature **410**(6824): 41-49.

Fernandez-Chacon, R., O. H. Shin, A. Konigstorfer, M. F. Matos, A. C. Meyer, J. Garcia, S. H. Gerber, J. Rizo, T. C. Sudhof and C. Rosenmund (2002). "Structure/function analysis of Ca2+ binding to the C2A domain of synaptotagmin 1." J Neurosci **22**(19): 8438-8446.

Fernandez, I., D. Arac, J. Ubach, S. H. Gerber, O. Shin, Y. Gao, R. G. Anderson, T. C. Sudhof and J. Rizo (2001). "Three-dimensional structure of the synaptotagmin 1 C2B-domain: synaptotagmin 1 as a phospholipid binding machine." Neuron **32**(6): 1057-1069.

Fernandez, I., J. Ubach, I. Dulubova, X. Zhang, T. C. Sudhof and J. Rizo (1998). "Three-dimensional structure of an evolutionarily conserved N-terminal domain of syntaxin 1A." Cell **94**(6): 841-849.

Fleming, K. G., T. M. Hohl, R. C. Yu, S. A. Muller, B. Wolpensinger, A. Engel, H. Engelhardt, A. T. Brunger, T. H. Sollner and P. I. Hanson (1998). "A revised model for the oligomeric state of the N-ethylmaleimide-sensitive fusion protein, NSF." J Biol Chem **273**(25): 15675-15681.

Fujiwara, T., T. Mishima, T. Kofuji, T. Chiba, K. Tanaka, A. Yamamoto and K. Akagawa (2006). "Analysis of knock-out mice to determine the role of HPC-1/syntaxin 1A in expressing synaptic plasticity." J Neurosci **26**(21): 5767-5776.

Gengyo-Ando, K., Y. Kamiya, A. Yamakawa, K. Kodaira, K. Nishiwaki, J. Miwa, I. Hori and R. Hosono (1993). "The C. elegans unc-18 gene encodes a protein expressed in motor neurons." Neuron **11**(4): 703-711.

Geppert, M., B. T. Archer, 3rd and T. C. Sudhof (1991). "Synaptotagmin II. A novel differentially distributed form of synaptotagmin." J Biol Chem **266**(21): 13548-13552.

Geppert, M., Y. Goda, R. E. Hammer, C. Li, T. W. Rosahl, C. F. Stevens and T. C. Sudhof (1994). "Synaptotagmin I: a major Ca2+ sensor for transmitter release at a central synapse." Cell **79**(4): 717-727.

Gerber, S. H., J. C. Rah, S. W. Min, X. Liu, H. de Wit, I. Dulubova, A. C. Meyer, J. Rizo, M. Arancillo, R. E. Hammer, M. Verhage, C. Rosenmund and T. C. Südhof (2008). "Conformational switch of syntaxin-1 controls synaptic vesicle fusion." Science **321**(5895): 1507-1510.

Gerber, S. H., J. C. Rah, S. W. Min, X. Liu, H. de Wit, I. Dulubova, A. C. Meyer, J. Rizo, M. Arancillo, R. E. Hammer, M. Verhage, C. Rosenmund and T. C. Sudhof (2008).

"Conformational switch of syntaxin-1 controls synaptic vesicle fusion." Science **321**(5895): 1507-1510.

Grabowski, R. and D. Gallwitz (1997). "High-affinity binding of the yeast cis-Golgi t-SNARE, Sed5p, to wild-type and mutant Sly1p, a modulator of transport vesicle docking." FEBS Lett **411**(2-3): 169-172.

Gracheva, E. O., G. Hadwiger, M. L. Nonet and J. E. Richmond (2008). "Direct interactions between C. elegans RAB-3 and Rim provide a mechanism to target vesicles to the presynaptic density." Neurosci Lett **444**(2): 137-142.

Grote, E., C. M. Carr and P. J. Novick (2000). "Ordering the final events in yeast exocytosis." J Cell Biol **151**(2): 439-452.

Guan, R., H. Dai and J. Rizo (2008). "Binding of the Munc13-1 MUN domain to membrane-anchored SNARE complexes." Biochemistry **47**(6): 1474-1481.

Gulyas-Kovacs, A., H. de Wit, I. Milosevic, O. Kochubey, R. Toonen, J. Klingauf, M. Verhage and J. B. Sorensen (2007). "Munc18-1: sequential interactions with the fusion machinery stimulate vesicle docking and priming." J Neurosci **27**(32): 8676-8686.

Hammarlund, M., M. T. Palfreyman, S. Watanabe, S. Olsen and E. M. Jorgensen (2007). "Open syntaxin docks synaptic vesicles." PLoS Biol **5**(8): e198.

Hanson, P. I., H. Otto, N. Barton and R. Jahn (1995). "The N-ethylmaleimide-sensitive fusion protein and alpha-SNAP induce a conformational change in syntaxin." J Biol Chem **270**(28): 16955-16961.

Hanson, P. I., R. Roth, H. Morisaki, R. Jahn and J. E. Heuser (1997). "Structure and conformational changes in NSF and its membrane receptor complexes visualized by quick-freeze/deep-etch electron microscopy." Cell **90**(3): 523-535.

Hashizume, K., Y. S. Cheng, J. L. Hutton, C. H. Chiu and C. M. Carr (2009). "Yeast Sec1p functions before and after vesicle docking." Mol Biol Cell **20**(22): 4673-4685.

Hata, Y., C. A. Slaughter and T. C. Sudhof (1993). "Synaptic vesicle fusion complex contains unc-18 homologue bound to syntaxin." Nature **366**(6453): 347-351.

Hayashi, T., H. McMahon, S. Yamasaki, T. Binz, Y. Hata, T. C. Sudhof and H. Niemann (1994). "Synaptic vesicle membrane fusion complex: action of clostridial neurotoxins on assembly." EMBO J **13**(21): 5051-5061.

Hazzard, J., T. C. Sudhof and J. Rizo (1999). "NMR analysis of the structure of synaptobrevin and of its interaction with syntaxin." J Biomol NMR **14**(3): 203-207.

Helm, C. A. and J. N. Israelachvili (1993). "Forces between phospholipid bilayers and relationship to membrane fusion." Methods Enzymol **220**: 130-143.

Hernandez, J. M., A. Stein, E. Behrmann, D. Riedel, A. Cypionka, Z. Farsi, P. J. Walla, S. Raunser and R. Jahn (2012). "Membrane fusion intermediates via directional and full assembly of the SNARE complex." Science **336**(6088): 1581-1584.

Hui, E., J. D. Gaffaney, Z. Wang, C. P. Johnson, C. S. Evans and E. R. Chapman (2011). "Mechanism and function of synaptotagmin-mediated membrane apposition." Nat Struct Mol Biol **18**(7): 813-821.

Jahn, R. and D. Fasshauer (2012). "Molecular machines governing exocytosis of synaptic vesicles." Nature **490**(7419): 201-207.

Jahn, R., T. Lang and T. C. Sudhof (2003). "Membrane fusion." Cell **112**(4): 519-533.

Jahn, R. and R. H. Scheller (2006). "SNAREs--engines for membrane fusion." Nat Rev Mol Cell Biol **7**(9): 631-643.

James, D. J., J. Kowalchyk, N. Daily, M. Petrie and T. F. Martin (2009). "CAPS drives trans-SNARE complex formation and membrane fusion through syntaxin interactions." Proc Natl Acad Sci U S A **106**(41): 17308-17313.

Khvotchev, M., I. Dulubova, J. Sun, H. Dai, J. Rizo and T. C. Südhof (2007). "Dual modes of Munc18-1/SNARE interactions are coupled by functionally critical binding to syntaxin-1 N terminus." J Neurosci **27**(45): 12147-12155.

Khvotchev, M., I. Dulubova, J. Sun, H. Dai, J. Rizo and T. C. Sudhof (2007). "Dual modes of Munc18-1/SNARE interactions are coupled by functionally critical binding to syntaxin-1 N terminus." J Neurosci **27**(45): 12147-12155.

Kozlov, M. M. and V. S. Markin (1983). "[Possible mechanism of membrane fusion]." Biofizika **28**(2): 242-247.

Kummel, D., S. S. Krishnakumar, D. T. Radoff, F. Li, C. G. Giraudo, F. Pincet, J. E. Rothman and K. M. Reinisch (2011). "Complexin cross-links prefusion SNAREs into a zigzag array." Nat Struct Mol Biol **18**(8): 927-933.

Kweon, D. H., C. S. Kim and Y. K. Shin (2003). "Regulation of neuronal SNARE assembly by the membrane." Nat Struct Biol **10**(6): 440-447.

Kyoung, M., A. Srivastava, Y. Zhang, J. Diao, M. Vrljic, P. Grob, E. Nogales, S. Chu and A. T. Brunger (2011). "In vitro system capable of differentiating fast Ca2+-triggered content mixing from lipid exchange for mechanistic studies of neurotransmitter release." Proc Natl Acad Sci U S A **108**(29): E304-313.

Latham, C. F., J. A. Lopez, S. H. Hu, C. L. Gee, E. Westbury, D. H. Blair, C. J. Armishaw, P. F. Alewood, N. J. Bryant, D. E. James and J. L. Martin (2006). "Molecular dissection of the Munc18c/syntaxin4 interaction: implications for regulation of membrane trafficking." Traffic **7**(10): 1408-1419.

Lee, H. K., Y. Yang, Z. Su, C. Hyeon, T. S. Lee, H. W. Lee, D. H. Kweon, Y. K. Shin and T. Y. Yoon (2010). "Dynamic Ca2+-dependent stimulation of vesicle fusion by membrane-anchored synaptotagmin 1." Science **328**(5979): 760-763.

Lee, J. and B. R. Lentz (1997). "Evolution of lipidic structures during model membrane fusion and the relation of this process to cell membrane fusion." Biochemistry **36**(21): 6251-6259.

Li, C., B. Ullrich, J. Z. Zhang, R. G. Anderson, N. Brose and T. C. Sudhof (1995). "Ca(2+)-dependent and -independent activities of neural and non-neural synaptotagmins." Nature **375**(6532): 594-599.

Li, W., C. Ma, R. Guan, Y. Xu, D. R. Tomchick and J. Rizo (2011). "The crystal structure of a Munc13 C-terminal module exhibits a remarkable similarity to vesicle tethering factors." Structure **19**(10): 1443-1455.

Li, Y., G. J. Augustine and K. Weninger (2007). "Kinetics of complexin binding to the SNARE complex: correcting single molecule FRET measurements for hidden events." Biophys J **93**(6): 2178-2187.

Lin, R. C. and R. H. Scheller (1997). "Structural organization of the synaptic exocytosis core complex." Neuron **19**(5): 1087-1094.

Link, E., L. Edelmann, J. H. Chou, T. Binz, S. Yamasaki, U. Eisel, M. Baumert, T. C. Sudhof, H. Niemann and R. Jahn (1992). "Tetanus toxin action: inhibition of neurotransmitter release linked to synaptobrevin proteolysis." Biochem Biophys Res Commun **189**(2): 1017-1023.

Liu, J., T. Guo, Y. Wei, M. Liu and S. F. Sui (2006). "Complexin is able to bind to SNARE core complexes in different assembled states with distinct affinity." Biochem Biophys Res Commun **347**(2): 413-419.

Liu, J., T. Guo, J. Wu, X. Bai, Q. Zhou and S. F. Sui (2007). "Overexpression of complexin in PC12 cells inhibits exocytosis by preventing SNARE complex recycling." Biochemistry (Mosc) **72**(4): 439-444.

Lu, J., M. Machius, I. Dulubova, H. Dai, T. C. Sudhof, D. R. Tomchick and J. Rizo (2006). "Structural basis for a Munc13-1 homodimer to Munc13-1/RIM heterodimer switch." PLoS Biol **4**(7): e192.

Ma, C., W. Li, Y. Xu and J. Rizo (2011). "Munc13 mediates the transition from the closed syntaxin-Munc18 complex to the SNARE complex." Nat Struct Mol Biol **18**(5): 542-549.

Ma, C., W. Li, Y. Xu and J. Rizo (2011). "Munc13 Mediates the Transition from the Closed Syntaxin/Munc18 complex to the SNARE complex." Nature structural & molecular biology, in press.

Mackler, J. M., J. A. Drummond, C. A. Loewen, I. M. Robinson and N. E. Reist (2002). "The C(2)B Ca(2+)-binding motif of synaptotagmin is required for synaptic transmission in vivo." Nature **418**(6895): 340-344.

Madison, J. M., S. Nurrish and J. M. Kaplan (2005). "UNC-13 interaction with syntaxin is required for synaptic transmission." Curr Biol **15**(24): 2236-2242.

Martens, S., M. M. Kozlov and H. T. McMahon (2007). "How synaptotagmin promotes membrane fusion." Science **316**(5828): 1205-1208.

Maximov, A., J. Tang, X. Yang, Z. P. Pang and T. C. Sudhof (2009). "Complexin controls the force transfer from SNARE complexes to membranes in fusion." Science **323**(5913): 516-521.

Mayer, A., W. Wickner and A. Haas (1996). "Sec18p (NSF)-driven release of Sec17p (alpha-SNAP) can precede docking and fusion of yeast vacuoles." Cell **85**(1): 83-94.

McMahon, H. T., M. Missler, C. Li and T. C. Sudhof (1995). "Complexins: cytosolic proteins that regulate SNAP receptor function." Cell **83**(1): 111-119.

Medine, C. N., C. Rickman, L. H. Chamberlain and R. R. Duncan (2007). "Munc18-1 prevents the formation of ectopic SNARE complexes in living cells." J Cell Sci **120**(Pt 24): 4407-4415.

Meinrenken, C. J., J. G. Borst and B. Sakmann (2003). "Local routes revisited: the space and time dependence of the Ca2+ signal for phasic transmitter release at the rat calyx of Held." J Physiol **547**(Pt 3): 665-689.

Mima, J., C. M. Hickey, H. Xu, Y. Jun and W. Wickner (2008). "Reconstituted membrane fusion requires regulatory lipids, SNAREs and synergistic SNARE chaperones." EMBO J **27**(15): 2031-2042.

Misura, K. M., L. C. Gonzalez, Jr., A. P. May, R. H. Scheller and W. I. Weis (2001). "Crystal structure and biophysical properties of a complex between the N-terminal SNARE region of SNAP25 and syntaxin 1a." J Biol Chem **276**(44): 41301-41309.

Misura, K. M., R. H. Scheller and W. I. Weis (2000). "Three-dimensional structure of the neuronal-Sec1-syntaxin 1a complex." Nature **404**(6776): 355-362.

Misura, K. M., R. H. Scheller and W. I. Weis (2001). "Self-association of the H3 region of syntaxin 1A. Implications for intermediates in SNARE complex assembly." J Biol Chem **276**(16): 13273-13282.

Nagiec, E. E., A. Bernstein and S. W. Whiteheart (1995). "Each domain of the N-ethylmaleimide-sensitive fusion protein contributes to its transport activity." J Biol Chem **270**(49): 29182-29188.

Neher, E. (2010). "Complexin: does it deserve its name?" Neuron **68**(5): 803-806.

Nichols, B. J., J. C. Holthuis and H. R. Pelham (1998). "The Sec1p homologue Vps45p binds to the syntaxin Tlg2p." Eur J Cell Biol **77**(4): 263-268.

Nickel, W., T. Weber, J. A. McNew, F. Parlati, T. H. Sollner and J. E. Rothman (1999). "Content mixing and membrane integrity during membrane fusion driven by pairing of isolated v-SNAREs and t-SNAREs." Proc Natl Acad Sci U S A **96**(22): 12571-12576.

Nishiki, T. and G. J. Augustine (2004). "Dual roles of the C2B domain of synaptotagmin I in synchronizing Ca2+-dependent neurotransmitter release." J Neurosci **24**(39): 8542-8550.

Novick, P., C. Field and R. Schekman (1980). "Identification of 23 complementation groups required for post-translational events in the yeast secretory pathway." Cell **21**(1): 205-215.

Ohya, T., M. Miaczynska, U. Coskun, B. Lommer, A. Runge, D. Drechsel, Y. Kalaidzidis and M. Zerial (2009). "Reconstitution of Rab- and SNARE-dependent membrane fusion by synthetic endosomes." Nature **459**(7250): 1091-1097.

Pabst, S., J. W. Hazzard, W. Antonin, T. C. Sudhof, R. Jahn, J. Rizo and D. Fasshauer (2000). "Selective interaction of complexin with the neuronal SNARE complex. Determination of the binding regions." J Biol Chem **275**(26): 19808-19818.

Pabst, S., M. Margittai, D. Vainius, R. Langen, R. Jahn and D. Fasshauer (2002). "Rapid and selective binding to the synaptic SNARE complex suggests a modulatory role of complexins in neuroexocytosis." J Biol Chem **277**(10): 7838-7848.

Parlati, F., T. Weber, J. A. McNew, B. Westermann, T. H. Sollner and J. E. Rothman (1999). "Rapid and efficient fusion of phospholipid vesicles by the alpha-helical core of a SNARE complex in the absence of an N-terminal regulatory domain." Proc Natl Acad Sci U S A **96**(22): 12565-12570.

Pei, J., C. Ma, J. Rizo and N. V. Grishin (2009). "Remote homology between Munc13 MUN domain and vesicle tethering complexes." J Mol Biol **391**(3): 509-517.

Peng, R. and D. Gallwitz (2002). "Sly1 protein bound to Golgi syntaxin Sed5p allows assembly and contributes to specificity of SNARE fusion complexes." J Cell Biol **157**(4): 645-655.

Pevsner, J., S. C. Hsu, J. E. Braun, N. Calakos, A. E. Ting, M. K. Bennett and R. H. Scheller (1994). "Specificity and regulation of a synaptic vesicle docking complex." Neuron **13**(2): 353-361.

Poirier, M. A., W. Xiao, J. C. Macosko, C. Chan, Y. K. Shin and M. K. Bennett (1998). "The synaptic SNARE complex is a parallel four-stranded helical bundle." Nat Struct Biol **5**(9): 765-769.

Rathore, S. S., E. G. Bend, H. Yu, M. Hammarlund, E. M. Jorgensen and J. Shen (2010). "Syntaxin N-terminal peptide motif is an initiation factor for the assembly of the SNARE-Sec1/Munc18 membrane fusion complex." Proc Natl Acad Sci U S A **107**(52): 22399-22406.

Reim, K., M. Mansour, F. Varoqueaux, H. T. McMahon, T. C. Sudhof, N. Brose and C. Rosenmund (2001). "Complexins regulate a late step in Ca2+-dependent neurotransmitter release." Cell **104**(1): 71-81.

Reim, K., H. Wegmeyer, J. H. Brandstatter, M. Xue, C. Rosenmund, T. Dresbach, K. Hofmann and N. Brose (2005). "Structurally and functionally unique complexins at retinal ribbon synapses." J Cell Biol **169**(4): 669-680.

Rhee, J. S., A. Betz, S. Pyott, K. Reim, F. Varoqueaux, I. Augustin, D. Hesse, T. C. Sudhof, M. Takahashi, C. Rosenmund and N. Brose (2002). "Beta phorbol ester- and diacylglycerol-induced augmentation of transmitter release is mediated by Munc13s and not by PKCs." Cell **108**(1): 121-133.

Richmond, J. E., W. S. Davis and E. M. Jorgensen (1999). "UNC-13 is required for synaptic vesicle fusion in C. elegans." Nat Neurosci **2**(11): 959-964.

Richmond, J. E., R. M. Weimer and E. M. Jorgensen (2001). "An open form of syntaxin bypasses the requirement for UNC-13 in vesicle priming." Nature **412**(6844): 338-341.

Rickman, C., F. A. Meunier, T. Binz and B. Davletov (2004). "High affinity interaction of syntaxin and SNAP-25 on the plasma membrane is abolished by botulinum toxin E." J Biol Chem **279**(1): 644-651.

Riento, K., T. Galli, S. Jansson, C. Ehnholm, E. Lehtonen and V. M. Olkkonen (1998). "Interaction of Munc-18-2 with syntaxin 3 controls the association of apical SNAREs in epithelial cells." J Cell Sci **111 (Pt 17)**: 2681-2688.

Rizo, J., X. Chen and D. Ara (2006). "Unraveling the mechanisms of synaptotagmin and SNARE function in neurotransmitter release." Trends in cell biology **16**(7): 339-350.

Rizo, J., X. Chen and D. Arac (2006). "Unraveling the mechanisms of synaptotagmin and SNARE function in neurotransmitter release." Trends Cell Biol **16**(7): 339-350.

Rizo, J. and C. Rosenmund (2008). "Synaptic vesicle fusion." Nature structural & molecular biology **15**(7): 665-674.

Rizo, J. and C. Rosenmund (2008). "Synaptic vesicle fusion." Nat Struct Mol Biol **15**(7): 665-674.

Rizo, J. and T. Südhof (2002). "Snares and Munc18 in synaptic vesicle fusion." Nature Reviews Neuroscience **3**(8): 641-653.

Rizo, J. and T. C. Sudhof (2002). "Snares and Munc18 in synaptic vesicle fusion." Nat Rev Neurosci **3**(8): 641-653.

Robinson, I. M., R. Ranjan and T. L. Schwarz (2002). "Synaptotagmins I and IV promote transmitter release independently of Ca(2+) binding in the C(2)A domain." Nature **418**(6895): 336-340.

Rodkey, T. L., S. Liu, M. Barry and J. A. McNew (2008). "Munc18a scaffolds SNARE assembly to promote membrane fusion." Mol Biol Cell **19**(12): 5422-5434.

Schiavo, G., F. Benfenati, B. Poulain, O. Rossetto, P. Polverino de Laureto, B. R. DasGupta and C. Montecucco (1992). "Tetanus and botulinum-B neurotoxins block neurotransmitter release by proteolytic cleavage of synaptobrevin." Nature **359**(6398): 832-835.

Schneggenburger, R. and E. Neher (2005). "Presynaptic calcium and control of vesicle fusion." Curr Opin Neurobiol **15**(3): 266-274.

Schoch, S., F. Deak, A. Konigstorfer, M. Mozhayeva, Y. Sara, T. C. Sudhof and E. T. Kavalali (2001). "SNARE function analyzed in synaptobrevin/VAMP knockout mice." Science **294**(5544): 1117-1122.

Schollmeier, Y., J. M. Krause, S. Kreye, J. Malsam and T. H. Sollner (2011). "Resolving the function of distinct Munc18-1/SNARE protein interaction modes in a reconstituted membrane fusion assay." J Biol Chem **286**(35): 30582-30590.

Shen, J., S. S. Rathore, L. Khandan and J. E. Rothman (2010). "SNARE bundle and syntaxin N-peptide constitute a minimal complement for Munc18-1 activation of membrane fusion." J Cell Biol **190**(1): 55-63.

Shen, J., D. Tareste, F. Paumet, J. Rothman and T. Melia (2007). "Selective activation of cognate SNAREpins by Sec1/Munc18 proteins." Cell **128**(1): 183-195.

Shen, J., D. C. Tareste, F. Paumet, J. E. Rothman and T. J. Melia (2007). "Selective activation of cognate SNAREpins by Sec1/Munc18 proteins." Cell **128**(1): 183-195.

Shin, O. H., J. Lu, J. S. Rhee, D. R. Tomchick, Z. P. Pang, S. M. Wojcik, M. Camacho-Perez, N. Brose, M. Machius, J. Rizo, C. Rosenmund and T. C. Sudhof (2010). "Munc13 C2B domain is an activity-dependent Ca2+ regulator of synaptic exocytosis." Nat Struct Mol Biol **17**(3): 280-288.

Shin, O. H., J. S. Rhee, J. Tang, S. Sugita, C. Rosenmund and T. C. Sudhof (2003). "Sr2+ binding to the Ca2+ binding site of the synaptotagmin 1 C2B domain triggers fast exocytosis without stimulating SNARE interactions." Neuron **37**(1): 99-108.

Siksou, L., F. Varoqueaux, O. Pascual, A. Triller, N. Brose and S. Marty (2009). "A common molecular basis for membrane docking and functional priming of synaptic vesicles." Eur J Neurosci **30**(1): 49-56.

Sivaram, M. V., J. A. Saporita, M. L. Furgason, A. J. Boettcher and M. Munson (2005). "Dimerization of the exocyst protein Sec6p and its interaction with the t-SNARE Sec9p." Biochemistry **44**(16): 6302-6311.

Sollner, T., M. K. Bennett, S. W. Whiteheart, R. H. Scheller and J. E. Rothman (1993). "A protein assembly-disassembly pathway in vitro that may correspond to sequential steps of synaptic vesicle docking, activation, and fusion." Cell **75**(3): 409-418.

Sorensen, J. B. (2009). "Conflicting views on the membrane fusion machinery and the fusion pore." Annu Rev Cell Dev Biol **25**: 513-537.

Starai, V., C. Hickey and W. Wickner (2008). "HOPS proofreads the trans-SNARE complex for yeast vacuole fusion." Molecular biology of the cell **19**(6): 2500.

Stein, A. and R. Jahn (2009). "Complexins living up to their name--new light on their role in exocytosis." Neuron **64**(3): 295-297.

Stein, A., A. Radhakrishnan, D. Riedel, D. Fasshauer and R. Jahn (2007). "Synaptotagmin activates membrane fusion through a Ca2+-dependent trans interaction with phospholipids." Nat Struct Mol Biol **14**(10): 904-911.

Stein, A., G. Weber, M. C. Wahl and R. Jahn (2009). "Helical extension of the neuronal SNARE complex into the membrane." Nature **460**(7254): 525-528.

Stevens, C. F. and J. M. Sullivan (2003). "The synaptotagmin C2A domain is part of the calcium sensor controlling fast synaptic transmission." Neuron **39**(2): 299-308.

Stevens, D. R., Z. X. Wu, U. Matti, H. J. Junge, C. Schirra, U. Becherer, S. M. Wojcik, N. Brose and J. Rettig (2005). "Identification of the minimal protein domain required for priming activity of Munc13-1." Curr Biol **15**(24): 2243-2248.

Stroupe, C., K. M. Collins, R. A. Fratti and W. Wickner (2006). "Purification of active HOPS complex reveals its affinities for phosphoinositides and the SNARE Vam7p." EMBO J **25**(8): 1579-1589.

Stroupe, C., C. M. Hickey, J. Mima, A. S. Burfeind and W. Wickner (2009). "Minimal membrane docking requirements revealed by reconstitution of Rab GTPase-dependent membrane fusion from purified components." Proc Natl Acad Sci U S A **106**(42): 17626-17633.

Sudhof, T. C. (2002). "Synaptotagmins: why so many?" J Biol Chem **277**(10): 7629-7632.

Sudhof, T. C. (2004). "The synaptic vesicle cycle." Annu Rev Neurosci **27**: 509-547.

Sudhof, T. C. and J. Rizo (2011). "Synaptic vesicle exocytosis." Cold Spring Harb Perspect Biol **3**(12).

Sudhof, T. C. and J. E. Rothman (2009). "Membrane fusion: grappling with SNARE and SM proteins." Science **323**(5913): 474-477.

Sutton, R. B., D. Fasshauer, R. Jahn and A. T. Brunger (1998). "Crystal structure of a SNARE complex involved in synaptic exocytosis at 2.4 A resolution." Nature **395**(6700): 347-353.

Tagaya, M., D. W. Wilson, M. Brunner, N. Arango and J. E. Rothman (1993). "Domain structure of an N-ethylmaleimide-sensitive fusion protein involved in vesicular transport." J Biol Chem **268**(4): 2662-2666.

Tellam, J. T., S. McIntosh and D. E. James (1995). "Molecular identification of two novel Munc-18 isoforms expressed in non-neuronal tissues." J Biol Chem **270**(11): 5857-5863.

Thurmond, D. C., M. Kanzaki, A. H. Khan and J. E. Pessin (2000). "Munc18c function is required for insulin-stimulated plasma membrane fusion of GLUT4 and insulin-responsive amino peptidase storage vesicles." Mol Cell Biol **20**(1): 379-388.

Togneri, J., Y. S. Cheng, M. Munson, F. M. Hughson and C. M. Carr (2006). "Specific SNARE complex binding mode of the Sec1/Munc-18 protein, Sec1p." Proc Natl Acad Sci U S A **103**(47): 17730-17735.

Toonen, R. F. and M. Verhage (2007). "Munc18-1 in secretion: lonely Munc joins SNARE team and takes control." Trends Neurosci **30**(11): 564-572.

Tripathi, A., Y. Ren, P. D. Jeffrey and F. M. Hughson (2009). "Structural characterization of Tip20p and Dsl1p, subunits of the Dsl1p vesicle tethering complex." Nat Struct Mol Biol **16**(2): 114-123.

Tucker, W. C., T. Weber and E. R. Chapman (2004). "Reconstitution of Ca2+-regulated membrane fusion by synaptotagmin and SNAREs." Science **304**(5669): 435-438.

Tugarinov, V., R. Sprangers and L. E. Kay (2004). "Line narrowing in methyl-TROSY using zero-quantum 1H-13C NMR spectroscopy." J Am Chem Soc **126**(15): 4921-4925.

Ubach, J., X. Zhang, X. Shao, T. C. Sudhof and J. Rizo (1998). "Ca2+ binding to synaptotagmin: how many Ca2+ ions bind to the tip of a C2-domain?" EMBO J **17**(14): 3921-3930.

Ullrich, B., C. Li, J. Z. Zhang, H. McMahon, R. G. Anderson, M. Geppert and T. C. Sudhof (1994). "Functional properties of multiple synaptotagmins in brain." Neuron **13**(6): 1281-1291.

van den Bogaart, G., M. G. Holt, G. Bunt, D. Riedel, F. S. Wouters and R. Jahn (2010). "One SNARE complex is sufficient for membrane fusion." Nat Struct Mol Biol **17**(3): 358-364.

van den Bogaart, G., S. Thutupalli, J. H. Risselada, K. Meyenberg, M. Holt, D. Riedel, U. Diederichsen, S. Herminghaus, H. Grubmuller and R. Jahn (2011). "Synaptotagmin-1 may be a distance regulator acting upstream of SNARE nucleation." Nat Struct Mol Biol **18**(7): 805-812.

Varoqueaux, F., A. Sigler, J. S. Rhee, N. Brose, C. Enk, K. Reim and C. Rosenmund (2002). "Total arrest of spontaneous and evoked synaptic transmission but normal synaptogenesis in the absence of Munc13-mediated vesicle priming." Proc Natl Acad Sci U S A **99**(13): 9037-9042.

Verhage, M., A. S. Maia, J. J. Plomp, A. B. Brussaard, J. H. Heeroma, H. Vermeer, R. F. Toonen, R. E. Hammer, T. K. van den Berg, M. Missler, H. J. Geuze and T. C. Südhof (2000). "Synaptic assembly of the brain in the absence of neurotransmitter secretion." Science **287**(5454): 864-869.

Verhage, M., A. S. Maia, J. J. Plomp, A. B. Brussaard, J. H. Heeroma, H. Vermeer, R. F. Toonen, R. E. Hammer, T. K. van den Berg, M. Missler, H. J. Geuze and T. C. Sudhof (2000). "Synaptic assembly of the brain in the absence of neurotransmitter secretion." Science **287**(5454): 864-869.

Verhage, M. and R. Toonen (2007). "Regulated exocytosis: merging ideas on fusing membranes." Current opinion in cell biology **19**(4): 402-408.

Verhage, M. and R. F. Toonen (2007). "Regulated exocytosis: merging ideas on fusing membranes." Curr Opin Cell Biol **19**(4): 402-408.

Voets, T., R. F. Toonen, E. C. Brian, H. de Wit, T. Moser, J. Rettig, T. C. Sudhof, E. Neher and M. Verhage (2001). "Munc18-1 promotes large dense-core vesicle docking." Neuron **31**(4): 581-591.

Washbourne, P., P. M. Thompson, M. Carta, E. T. Costa, J. R. Mathews, G. Lopez-Bendito, Z. Molnar, M. W. Becher, C. F. Valenzuela, L. D. Partridge and M. C. Wilson (2002). "Genetic ablation of the t-SNARE SNAP-25 distinguishes mechanisms of neuroexocytosis." Nat Neurosci **5**(1): 19-26.

Weber, T., F. Parlati, J. A. McNew, R. J. Johnston, B. Westermann, T. H. Sollner and J. E. Rothman (2000). "SNAREpins are functionally resistant to disruption by NSF and alphaSNAP." J Cell Biol **149**(5): 1063-1072.

Weber, T., B. V. Zemelman, J. A. McNew, B. Westermann, M. Gmachl, F. Parlati, T. H. Sollner and J. E. Rothman (1998). "SNAREpins: minimal machinery for membrane fusion." Cell **92**(6): 759-772.

Weimer, R. M., E. O. Gracheva, O. Meyrignac, K. G. Miller, J. E. Richmond and J. L. Bessereau (2006). "UNC-13 and UNC-10/rim localize synaptic vesicles to specific membrane domains." J Neurosci **26**(31): 8040-8047.

Weimer, R. M., J. E. Richmond, W. S. Davis, G. Hadwiger, M. L. Nonet and E. M. Jorgensen (2003). "Defects in synaptic vesicle docking in unc-18 mutants." Nat Neurosci **6**(10): 1023-1030.

Whiteheart, S. W., I. C. Griff, M. Brunner, D. O. Clary, T. Mayer, S. A. Buhrow and J. E. Rothman (1993). "SNAP family of NSF attachment proteins includes a brain-specific isoform." Nature **362**(6418): 353-355.

Williams, R. W. and K. Herrup (1988). "The control of neuron number." Annu Rev Neurosci **11**: 423-453.

Wilson, D. W., S. W. Whiteheart, M. Wiedmann, M. Brunner and J. E. Rothman (1992). "A multisubunit particle implicated in membrane fusion." J Cell Biol **117**(3): 531-538.

Wu, M. N., J. T. Littleton, M. A. Bhat, A. Prokop and H. J. Bellen (1998). "ROP, the Drosophila Sec1 homolog, interacts with syntaxin and regulates neurotransmitter release in a dosage-dependent manner." EMBO J **17**(1): 127-139.

Xu, H., Y. Jun, J. Thompson, J. Yates and W. Wickner (2010). "HOPS prevents the disassembly of trans-SNARE complexes by Sec17p/Sec18p during membrane fusion." EMBO J **29**(12): 1948-1960.

Xu, Y., A. B. Seven, L. Su, Q. X. Jiang and J. Rizo (2011). "Membrane bridging and hemifusion by denaturated Munc18." PLoS One **6**(7): e22012.

Xu, Y., L. Su and J. Rizo (2010). "Binding of Munc18-1 to synaptobrevin and to the SNARE four-helix bundle." Biochemistry **49**(8): 1568-1576.

Xue, M., T. K. Craig, J. Xu, H. T. Chao, J. Rizo and C. Rosenmund (2010). "Binding of the complexin N terminus to the SNARE complex potentiates synaptic-vesicle fusogenicity." Nat Struct Mol Biol **17**(5): 568-575.

Xue, M., C. Ma, T. K. Craig, C. Rosenmund and J. Rizo (2008). "The Janus-faced nature of the C(2)B domain is fundamental for synaptotagmin-1 function." Nat Struct Mol Biol **15**(11): 1160-1168.

Xue, M., K. Reim, X. Chen, H. T. Chao, H. Deng, J. Rizo, N. Brose and C. Rosenmund (2007). "Distinct domains of complexin I differentially regulate neurotransmitter release." Nat Struct Mol Biol **14**(10): 949-958.

Yang, B., M. Steegmaier, L. C. Gonzalez, Jr. and R. H. Scheller (2000). "nSec1 binds a closed conformation of syntaxin1A." J Cell Biol **148**(2): 247-252.

Yang, X., Y. J. Kaeser-Woo, Z. P. Pang, W. Xu and T. C. Sudhof (2010). "Complexin clamps asynchronous release by blocking a secondary Ca(2+) sensor via its accessory alpha helix." Neuron **68**(5): 907-920.

Zhang, F., Y. Chen, D. H. Kweon, C. S. Kim and Y. K. Shin (2002). "The four-helix bundle of the neuronal target membrane SNARE complex is neither disordered in the middle nor uncoiled at the C-terminal region." J Biol Chem **277**(27): 24294-24298.

Zhao, C., E. C. Smith and S. W. Whiteheart (2012). "Requirements for the catalytic cycle of the N-ethylmaleimide-Sensitive Factor (NSF)." Biochim Biophys Acta **1823**(1): 159-171.

Zucchi, P. C. and M. Zick (2011). "Membrane fusion catalyzed by a Rab, SNAREs, and SNARE chaperones is accompanied by enhanced permeability to small molecules and by lysis." Mol Biol Cell **22**(23): 4635-4646.